

**Investigations of Novel N_xS_y
Technetium and Rhenium Chelants**

Investigations of Novel N_xS_y Technetium and Rhenium Chelants

by

SAMANTHA ELIZABETH BENNETT, B. Sc.

A Thesis

Submitted to the School of Graduate Studies

in Partial Fulfilment of the Requirements

for the Degree

Masters of Science

McMaster University

©Copyright by Samantha E. Bennett, June 1997.

MASTERS OF SCIENCE (1997)
(Chemistry)

McMASTER
UNIVERSITY
Hamilton, Ontario

TITLE: Investigations of Novel N_xS_y Technetium and Rhenium
Chelants

AUTHOR: Samantha Elizabeth Bennett, B. Sc. (McMaster University)

SUPERVISORS: Professor Russell Arthur Bell
Professor Colin James Lyne Lock

NUMBER OF PAGES: xii, 101

Abstract

This thesis describes the synthesis and complexation of amino acid based chelants for technetium and rhenium. All of the chelates were of the N_xS_y type. An initial N_2S_2 diamido dithiol peptide of the type mercaptoacetic acid-serine-cysteine was synthesized and coordinated with both rhenium and technetium. The complexes were analysed by NMR spectroscopy and found to retain the benzyl moieties. *Syn* and *anti* diastereomers were produced with one conformation preferred over the other.

This was not true of another chelant RP294 supplied by Resolution Pharmaceuticals. The $N_2N_1'S_1$ chelant consisted of dimethyl-glycine-serine-cysteine-glycine and was a novel variation of the N_2S_2 tripeptide used initially. The coordination of this N_3S chelant to technetium resulted in the formation of equal 1:1 quantities of diastereomers. Analysis was done by NMR spectroscopy and electrospray mass spectrometry. The two diastereomers were found to slowly interconvert and a mechanism for the interconversion proposed. The radiopharmaceutical RP128 (dimethylglycine-serine-cysteine-glycine-threonine-lysine-proline-proline-arginine), of which the RP294 is the chelating portion, was coordinated to technetium. Analysis of the bifunctional chelant and its coordination complex by NMR spectroscopy demonstrated that the targeting portion of the molecule was unaffected by the technetium. Two diastereomers of the $TcO(RP128)$ complex were found, as seen for the chelating portion of the molecule, $TcO(RP294)$.

Acknowledgements

There are so many people whose encouragement and guidance have aided me in my quest to achieve this goal. First and foremost are those whose constant, cheery assistance and unfathomable knowledge of this subject have helped make this thesis what it is. I owe a debt of gratitude to Professor Russell Bell for his willingness to step in when needed and help guide me through the perils of NMR and synthetic chemistry. To Ernest Wong my heartfelt appreciation and life-long admiration for the caring guidance given throughout my collaboration with Resolution Pharmaceuticals Inc.. John Thornback for his support and presence throughout my research at McMaster. Alan Guest, a constant support, a good laugh and a wealth of knowledge. My lab mates, Theresa Fauconnier, Dave Green and John Valliant - thanks for being there. Don Hughes, Richard Smith, Dr. Brian McCarry and Laurie Allan and everyone else who looked kindly on me and gave me a hand, I thank you for your patience and understanding. Janis Gulens, thanks for being a wonderful friend and talking me into this, you were right. I am indebted to the late Professor Colin Lock for having the forbearance to let me be a part of his group. I trust he is not disappointed. This ambitious undertaking was not done without the support of those closest to me. Mom, Jennifer and Santino, I thank you for your patience and for being there when I needed the help or just a saner voice to listen to. Susan Nagy, my lunch partner, thanks for everything and letting me bend your ear from noon til one pm. Lorne, for all the great times, the tough times and the times to come as always, I am "Overjoyed". I would like to dedicate this to the loving memory of my father, Hugh Robert Bennett. Thanks Dad for making "me" me.

Table of Contents

	Page
Title	i
Abstract	iv
Acknowledgements	v
Table of Contents	vi
List of Figures	ix
List of Abbreviations	xi
Chapter 1: Introduction	
<i>1.0 Rationale</i>	1
<i>1.1 Objectives</i>	1
<i>1.2 Technetium</i>	2
<i>1.3 ^{99m}Technetium</i>	5
<i>1.4 Tc Based Radiopharmaceuticals</i>	5
<i>1.5 Tc Based Bifunctional Chelants</i>	7
<i>1.6 Spectroscopic and Spectrometric Analytical Methods</i>	10
Chapter 2: Amino Acid Based Chelants	
<i>2.0 Introduction</i>	12
<i>2.1 Retrosynthesis</i>	14
<i>2.2 Synthesis of Mer-Ser-Cys</i>	- 16

2.3	<i>NMR Spectroscopy of Mer-Ser-Cys</i>	26
2.4	<i>Reaction of Tr-S-Mer-L-Ser-S-Bn-L-Cys OMe with ReOCl₃(PPh₃)₂</i>	29
2.5	<i>Reaction of Tr-S-Mer-L-Ser-S-Bn-L-Cys OMe with K⁹⁹TcOCl₄</i>	36
2.6	<i>Complex Formation</i>	40
2.7	<i>Experimental Section</i>	41
Chapter 3:	Technetium(V) Oxo complex of an N₂N₁'S₁ Peptidic Chelator	
3.0	<i>Introduction</i>	48
3.1	<i>Chelant Design</i>	49
3.2	<i>NMR Spectroscopy of Chelant RP294</i>	50
3.3	<i>Technetium-99 Complex of RP294, 16</i>	55
3.4	<i>Syn and Anti Interconversion</i>	65
3.5	<i>^{99m}Tracer Studies</i>	68
3.6	<i>Experimental Section</i>	69
Chapter 4:	Chelation of a Nine Amino Acid Peptide to ⁹⁹Tc	
4.0	<i>Introduction</i>	72
4.1	<i>NMR Spectroscopy of RP128, 21</i>	74
4.2	<i>Synthesis of ⁹⁹TcO(RP128), 23</i>	77
4.3	<i>NMR Spectroscopy of ⁹⁹TcO(RP128), 23</i>	- 80

<i>4.4 $^{99m}\text{TcO}(\text{RP128})$ as an Imaging Agent</i>	85
<i>4.5 Experimental Section</i>	87
Chapter 5: Conclusions and Future Work	
<i>5.0 Conclusions</i>	90
References	92
Appendix I: Experimental Methods	98

List of Figures

Figure		Page
1-1	Cores of technetium	3
1-2	Schematic of TcOCl_4^- unit	4
1-3	HMPAO and MRP20	6
1-4	Cardiolite® and Myoview®	6
1-5	HYNIC Bifunctional chelant	8
1-6	Digitoxin and Digitoxigenin chelant derivatives	9
2-1	Diamino Dithiol ligand and ECD	12
2-2	Diamido Dithiol and Cys-Thr-Cys	13
2-3	Retrosynthesis of Mer-Ser-Cys	15
2-4	Synthesis of Mer-Ser-Cys	16
2-5	Borontrifluoride etherate mechanism	17
2-6	EDAC coupling of S-tritylthioglycolic to N-hydroxysuccinimide	19
2-7	200 ^1H NMR MHz spectrum of N-hydroxysuccinimido(triphenylmethylthio)-ethanoate in CDCl_3	20
2-8	Mechanism of <i>p</i> -TsOH catalysed esterification of cysteine	21
2-9	Mechanism of EDAC coupling of N-t-Boc-L-serine-S-benzyl-L-cysteine methyl ester	23
2-10	Mechanism of TFA deprotection of N-t-Boc-L-serine-S-benzyl-L-cysteine methyl ester	24
2-11	500 MHz ^1H NMR Spectrum of 6 in CDCl_3	26
2-12	Synthesis of Mer-Ser-Cys metal complexes	30

2-13	HPLC Chromatogram of 12	32
2-14	500 MHz ¹ H NMR Spectrum of aliphatic region of 12 in CD ₃ CN	32
2-15	Possible conformers of the metal complex	35
2-16	500 MHz ¹ H NMR Spectrum of aliphatic region of 14 in CD ₃ CN	38
3-1	MAG ₃ structure	48
3-2	RP294 Chelant 15	49
3-3	500 MHz ¹ H NMR Spectrum of Aliphatic region of 15 in D ₂ O	51
3-4	HMBC connectivity	52
3-5	HMBC of 15	54
3-6	Synthesis of 16	56
3-7	<i>Syn</i> and <i>anti</i> isomers of MO(RP294)	57
3-8	Selective TOCSY irradiation of cys α proton at 5.30 ppm	61
3-9	500 MHz ¹ H NMR spectrum of the aliphatic region of 16 in D ₂ O	62
3-10	Conformers of <i>syn</i> and <i>anti</i> side arm	63
3-11	¹⁸ O <i>syn</i> and <i>anti</i> conversion mechanism	67
3-12	HPLC coinjection of Re and Tc complexes of RP294	69
4-1	The bifunctional chelant RP128, 21	74
4-2	Reaction scheme for RP128 coordination of technetium	78
4-3	Infrared spectrum of 23	79
4-4	500 MHz ¹ H NMR Aliphatic region of 23 in D ₂ O	82
4-5	HPLC of ^{99m} TcO(RP128) and ReO(RP128)	85
4-6	^{99m} Tc scintigraph of rheumatic arthritis sufferer	86

List of Abbreviations and Symbols

AN	Acetonitrile
Bn	Benzyl
Boc	Tert-Butoxycarbonyl
¹³ C NMR	C-13 Nuclear Magnetic Resonance Spectroscopy
COSY	Correlation Spectroscopy
Cys	Cysteine
DADS	Diamido Disulfide
DADT	Diamido Dithiol
DCC	Dicyclohexylcarbodiimide
DCM	Dichloromethane
DIPEA	Diisopropylethylamine
DW	Distilled water
ECD	N,N'-1,2-Ethylene-bis-L-cysteine diethyl ester
EDAC	Ethyl-3-(3'-dimethylamino)-propylcarbodiimide hydrochloride
ESMS	Electrospray Mass Spectrometry
EtOH	Ethanol
Fmoc	9-Fluorenylmethoxycarbonyl
Gly	Glycine
HPLC	High Performance Liquid Chromatography
¹ H NMR	Proton Nuclear Magnetic Resonance Spectroscopy
HMBC	Heteronuclear multiple bond correlation
HMQC	Heteronuclear multiple quantum coherence
h	Hours
HSQC	Heteronuclear single quantum coherence
HYNIC	Hydrazino nicotinamide
IR	Infrared Spectroscopy
MAG ₃	Mercaptoacetamide-glycine-glycine-glycine
Me	Methyl
MeOH	Methanol
Mer	Mercaptoacetic acid
mp	Melting point
MRP20	N-(2-(1H pyrrolylmethyl)) N'-(4-pentene-3-one-2) ethane-1,2-diamine
MS	Mass Spectrometry

NOE	Nuclear Overhauser Effect
PnAO	Propylene Oxime
PPh ₃	Triphenylphosphine
ppm	Parts per million
Re	Rhenium
RP128	Dimethylglycine-serine-cysteine-glycine-threonine-lysine-proline-proline-arginine
RP294	Dimethylglycine-serine-cysteine-glycine
Ser	Serine
Tc	Technetium
TFA	Trifluoroacetic acid
TKPR	Theonine-lysine-proline-arginine
TKPPR	Threonine-lysine-proline-proline-arginine
TLC	Thin Layer Chromatography
TOCSY	Total correlation spectroscopy
TsOH	<i>p</i> -Toluenesulfonic acid
Tr	Tryl

Chapter 1

Introduction

1.0 Rationale

To the human eye, the internal structures and functions of the human body are invisible. However, with the technology of today, images can be created through which the medical profession can look into the body and diagnose abnormal conditions much more accurately than in the past. Radiopharmaceuticals have become a means through which much of this imaging is done. Research in this area has flourished over the last two decades as a result of the interest in radiopharmaceuticals as a diagnostic as well as a therapeutic tool.

1.1 Objectives

The main objective of this thesis was to pursue the synthesis of novel chelants for both technetium and rhenium which are used extensively in nuclear medicine. A second objective was to work in collaboration with Resolution Pharmaceuticals Inc.¹ to coordinate ⁹⁹Tc to a chelant and its bifunctional counterpart in order to study their structure and properties in solution. This thesis discusses, in detail, the synthesis of the chelant and the analytical techniques used to examine the complexes produced. In addition, a new model tripeptide chelant was prepared and the spectroscopic properties of the ⁹⁹Tc and Re complexes examined. The results of these studies are presented herein.

¹Resolution Pharmaceuticals Inc. 6850 Goreway Drive, Mississauga, Ontario, Canada

1.2 Technetium

Until the mid 1970s, technetium(V) had been widely ignored and its chemistry misinterpreted. As the needs of nuclear medicine grew, the development of the chemistry of technetium(V) grew rapidly as technetium-99m became the predominant radionuclide to be used in radiopharmaceuticals. The better known rhenium(V) chemistry is also of great interest, not only because it resembles the second-row congener technetium and easily permits non-radioactive model studies, but because ^{186}Re and ^{188}Re are attractive isotopes in their own right [1]. ^{186}Re is an ideal radionuclide for radioimmunotherapy. The 3.7 day half-life is compatible with the pharmacokinetics of tumour localization and clearance, and this isotope has a medium energy beta particle that is suitable for radioimmunotherapy. Its maximum energy is 1.07 MeV and 90% of its energy is delivered to within 2 mm of the source [2]. Frequently, $^{99\text{m}}\text{Tc}$ and ^{186}Re are called a matched pair in radiopharmaceuticals as one is ideal for imaging while the other can be used for therapeutics.

Among the various oxidation states, Tc(V) has proven to be the most successful in radiotracer design. It provides the most suitable synthesis of well-defined monomeric complexes that are sufficiently stable in aqueous solution and permit great variability in molecular structure and properties [1].

Technetium is found at a central position in the d-block elements, giving it a wide variety of oxidation states, coordination numbers and coordination geometries. For use in radiopharmaceuticals, the relevant chemical aspects of Tc(V) are concerned mostly with the oxotechnetium species. The reason for the appearance of the oxo species is the need

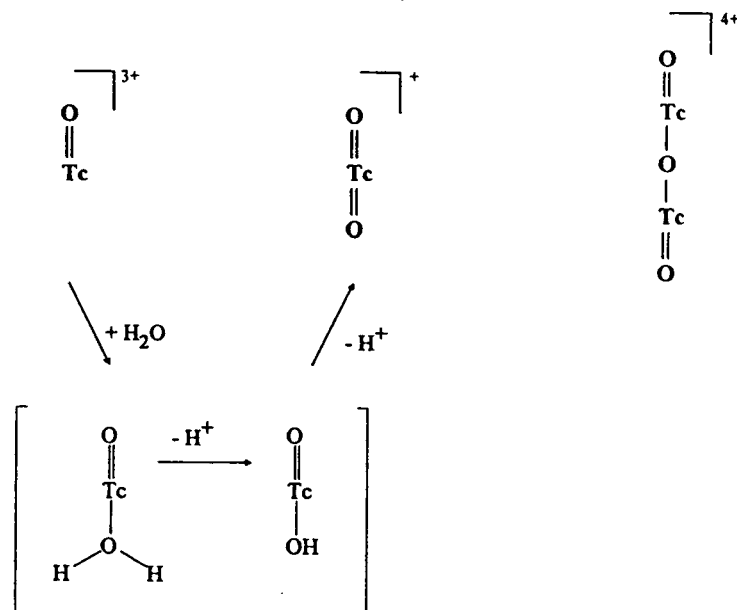


Figure 1-1 Cores of technetium

for neutralization of the high formal charge on the Tc(V). Tc(V) can contain either one or two oxo atoms depending on the ability of the coordinating ligands to donate negative charge to the metal [3,4]. Oxotechnetium species are most conveniently categorized on the basis of their cores (Fig. 1-1). The dominant structural element, especially in this thesis, is found in the monoxotechnetium, TcO^{3+} . The presence of the *oxo* ligand has a significant effect on the reactivity and structure of the derived complexes. A typical consequence of the presence of this TcO^{3+} group is the induction of a large *trans* effect, which favours the formation of a five-coordinate complex by making the *trans* position labile [1].

Furthermore, the TcO bond is a relatively short bond imposing a large steric

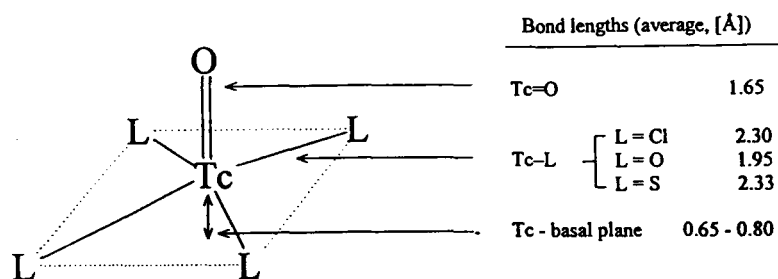


Figure 1-2 Schematic of $TcOL_4^-$ unit

requirement such that the Tc centre is usually located significantly above the plane of the four donor atoms (Fig.1-2). This can be seen in a large variety of complexes ranging from one of the simplest - a five-coordinate $TcOCl_4^-$ with four monodentate ligands - to those with more complicated ligands having two or more donor groups. A general feature of oxotechnetium complexes is that the metal lies above the equatorial plane of the four basal ligand atoms and the oxo group is at the apex. The TcO bond lengths correlate with the displacement of the Tc atom from the basal plane towards the oxygen at the apical position [5,6,7].

One of the best diagnostic tools for determining the presence of a TcO bond is its stretching vibration. This can be observed in the infrared spectrum as a sharp intense band between 890 cm^{-1} and 1020 cm^{-1} [8]. These values are related to the electronegativities of the ligands in the equatorial planes, as well as the presence and nature of a *trans* ligand [1].

1.3 ^{99m}Techneium

^{99m}Tc is a low energy gamma emitter ($E_{\max} = 140$ keV) and has a short half-life (6.02 h) which makes it favourable for use as a diagnostic radionuclide [9]. About eighty-five percent of the radiopharmaceuticals used in clinics today are labelled with ^{99m}Tc because of these ideal properties. Also advantageous is its relative ease of production and the low cost of maintaining a generator for the ^{99m}Tc [10]. The low energy gamma is enough to study organs deep within the body whilst minimizing the radiation dose to the patient. The half-life is short enough to allow enough time to perform *in vivo* measurements and also not produce contamination problems.

^{99m}Tc is a decay product of 99-molybdenum. The ⁹⁹Mo is a product of ²³⁵U fission and is produced commercially by extraction from irradiated uranium targets. The ⁹⁹MoO₄⁻ is loaded onto a shielded column and the ^{99m}Tc is “milked off” of this “moly-cow” by elution in a saline solution. Technicians can calculate the exact amount of ^{99m}Tc milked off by knowing the initial activity of the ⁹⁹Mo within the column [5, 11].

1.4 Tc Based Radiopharmaceuticals

Radiopharmaceuticals, drugs containing radionuclides, are a fundamental and essential component in nuclear medicinal studies directed towards both diagnosis and therapy. The development of ^{99m}Tc-radiopharmaceuticals offers many challenges, since this metal is not a component of any naturally occurring biological molecule. Thus, in designing ^{99m}Tc-radiopharmaceuticals, two approaches are used for the incorporation of the ^{99m}Tc into compounds that are produced as final drug products. There is first the

^{99m}Tc -essential, where the biological distribution of the molecule is based on the presence of the ^{99m}Tc and the properties it conveys to the coordination compound and second,

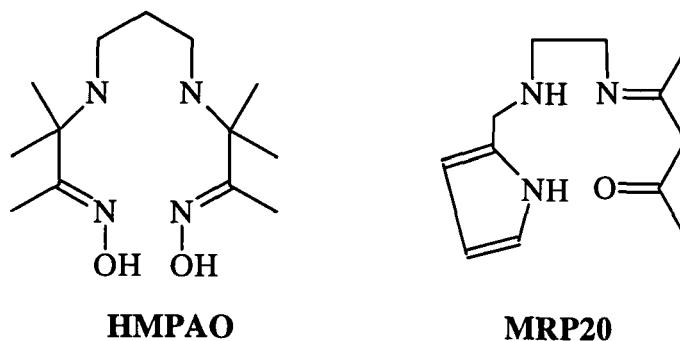


Figure 1-3 HMPAO and MRP20

bifunctional chelants where a biologically active targeting molecule is covalently bound to the ^{99m}Tc chelate, (*vide infra*) [12].

^{99m}Tc -essential drugs are currently being extensively used in nuclear medicine.

Some examples that exist include those that image the brain, heart and kidneys. In imaging the brain both the propyleneamine oxime, PnAO [13, 14] and MRP20 (N-(2(1H-pyrolylmethyl)) N'-(4-pentene-3-one-2) ethane-1,2-diamine) [15] have been successful at

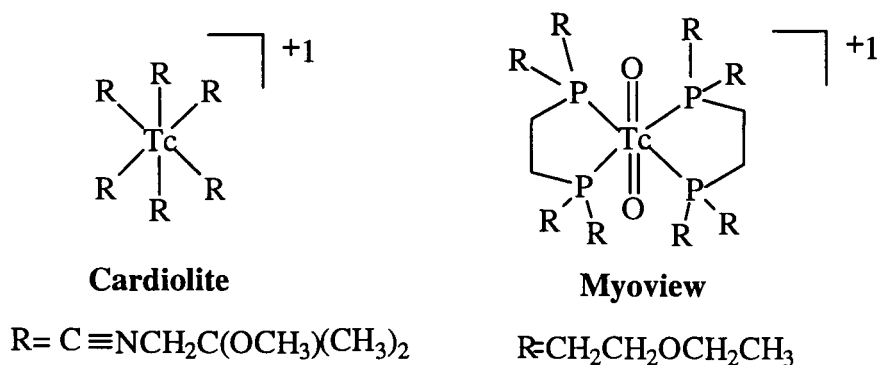


Figure 1-4 Cardiolite® and Myoview®

producing neutral lipophilic complexes that penetrate the blood brain barrier (Fig. 1-3).

All of the ^{99m}Tc -complexes currently in use for myocardial imaging have a +1 charge associated with them. One of the most important imaging agents in use is Cardiolite® [16, 17, 18]. This Tc(I) complex was the first myocardial-perfusion agent to receive worldwide approval and is the most widely used (Fig. 1-4). Another well known heart imaging agent is Myoview®. It is a Tc(V) complex that exhibits high myocardial uptake and retention in the heart [19, 20] (Fig. 1-4).

Kidney function is currently being looked at with two different types of imaging agents, ^{99m}Tc -DTPA and ^{99m}Tc -MAG₃. These agents are used to monitor passage into and through the renal system, and to assess the glomerular filtration and tubular secretion functions. The oxidation states of the ^{99m}Tc -DTPA are suspected to be +4 or +5 [21, 22] although the real chemistry is unknown at this moment. The MAG₃ is an amino acid based chelant and will be discussed in more detail in Chapter 3.

1.5 Tc Based Bifunctional Chelants

A bifunctional chelant is a metal-binding ligand which possesses a reactive functional group that can be used to covalently link the ligand or its chelate to a targeting molecule. When using bifunctional chelants, a new molecule is produced that resembles a ball and chain assembly. The ball is the radionuclide that is to be used for either imaging or therapy. The chain is the linking portion that contains both a linker group and the

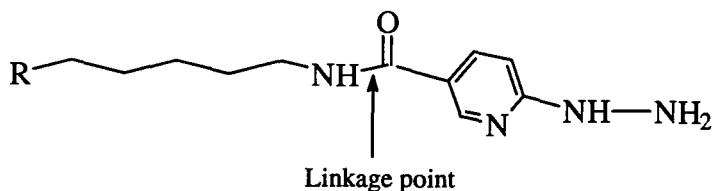


Figure 1-5 HYNIC Bifunctional Chelant

targeting molecule which contains the functionality of the radiopharmaceutical [23]. One particularly good example of this is the hydrazino nicotinamide (HYNIC) bifunctional chelant (Fig. 1-5). While the structure of the complex from HYNIC derivatized proteins remains uncertain, it provides for an easy and effective way to derivatize peptides (eg. by an active ester coupling) and allow for technetium attachment. It is likely that the hydrazine forms a multiple bond ligand to the technetium and it appears to be quite robust *in vivo*.

The use of bifunctional chelants has been of great interest to our research group in the past. Nitrogen and sulfur are good ligands for Tc(V) and chelants having two nitrogens and two sulfurs (N_2S_2) or three nitrogens and one sulfur (N_3S) have proven to give rise to very stable Tc(V) complexes [1]. In the pursuit of site specific radiopharmaceuticals, work done by the group has resulted in the preparation of a potential heart imaging agent by the derivatization of the cardiac glycosides digitoxin [25] and digitoxigenin [26] (Fig. 1-6). Both of these molecules bind to ATPase which is abundantly found in heart muscle. Other derivatizable steroids and DNA reactive drugs currently being studied include estradiol and chlorambucil [27].

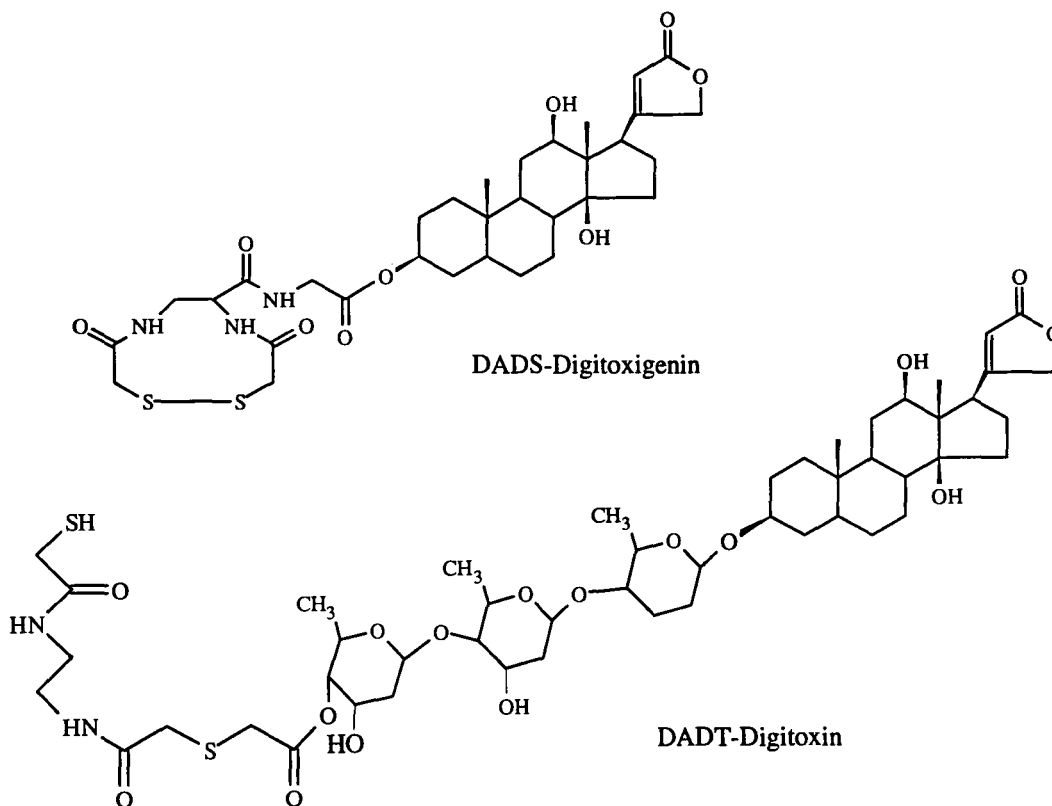


Figure 1-6 Digitoxin and digitoxigenin chelant derivatives

The latest attempts at producing novel ^{99m}Tc -radiopharmaceuticals involve the use of amino acids. Part of this work presents the synthesis of a Tc coordinating chelant designed almost exclusively with amino acids. This provides an excellent opportunity for derivatization as the end group on either side of the chelant can be used for attachment of a functional moiety. In other words, the chelant becomes an excellent ball to which an endless variety of amino acid based chains or other species can be attached [28].

This thesis covers the synthesis of a novel amino acid based technetium chelant of the N_2S_2 type. It also describes an investigation of the coordination properties of another amino acid based chelant of the N_3S type and its subsequent bifunctional chelant as they are bound to technetium.

1.6 Spectroscopic and Spectrometric Analytical Methods

Various types of analytical methods were employed to examine the compounds synthesized in this thesis. Nuclear Magnetic Resonance (NMR) is the technique primarily employed, as the spectrum is dependent on the molecular structure and conformation of the molecule. Electrons shield the nucleus from the effects of the applied magnetic field, and the resonance frequency, or chemical shift, observed for a given nucleus is a reflection of the overall electronic environment of the nucleus. Consequently, the observed chemical shifts in an NMR spectrum are dictated by the three-dimensional structure of the molecule. Additional information about molecular structure can be obtained from observation of scalar coupling (*J* coupling) between nuclei. The magnitude of this through-bond interaction is dependent on both the bonding network, connecting the *J*-coupled nuclei and the molecular geometry [29].

Additional analysis was achieved through the use of two dimensional (2D) NMR techniques such as Correlation Spectroscopy (COSY) that relates *J*-coupled proton signals; Total Correlation (TOCSY) that relates specific spin systems; Heteronuclear Single Quantum Coherence (HSQC) that relates carbon signals to their directly bonded protons; and Heteronuclear Multiple Bonded Coherence (HMBC) that relates three and four bond coupling systems.

Also extremely useful was the use of Electrospray Mass Spectroscopy (ESMS). This is a procedure in which a solution of the sample is sprayed, at atmospheric pressure, through a several-kilovolt potential difference toward the differentially pumped entrance

to a mass spectrometer. The resulting droplets are electrostatically charged and as the solvent evaporates, electrostatic repulsion produces smaller and smaller droplets, until the macromolecule is expelled “saturated” with charge. This ion is then detected in a quadrupole as presented in detail by McLafferty and Turecek [30]. Both negative and positive ESMS experiments can be carried out.

Chapter 2

Amino Acid Based Chelants

2.0 Introduction

The major thrust of this thesis is the investigation of amino acid based chelants and their use in radiopharmaceuticals. This approach has its historical roots in the successful use of *diamino* dithiols (DADT) and *diamido* dithiols (DADS) ligands as imaging agents. The tetradentate DADT (Fig. 2-1A) chelants form neutral, lipid-soluble technetium complexes [31]. Their neutrality stems from the ability of one amino group to deprotonate on complexation, along with both thiol groups. This action allows these types of chelates to be used in brain imaging as they are able to diffuse across the blood brain barrier (BBB) [7]. N,N'-1,2-Ethylene-bis-L-cysteine diethyl ester, ECD, is an excellent example of one such radiopharmaceutical. It demonstrates remarkable brain retention because of enzymatic cleavage of its ester groups to give ionic products that become trapped in the brain. (Fig. 2-1B) [32].

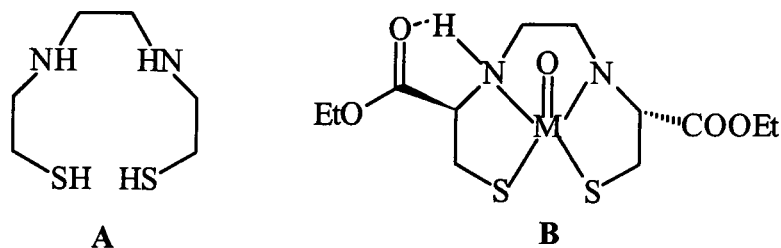


Figure 2-1 A) Diamino Dithiol ligand B) ECD

The presence of amino acids in the backbone of the ECD chelant has led to further investigations of another subclass of the DADS chelants noted above. The inclusion of a second amide group (Fig. 2-2A) results in the formation of very stable oxotechnetium anions. Although previously prepared with ethylene diamines and mercaptoethanoic acid, these ligands can have their amide connections made through the use of amino acids. The use of these types of synthons provides a wide degree of flexibility in properties and allows for the problem of solubility to be addressed. Knight *et al.*[33] used a hexapeptide lysine-cysteine-threonine-cysteine-cysteine-alanine (KCTCCA), which was known to bind to thrombi, as a basis for a technetium binding imaging agent. It was postulated that the presence of an interior DADS chelant, with the tripeptide cysteine-threonine-cysteine, would induce binding to technetium in a manner superior to that of the standard, nonspecific monoclonal antibodies method, providing a highly specialized radiopharmaceutical (Fig. 2-2B). Initial indications have provided images with ^{99m}Tc but the receptor binding has not been as specific as predicted. Some design improvement would be necessary before it can be used as a radiopharmaceutical.

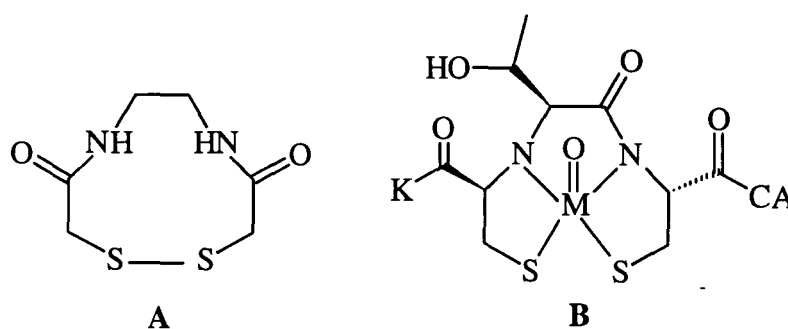
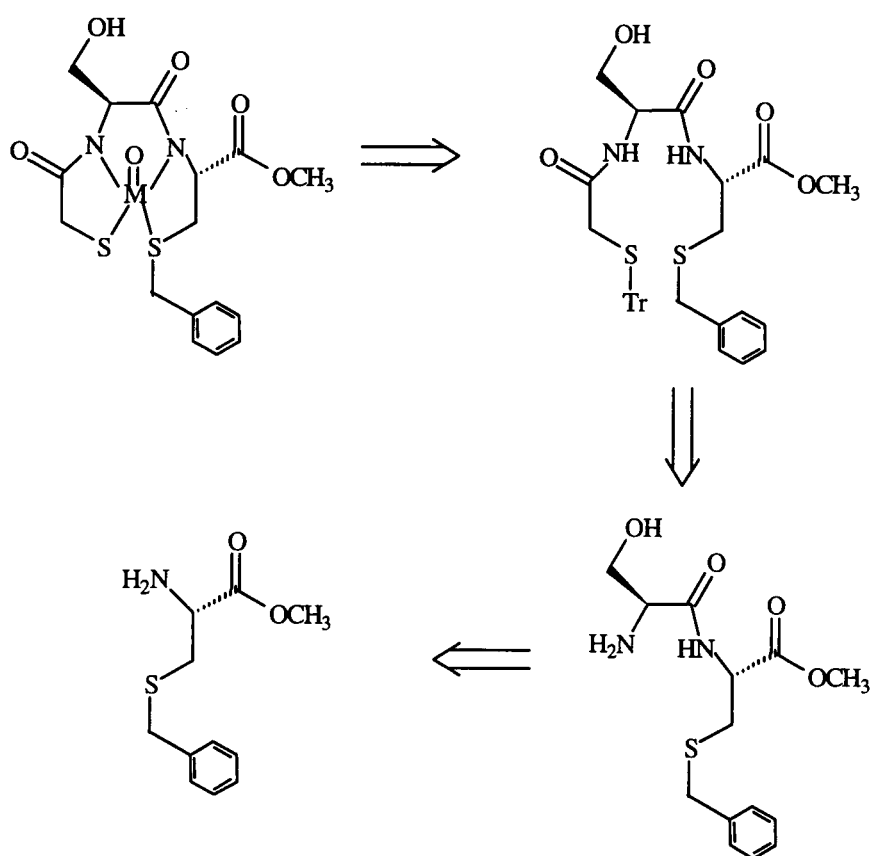


Figure 2-2 A) Diamido Dithiol B) Cys-Thr-Cys

This new impetus in the design of chelants using amino acids is looked at in the synthesis of a mercaptoacetamido-serine-cysteine DADS type of ligand. The use of serine as the “X” amino acid in a mercaptoacetamido-serine-cysteine (mer-X-cys) arrangement is intended to provide water solubility, an important aspect of flexibility in chelant design. The synthesis of mer-ser-cys and formation of its technetium and rhenium complexes were studied and are described in this chapter.

2.1 Retrosynthesis

The retrosynthesis of mer-ser-cys metal complexes with rhenium and technetium is shown in Fig. 2-3. The first retrosynthetic step in the process of chelate formation was the coordination of the technetium or rhenium. This was to be accomplished by activating the ligand through the removal of the trityl S-protecting group and it was anticipated that upon coordination to the metal, the S-benzyl thioether present on the cysteine, would cleave, and thereby produce a DADS-like coordination complex. The approach that was taken in the synthesis of the chelant itself involved the coupling of a dipeptide to an activated mercaptoacetic acid unit. The dipeptide consisted of the N-t-Boc protected L-serine and S-benzyl-L-cysteine and it was available from the condensation of N-protected L-serine and S-benzyl-L-cysteine.



M= Tc or Re, Tr= Trityl

Figure 2-3 Retrosynthesis of Mer-Ser-Cys

2.2 Synthesis of Mer-Ser-Cys

The synthesis of protected mer-ser-cys **6** is outlined in Fig. 2-4. The first step in the synthesis was protection of the thiol group on the mercaptoacetic acid. The protection of the sulfhydryl group was necessary to avoid side reactions in subsequent

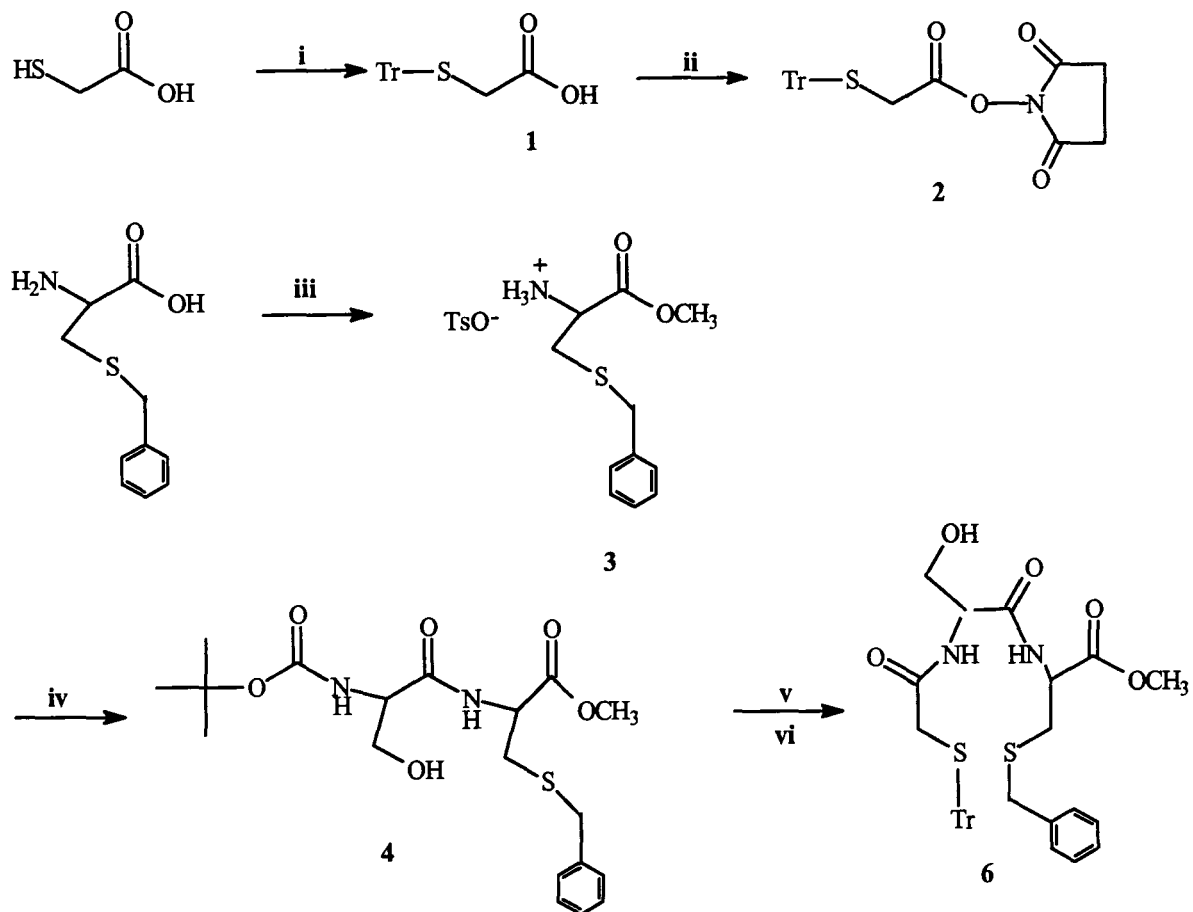


Figure 2-4 Synthesis of Mer-ser-cys

i) TrOH , $\text{BF}_3\text{-Et}_2\text{O}$, AcOH , 70°C ii) *N*-hydroxysuccinimide, EDAC, MeCN iii) *p*- TsOH , MeOH, Δ iv) **3**, *N*-*t*-Boc-L-serine, EDAC v) **4**, TFA, Et_3SiH vi) **2**, **5** CH_2Cl_2 , DIPEA

steps, since SH is a very good nucleophile. This was achieved in a standard method by Brenner *et.al* [34] in which borontrifluoride etherate ($\text{BF}_3\text{-OEt}$) was used as a Lewis acid catalyst (Fig. 2-5). The slow addition of $\text{BF}_3\text{-OEt}$ allows it to complex to

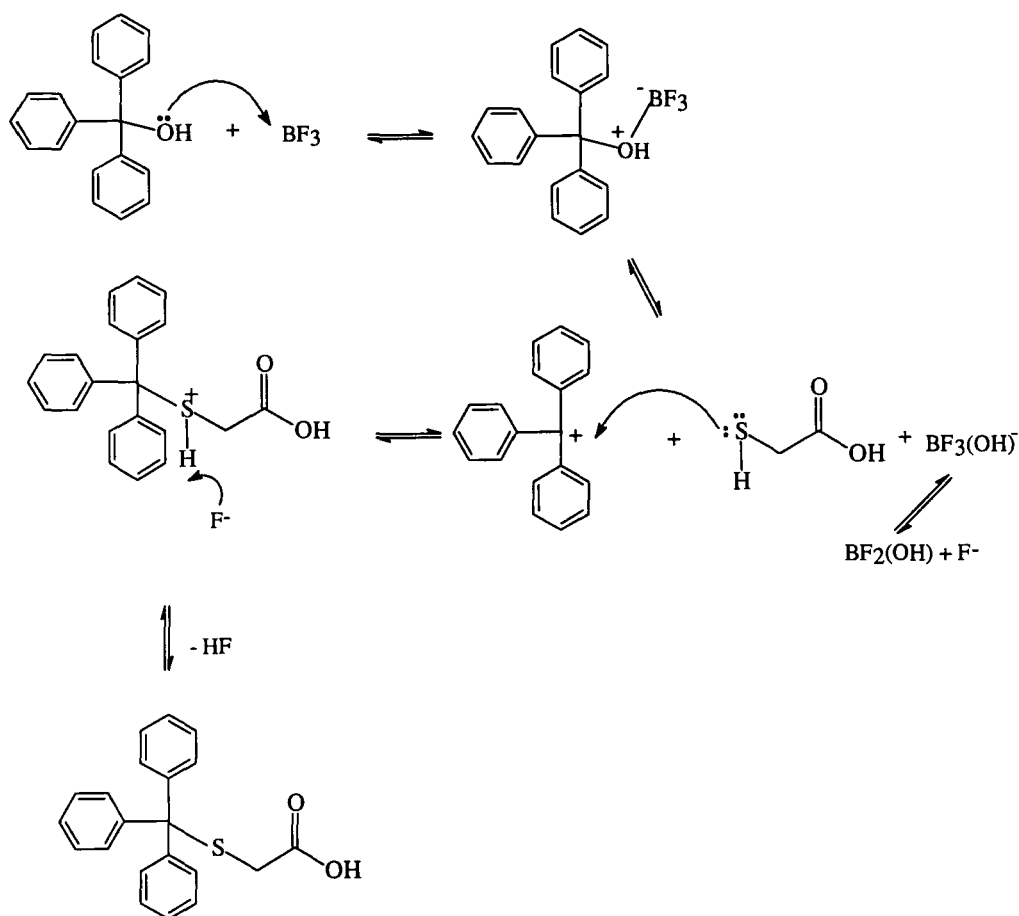


Figure 2-5 Borontrifluoride etherate mechanism

triphenylmethanol and promote the formation of a carbocation which the mercaptoacetic acid easily trapped to form the initial mercapto-protected synthon **2** [35, 36]. The poor yield (31%) resulted from solubility problems and difficulty in maintaining the reaction temperature. These factors were overcome by J. F. Valliant [27] who used dichloromethane as a cosolvent and completed the reaction at room temperature. Under

these conditions, the yields improved dramatically (80-90 %).

To carry out the final condensation of the dipeptide **4** to the S-tritylthioglycolic acid, the initial S-trityl synthon required activation at the carboxyl group. This was achieved by attaching N-hydroxysuccinimide to the carboxyl of **2** using 1-(3-dimethylaminopropyl)-3-ethylcarbodiimide (EDAC) as a coupling agent. Previously, amides were synthesized in the presence of dialkyl carbodiimides as aids to coupling. The use of such coupling agents alone, with unactivated carboxylic acids, often resulted in rearrangement problems and purification problems because of the co-formation of alkyl ureas. In the present method, the synthon was activated by formation and isolation in the crystalline form of the N-hydroxysuccinimide derivative **2**. The intermediate **2** was prepared by condensation of N-hydroxysuccinimide and S-trityl-thioglycolic acid in the presence of EDAC, a water soluble carbodiimide, the urea of which is easily removed by extraction, was formed. This then allowed for the final coupling in the last step to be done without a carbodiimide, thus avoiding difficult rearrangement and separation problems that would have existed had it been present. The succinimide activated the carboxyl group by increasing its electrophilicity at the carbonyl carbon.

As the mechanism in Fig. 2-6 shows, the carboxylic acid reacts quickly on the electrophilic carbon of the EDAC, via a 6 membered transition state which leads to the formation of the imino-anhydride **7**. The imino-anhydride is a reactive acylating agent, the driving force being the elimination of a urea unit. Here, the hydroxy of the succinimide serves as the nucleophile and produces compound **2** along with the urea [37]. The use of EDAC over the standard dicyclohexylcarbodiimide (DCC), improved the yields

of the reaction mainly because of the ease with which the urea **8** could be removed from the ester **2**. By using acetonitrile as a solvent, both the EDAC and the urea **8** were found to be soluble while the product was not. This simplification provided excellent yields and

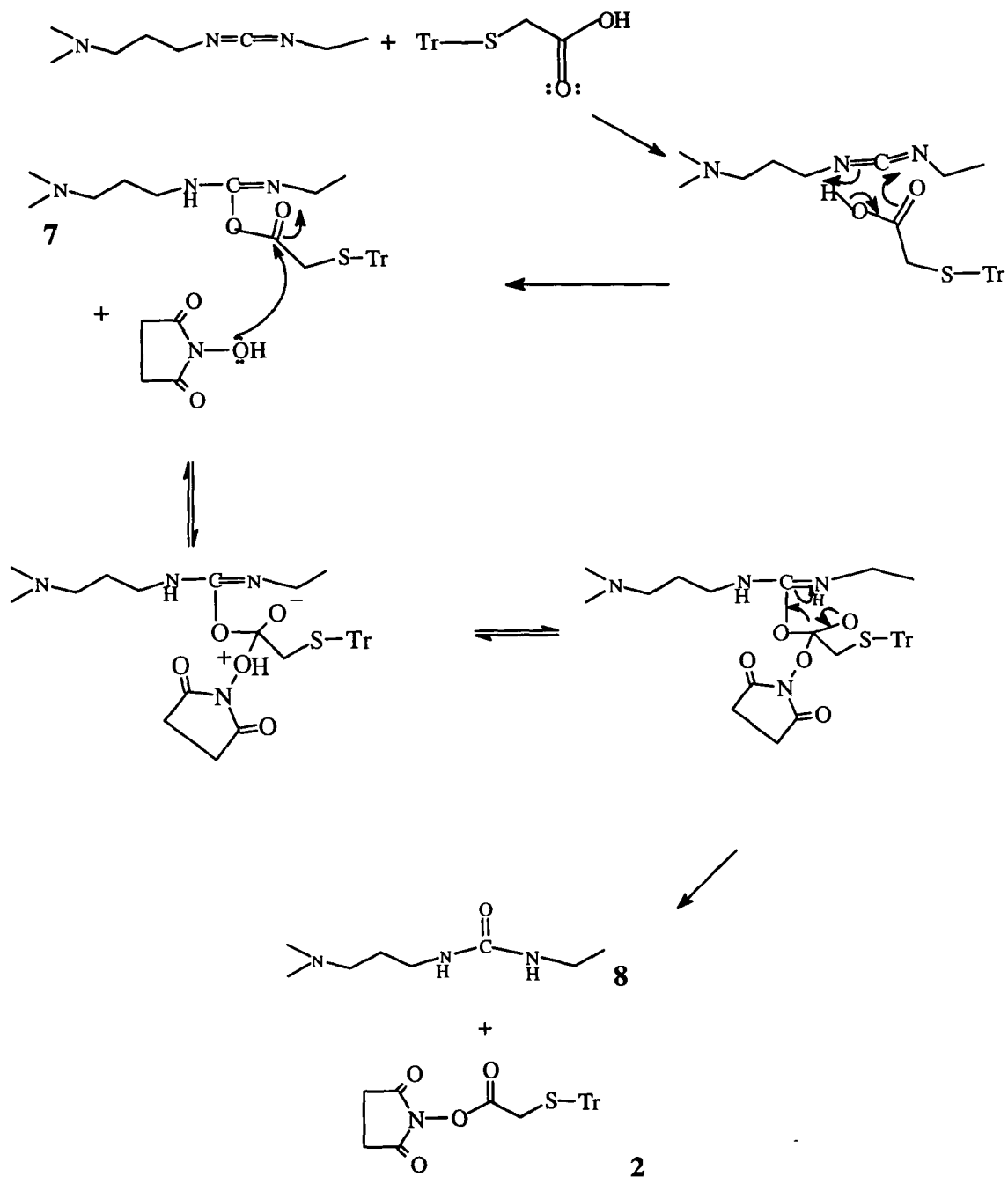


Figure 2-6 EDAC Coupling of *S*-tritylthioglycolic acid to *N*-hydroxysuccinimide

the purity can be seen in the ^1H NMR spectrum of the crude precipitate obtained directly by filtration of the reaction mixture (Fig. 2-7). The clean singlets at 3.118 ppm and 2.696 ppm for the acyl methylene and succinimido protons, respectively, show the excellent purity of the product.

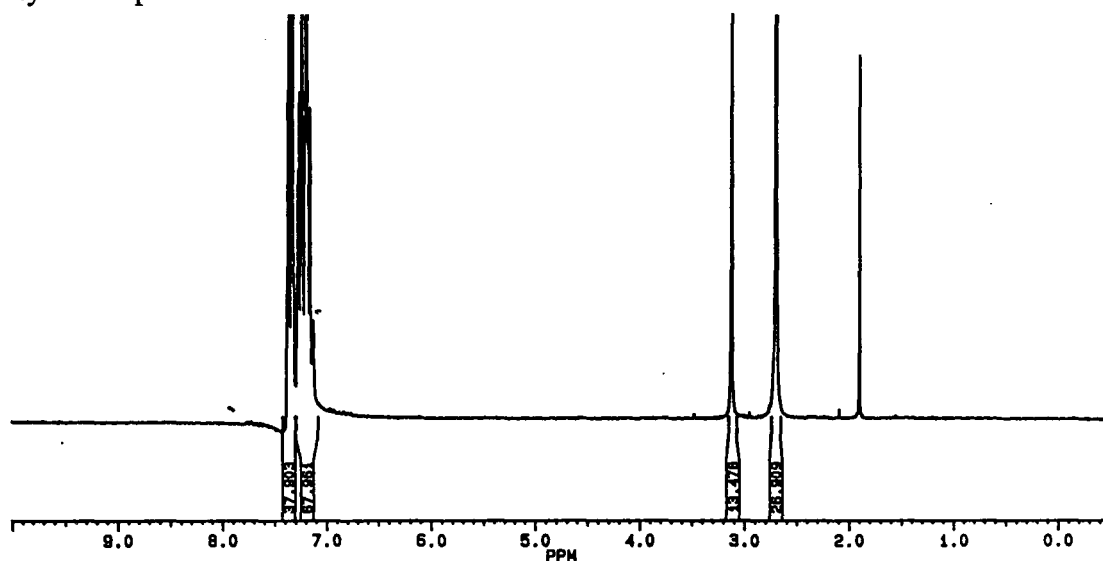


Figure 2-7 ^1H 200 NMR MHz spectrum of *N*-hydroxysuccinimido-(triphenylmethylthio)ethanoate in CDCl_3

The conversion of the *S*-benzyl-*L*-cysteine to its methyl ester **4** was accomplished using a slightly modified Fischer esterification. In previous work [38], HCl was used in the activation of the carbonyl group which then led to the nucleophilic attack by the alcohol. However because of the volatility of HCl and the long reaction times required, much catalyst was lost and additional side reactions took place. The use of the non-volatile *p*-toluenesulfonic acid kept the yields high and improved purity. The mechanism is shown in Fig. 2-8. The presence of the sulfonic salt allowed for a simplified purification procedure as the product precipitated out of solution in diethyl ether. The ^1H NMR spectrum of **4** showed a singlet at 3.652 ppm for the methyl ester protons and the ^{13}C

NMR spectrum showed a carbonyl carbon downfield from the original starting material.

The coupling of the cysteine to the serine, the next step in the tripeptide synthesis, was

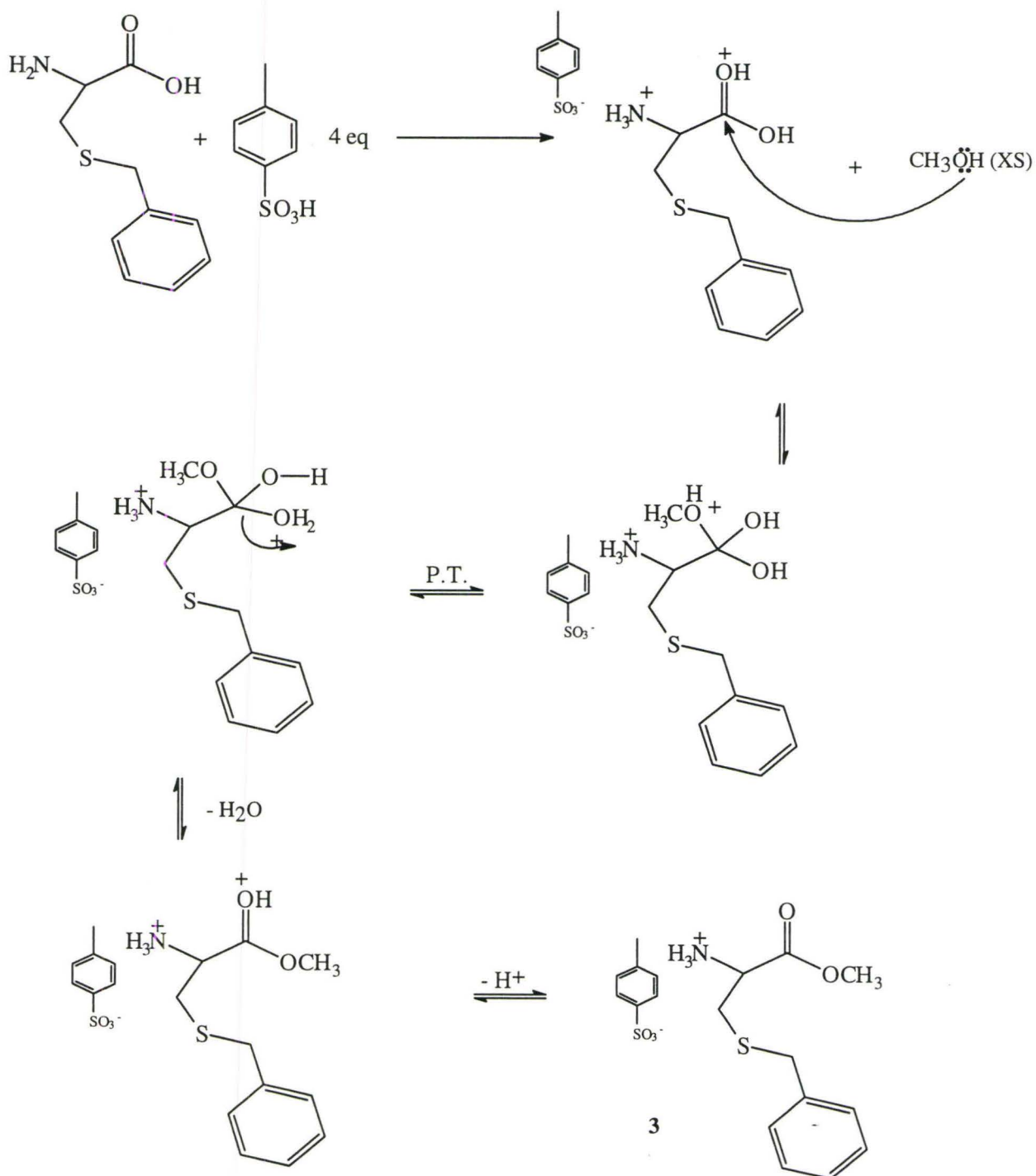


Figure 2-8 Mechanism of *p*-TsOH catalyzed esterification of *S*-benzyl cysteine

carried out after the cysteine was desalinated. The use of the organic sulfonic acid allowed for the dissolution of the ester salt, **3**, into organic solvents and facilitated the isolation of the free amine of the methyl ester with a 10% sodium carbonate extraction. The coupling was carried out in the presence of EDAC which gave a water soluble urea product. Initial synthetic attempts had been made with dicyclohexylcarbodiimide (DCC) but the yields had been poor and it was postulated that the problem was in purification, as noted above for the purification of the N-hydroxysuccinimido ester **2**. Thus, when EDAC was substituted, because of the solubility of both EDAC and the urea by-product in water, an extraction procedure led to even better yields of the dipeptide **4**.

To prevent the formation of an oily product, a solution of the dipeptide in dichloromethane (DCM) was extracted with water to remove the carbodiimide and urea that had been produced. The solvent was removed from the DCM fraction and replaced with anhydrous diethyl ether. Early preparations were carried out without this further ether extraction and had failed to produce **4** in a crystalline form. The aqueous extraction was then repeated and the ether dried with sodium sulfate. This was stored overnight at -4°C and gave the crystalline dipeptide **4** in 74% yield. The dipeptide was characterized by ^1H and ^{13}C NMR. The α -proton of the cysteine was the most evident as it was a part of an ABX system with the H_{α} at 4.75 ppm, a lower field than for the H_{α} of the cysteine itself at 4.69 ppm. The serine α -proton at 4.16 ppm is at a higher field compared to 4.50 ppm for serine itself.

The introduction of carbodiimides as coupling agents was a major event in peptide

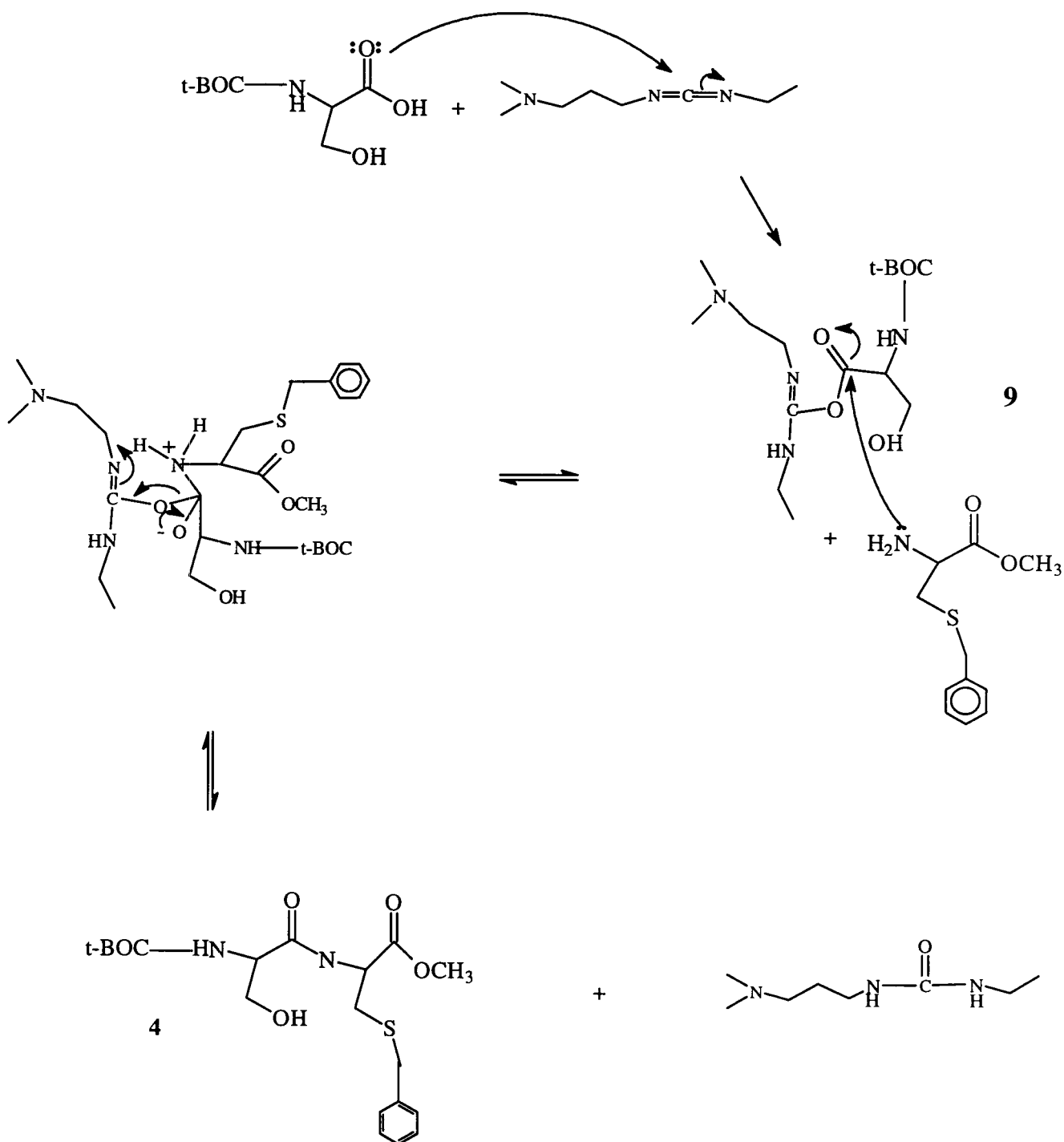


Figure 2-9 Mechanism of EDAC coupling of *N*-*t*-Boc-L-serine and *S*-benzyl-L-cysteine methyl ester

synthesis. The novel feature was that these reagents could be added to the mixture of the carboxyl component and the amine component. This then allowed for activation and coupling to proceed concurrently. In general, amines do not react as fast as carboxylic acids with carbodiimides. Once the carboxyl oxygen reacts first, it activates the carbonyl carbon. As can be seen in the mechanism, Fig. 2-9, the O-acylisourea produced has a N=C group that provides a powerful activation by way of urea elimination which, as noted above, is the major driving force for the coupling reaction. If it is assumed that the O-acylisourea **9** has some basic character, then a general, cyclic base catalysis can be invoked as the explanation for the surprisingly high reactivity in the aminolysis [39].

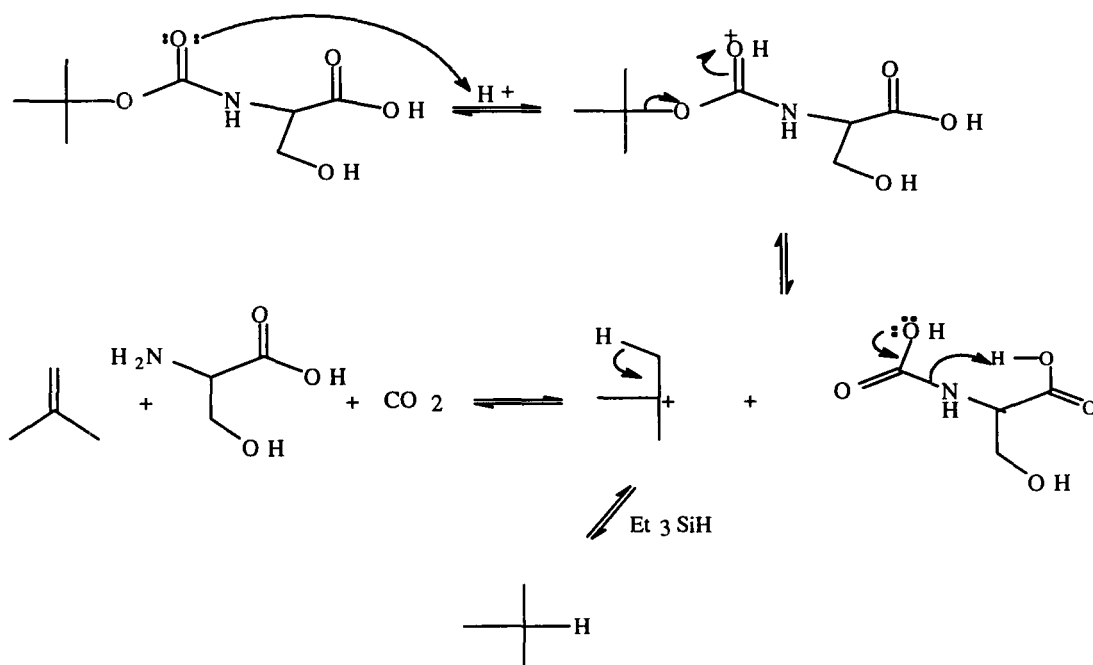


Figure 2-10 Mechanism of TFA deprotection of *N*-*t*-Boc-*L*-serine-*S*-benzyl-*L*-cysteine methyl ester

The final step in the synthesis of the tripeptide was the condensation of the N-hydroxy succinimido ester **2** to the dipeptide **4**. In order to achieve this, the serine portion of the amino acid had to be deprotected. The t-butoxycarbonyl (t-BOC) group was removed using trifluoroacetic acid (TFA) and triethylsilane (Et_3SiH) in CH_2Cl_2 . It is considered an “orthogonal” protecting group because it can be removed without affecting other protecting groups such as the methyl ester on the cysteine residue. Once the TFA was added, the reaction occurred quickly. As shown in Fig. 2-10, it has been proposed that the initial step involves the protonation of the carbamate oxygen followed by the formation of carbamic acid and a t-butyl cation. This cation subsequently undergoes either an elimination to form isobutene or reacts with a nucleophile. The carbamic acid is unstable and decomposes to form carbon dioxide and the free amine. The presence of the Et_3SiH enhances the reaction by acting as a hydride donor (nucleophile) to the t-butyl cation directly after its formation, preventing other undesirable side reactions [40]. The final product of this deprotection was in the form of a trifluoroacetate salt contaminated with excess TFA. This complicated matters for the next coupling step as it kept the amino group protonated and decreased its overall nucleophilicity. To overcome this, the deprotected product was taken up in DCM several times and the solvent evaporated under a stream of nitrogen while stirring. In this way, all but a small trace of TFA was removed.

The final coupling step of deprotected **4** with **2** was carried out in the presence of an excess of diisopropylethylamine (DIPEA) to facilitate the deprotonation of the free amine during the condensation. The reaction was monitored using thin layer

chromatography (TLC) and required stirring for two days at room temperature for completion. A moderate yield (44%) of protected tripeptide **6** was obtained after radial chromatography on silica gel.

2.3 NMR Spectroscopy of Mer-Ser-Cys

As a preliminary to the complete understanding of metal chelation by this ligand, detailed NMR spectroscopy was carried out on the ligand before complexation. The experiments included both proton and carbon-13 spectroscopy as well as two dimensional techniques known as ^1H - ^1H correlation spectroscopy (COSY) and heteronuclear single quantum coherence spectroscopy (HSQC). The data is shown in Table 2-1.

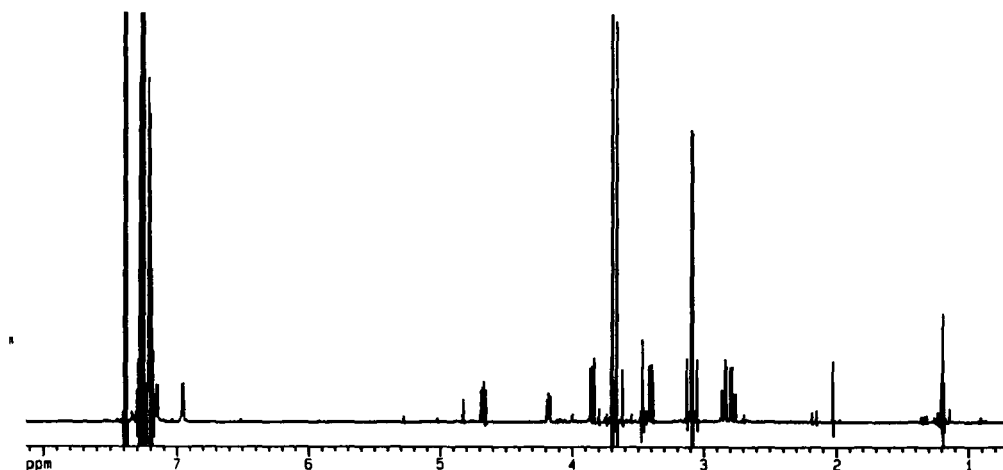


*Figure 2-11 500 MHz ^1H NMR Spectrum of **6** in CDCl_3*

The ^1H NMR spectrum is shown in Fig. 2-11. The multiplets at 7.386 and 7.241 ppm correspond to the aryl protons of the triphenylmethyl protecting group and the S-benzyl thioether. The doublet that was seen at 7.149 ppm is associated with the amide proton for the cysteine residue and the doublet at 6.955 ppm for the amide proton of the

serine residue. These amide protons were detected because dry deuteriochloroform was used as a solvent where the lack of any exchangeable protons in the deuterated solvent prevents any exchange from taking place. This would not have been the case had a protic solvent such as deuteromethanol been used. The multiplets at 4.677 ppm and 4.180 ppm arise from the α protons for cysteine and serine respectively. These multiplets are the X parts of ABX spin systems with the AB portions visible at 3.842 ppm and 3.401 ppm for serine and 2.848 ppm and 2.777 ppm for the cysteine. The remaining singlets were assigned to the methyl ester at 3.697 ppm, the benzyl-CH₂ at 3.658 ppm and the mercapto-CH₂ at 3.088 ppm.

The α proton assignments were tentatively made through standard NMR assignments for amino acids as found in the work by Wurthrich [41]. Once these protons were assigned, 2D COSY NMR as well as coupling constants were used to identify the β protons. Likewise it was possible to assign both amide protons using the same COSY correlation.

The COSY experiment is used to provide a map of the ¹H-¹H J-coupling network in a molecule. The basic pulse sequence starts with a relaxation delay during the preparation period to allow for the spin system to come into equilibrium. The first 90° pulse causes each spin to precess at its characteristic frequency, defined by its chemical shift, during the evolution period. This effectively labels the spin according to its initial precession frequency ω_1 . The second 90° pulse, the mixing pulse, causes an exchange of magnetization between J-coupled spins. The final precession frequency ω_2 is observed during the detection period. This magnetization exchange is often referred to as .

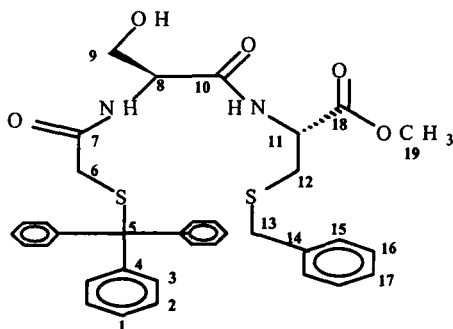


Table 2-1 Proton and Carbon-13 NMR Spectral Assignments of Mer-Ser-Cys

δ (ppm)	^1H Assignment		^{13}C Assignment	
	Assignment	J (Hz)	δ (ppm)	Assignment
7.386	aryl		170.929	18
7.241	aryl		170.407	10
7.149	NH (cys)	$^3J=7.8$	169.102	7
6.955	NH (ser)	$^3J=6.8$	143.901	4
4.677	11	$^3J_{\text{AX}}=4.9$	137.437	14
		$^3J_{\text{BX}}=6.8$	129.519	3
4.180	8	$^3J_{\text{AX}}=3.6$	128.891	15
		$^3J_{\text{BX}}=5.8$	128.631	16
3.842	9A	$^3J_{\text{AX}}=3.4$	128.132	2
		$^2J_{\text{AB}}=11.4$	127.324	17
3.697	19		127.035	1
3.658	13		67.819	5
3.401	9B	$^3J_{\text{BX}}=5.8$	62.459	9
		$^2J_{\text{AB}}=11.5$	54.222	8
3.088	6	$^2J_{\text{AB}}=16.0$	52.747	19
2.848	12A	$^3J_{\text{AX}}=5.0$	51.766	11
		$^2J_{\text{AB}}=14.0$	36.462	13
2.777	12B	$^3J_{\text{BX}}=6.8$	35.976	6
		$^2J_{\text{AB}}=13.9$	32.883	12

coherence transfer since the exchange involves in-phase, transverse magnetizations. For those spins that do exchange magnetizations due to J coupling, the final frequency is different from their initial one and this exchange gives rise to off diagonal signals or cross-correlation peaks. As a result, peaks that correspond to J-coupled protons are connected by symmetrical off diagonal peaks allowing for the entire J-coupled network to be traced [42].

With the protons assigned, the HSQC experiment, which correlates proton signals to their corresponding carbons, could be used to assign the ^{13}C spectrum. It is interesting to note that the α carbon for the cysteine was found at 51.77 ppm and the serine α carbon at 54.22 ppm. The methyl ester carbon could be identified at 52.75 ppm by correlating it to the singlet found at 3.697 ppm on the ^1H spectrum. The benzyl CH_2 was also found at 36.46 ppm and corresponded to the singlet at 3.658 ppm as was the methylene singlet at 3.088 ppm which corresponded to the carbon at 35.98 ppm. The serine and cysteine β carbons showed a large difference in chemical shifts with values of 64.46 ppm and 32.883 ppm respectively which can be rationalized by the difference in electronegativities of the neighbouring oxygen or sulfur. Oxygen is more electronegative and therefore has a larger deshielding effect resulting in the downfield shift of the carbon.

2.4 Reaction of Mer-L-Ser-S-Bn-L-Cys-OMe with $\text{ReOCl}_3(\text{PPh}_3)_2$

The tripeptide **6** was deprotected using TFA and Et_3SiH (Fig. 2-12). The mechanism is the same as mentioned above except that DCM was not used. This caused the triphenylmethane to precipitate out from the solution and therefore be removed by

filtration. The free thiol, **10**, was then produced via evaporation of the TFA using stirring and a stream of nitrogen as stated above; it was necessary to remove the TFA completely as the complexation step with rhenium was pH sensitive.

The thiol **10** was then reacted with a commonly used rhenium starting material,

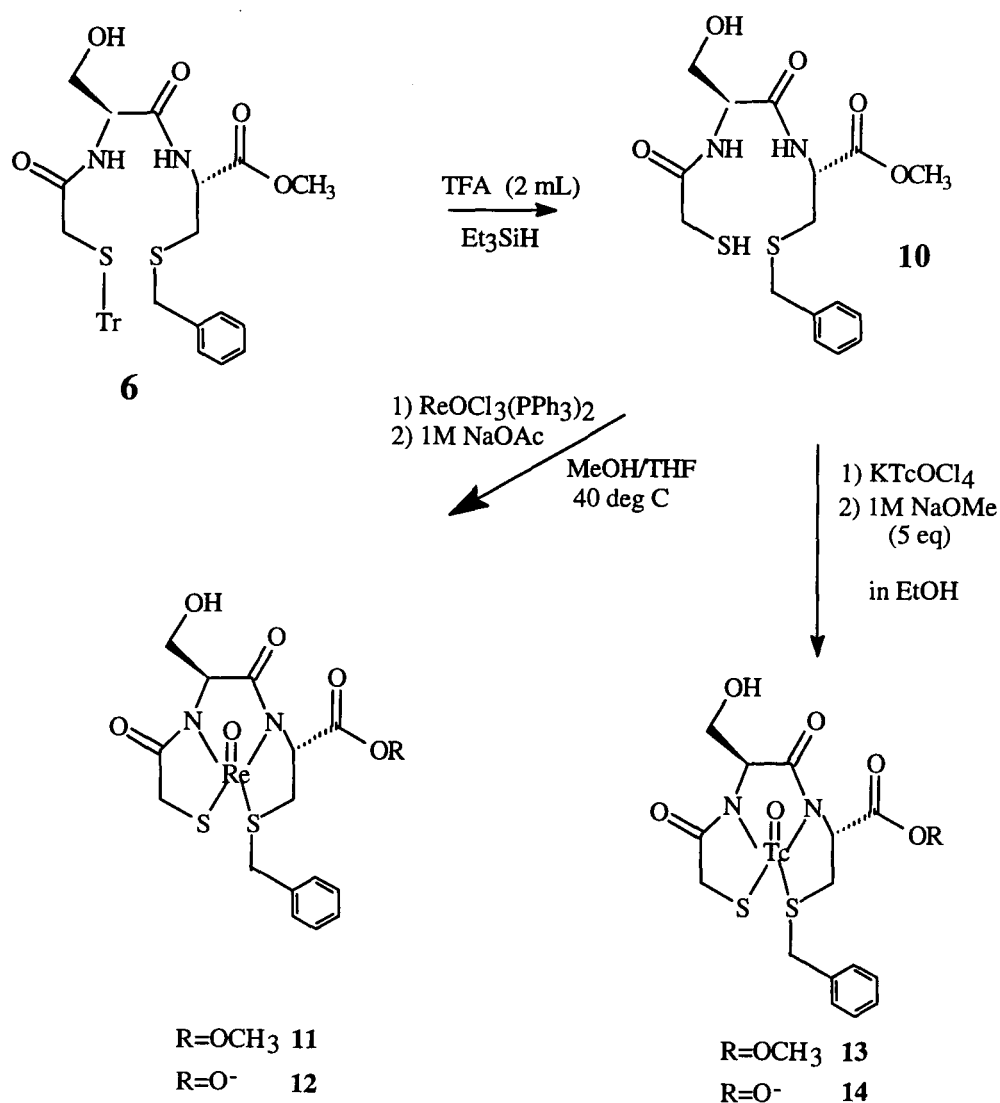


Figure 2-12 Synthesis of Mer-Ser-Cys Metal Complexes

$\text{ReOCl}_3(\text{PPh}_3)_2$ in MeOH/THF, to form the peptide-chelate **12**. The rhenium was in a +5 oxidation state, making this a substitution type of chelation reaction. The $\text{ReOCl}_3(\text{PPh}_3)_2$ came as a yellowish-green powder, indicative of the presence of *cis* and *trans* isomers [43]. The presence of the two isomers complicated the substitution reaction because one isomer was more soluble than the other. The solution to this problem was found by heating the reaction mixture at 40°C for the duration of the reaction. Sodium acetate was added at the beginning of the reaction as a buffer to maintain the pH because two amide protons were lost during the chelation.

After 4 hours at reflux, the initial yellow green solution had turned orange-red and a TLC in 5% $\text{CH}_3\text{OH}/\text{CH}_2\text{Cl}_2$ showed a coloured spot at $R_f=0.0$ which indicated chelation of the rhenium had occurred. Further evidence came in the form of electrospray mass spectroscopy (ESMS) which, in the negative ion mode, showed ions of masses of 569 and 571. These corresponded to the complex with the loss of the methyl group of the methyl ester. The ratio of the two masses was indicative of the ratio of the natural abundances of the 186/188 rhenium isotopes, providing further evidence that the metal had been complexed. The de-esterification was not unexpected as under basic conditions, such as acetate, and with refluxing, esters hydrolyse. It was possible that the metal could have been acting as a Lewis acid to help catalyse this normally slow process.

A ^1H NMR spectrum of this reaction mixture produced a complex set of signals with excessive interferences from both the acetate and triphenylphosphine peaks. Several attempts were made to clean-up the mixture by silica gel chromatography and triphenylphosphine recrystallization but these proved unsuccessful. Reverse phase High

Pressure Liquid Chromatography (HPLC) was successful in isolating the desired compound and Fig. 2-13 shows a typical chromatogram in acetonitrile and water. The

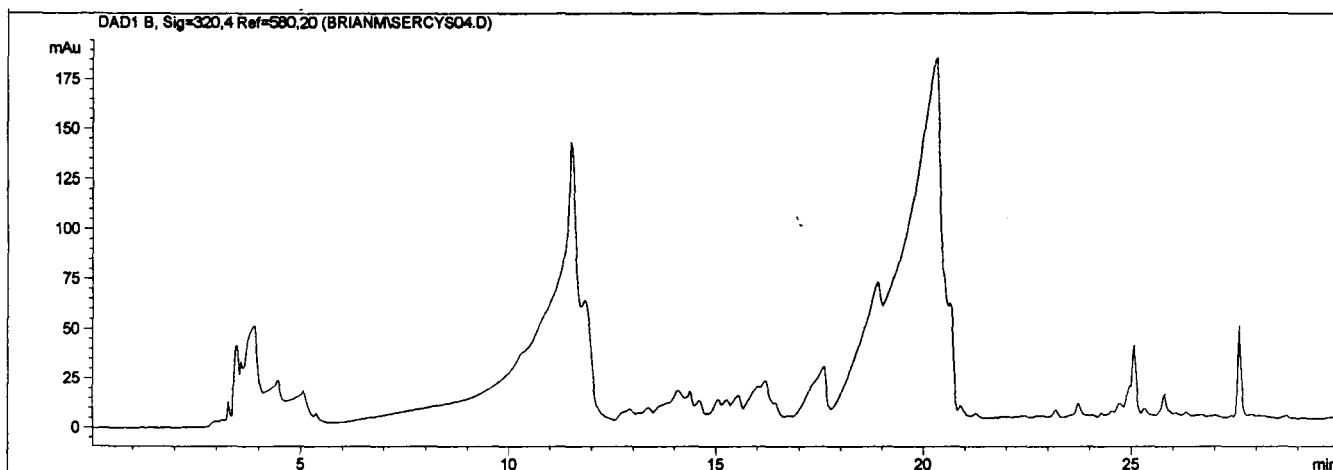


Figure 2-13 HPLC Chromatogram of 12 ($\lambda_{obs} = 320 \text{ nm}$)

largest peak was isolated and examined spectroscopically. An ESMS was run for all fractions collected and showed a clean 569/571 negative ion for several of them. These

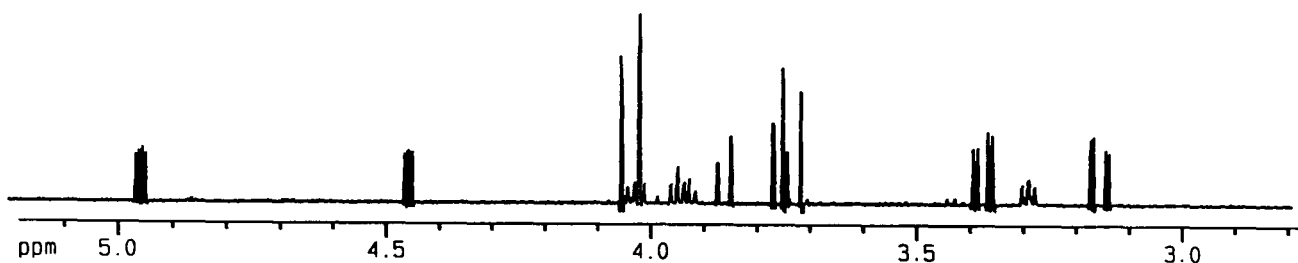


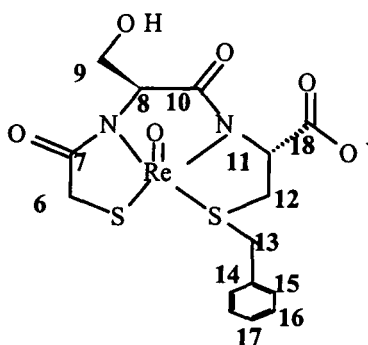
Figure 2-14 500 MHz ^1H NMR Spectrum of aliphatic region for 12 in CD_3CN

were then examined using 200 MHz proton NMR for evidence of purity and the most pure fractions were then combined and evaporated under a stream of nitrogen. The

combined sample of **12** was then dissolved in deuterated acetonitrile and used for 500 MHz NMR studies.

One dimensional and two dimensional NMR experiments were carried out on this sample. The ^1H NMR spectrum can be seen in Fig. 2-14 with its aliphatic region expanded. It was originally expected that two diastereomers would be present, as this had been the case for similar tripeptide complexes [27, 44, 45, 46, 47]. The appearance of only one large unresolved peak in the HPLC chromatogram seemed to indicate that the isomers were not separating. However, as the NMR showed, in fact only 1 isomer was present in large amounts in the combined sample of **12**. There was the presence of a small triplet and doublet of doublets at 4.86 ppm and 4.75 ppm respectively. The appearance of these and other small multiplets throughout the spectrum indicated that in fact two diastereomers were produced but the second was not isolated in sufficient amounts in any of the HPLC fractions to give useful NMR data.

The diastereomer of **12** that was isolated produced a clean ^1H NMR (see Table 2-2) spectrum that showed the presence of the benzyl group, the multiplet at 7.40 ppm, and no sign of a singlet for the ester methyl as demonstrated by the ESMS spectrum. It exhibited two downfield doublets of doublets at 4.937 and 4.437 ppm that were assigned to the alpha protons of the serine and cysteine amino acids respectively. The doublet of doublets at 4.937 ppm, which is the X of an ABX spin system, showed a COSY correlation to two sets of doublets of doublets at 4.005 and 3.923 ppm which were assigned to the H_A and H_B protons the β CH_2 of the serine. The coupling constants for these are $^3\text{J}_{8-9\text{A}}=3.9$ Hz and $^3\text{J}_{8-9\text{B}}=6.0$ Hz. As will be discussed in Chapter 3,

Table 2-2 ^1H and ^{13}C NMR Assignments for 12

^1H Assignment			^{13}C Assignment		
δ (ppm)	Assignment	J (Hz)	δ (ppm)	Assignment	
7.295	aryl		140.2	14	
4.937	8	$^3J_{9A-8}=3.9$	130.1	15	
		$^3J_{9B-8}=6.0$	129.3	16	
4.437	11	$^3J_{12A-11}=4.0$	127.8	17	
		$^3J_{12B-11}=2.9$	69.9	8	
4.017	6A	$^2J_{6A-6B}=17.0$	65.9	9	
4.005	9A	$^3J_{9A-8}=3.9$	61.3	11	
		$^2J_{9A-9B}=11.0$	39.9	13	
3.923	9B	$^3J_{9B-8}=6.0$	38.5	6	
		$^2J_{9B-9A}=11.0$	35.4	12	
3.841	13A	$^2J_{13A-13B}=12.7$			
3.755	13B	$^2J_{13B-13A}=12.7$			
3.712	6B	$^2J_{6B-6A}=17.0$			
3.355	12A	$^3J_{12A-11}=4.0$			
		$^2J_{12A-12B}=14.3$			
3.134	12B	$^3J_{12B-11}=2.9$			
		$^2J_{12B-12A}=14.3$			

results of a N_3S type of chelant with a serine in its backbone show rather smaller coupling constants in the serine spin system. The CH_2 of the serine "R" group does not become part of the chelant ring upon complexation to rhenium. E. Wong *et al.* [45] have suggested that the serine hydroxyl in the N_3S metal complex lies above the plane of the molecule and is oriented towards the metal and is held there by the steric interactions of the amide oxygens on either side. The larger coupling constants found for **12** seem to

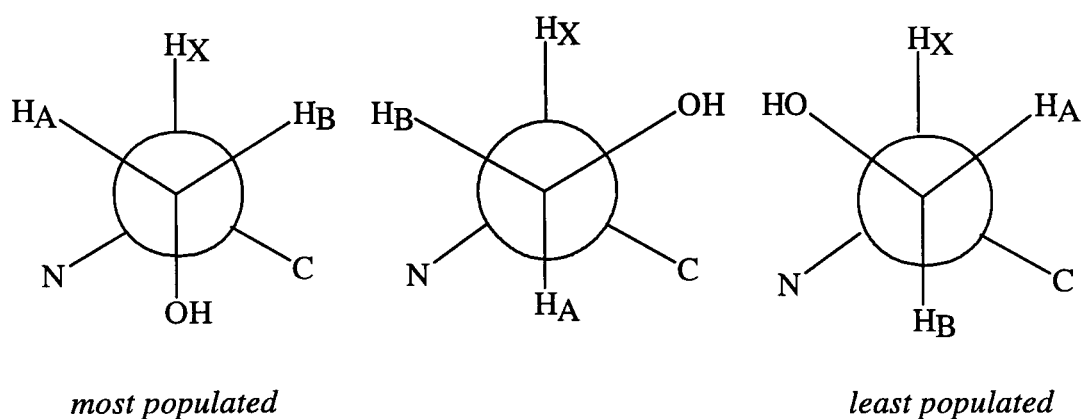


Figure 2-15 Possible conformers of the serine side chain of the metal complex, **12**

indicate a freer motion of the serine arm; i.e. increased populations of the conformers where the OH is directed away from the metal. The slight downfield shift of the serine β protons in **12** may then be a result of more conformations where the β protons are closer to the metal (see Fig. 2-15).

A large chemical shift change can be seen with the cysteine β protons. The α proton was assigned at 4.437 ppm in the COSY spectrum and correlated to two sets of doublets of doublets at 3.355 and 3.134 ppm. The cysteine β protons were part of the chelant ring and were consequently affected to a larger extent by the magnetic anisotropy

induced by the metal. This resulted in a 0.4 ppm downfield shift, larger than that obtained for the serine β protons.

The mercaptoacetyl CH_2 protons became diastereotopic when the tripeptide **5** complexed with the rhenium and this was indicative of their inclusion into a chelant ring system. The large difference in chemical shift between the H_A , at 4.017 ppm, and H_B , at 3.712 ppm, showed that the H_A proton was affected by the magnetic anisotropy to a larger extent than that of H_B . Both, however, were affected, as seen in their average chemical shift difference of 0.8 ppm from the original peptide (Table 2-1). The ^1H NMR data obtained do not permit assignment of H_A and H_B with respect to the ReO core.

A doublet of doublets was also found for the benzyl CH_2 protons. These became diastereotopic on complexation although they were not part of the chelant ring. There was some indication that they may have been affected by the magnetic anisotropy of the metal although the reason for this is unclear. Also unclear is the orientation of the benzyl group with respect to the ReO core. Additional NMR studies and a crystal structure would be necessary to make a better assessment.

2.5 Reaction of Tr-S-Mer-L-Ser-S-Bn-L-Cys-OMe with KTcOCl_4

Compound **6** was deprotected as in Fig. 2-12. The free thiol was isolated, dissolved in ethanol and combined with a solution of KTcOCl_4 in ethanol. An immediate colour change was expected as the KTcOCl_4 had been completely dissolved in the solvent. When this did not happen, the base sodium methoxide was used to adjust the pH of the

acidic solution to approximately neutral and immediately the reaction mixture turned a yellow-orange colour. It was found necessary to add 5 equivalents of the base to produce this colour change. Earlier attempts had been made at chelating technetium to the deprotected ligand using a reduction/substitution strategy with ammonium pertechnetate and $\text{NH}_4\text{OH}/\text{SnCl}_2/\text{pyridine}$. These attempts, however, were not successful and it was considered that a direct substitution of a Tc(V) species should be tried. The oxochloride KTcOCl_4 was used because it possessed no signals that would interfere with the ^1H NMR spectrum of the product. The poor solubility of the KTcOCl_4 was a potential problem but absolute ethanol was found to dissolve the salt sufficiently for a suitable reaction rate. The base, sodium methoxide, was used because of its availability as the dry solid and its solubility in the ethanol. The reaction was carried out at room temperature and its progress followed by ESMS which showed a negative ion with a mass/charge ratio of 483. This was indicative of the compound **13** minus the methyl ester, that is **14**. An NMR spectrum of the complete reaction mixture was recorded in deuterated acetonitrile and it showed what appeared to be α proton multiplets in the 5.0 ppm to 4.5 ppm region, but other interfering signals made assignments difficult. Reverse phase HPLC was once again used for separation of the mixture.

The large peak, with a retention time of 13 minutes, was isolated and ^1H NMR spectroscopy used to examine it. The strong peak proved to be the the required Tc-complex **14** and an expansion of the aliphatic region can be seen in Fig. 2-16. The loss of the methyl group of the methyl ester was not unexpected under the conditions of the reaction and therefore the methyl peak was not present in the spectrum. The assignments

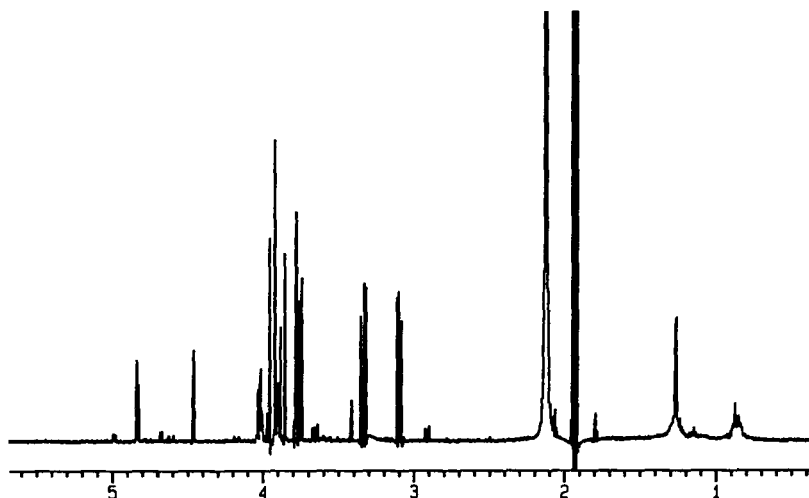
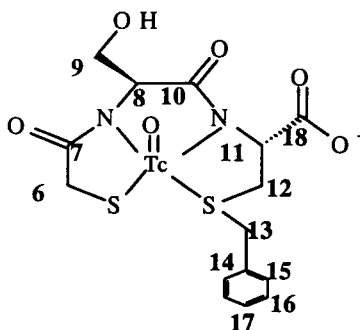


Figure 2-16 500 MHz ^1H NMR of aliphatic region of **14** in CD_3CN

were made following the procedure used for the Re-complex **12**, discussed above and the chemical shift trends were found to be similar to that for the rhenium complex. Again the benzyl group was retained, a doublet of doublets was seen for both α protons and by use of the 2D COSY spectrum, the corresponding β protons could be located. They were found to have similar chemical shifts to the corresponding β protons of the serine and cysteine residues in the rhenium complex **12**. The same trend was also noted for the coupling constants of the α and β protons. In each case, the coupling constants were almost identical, as shown in Table 2-3. It was also interesting to note that one isomer appeared to be isolated only. However, upon closer examination of the proton spectrum, the appearance of multiplets at 4.90 ppm, 4.68 ppm, 3.18 ppm and 2.92 ppm indicated the presence of a second isomer. Further evidence could be seen in a closer examination of the COSY spectrum where there were traces of off-diagonal peaks that had symmetrical partners similar to the more prevalent isomer that was being assigned. Again it was considered that the *syn* isomer was the more prevalent in this isolated HPLC

Table 2-3 ^1H and ^{13}C NMR Assignments for 14

^1H Assignment			^{13}C Assignment		
δ (ppm)	Assignment	J (Hz)	δ (ppm)	Assignment	
7.293	aryl		188.1	18	
4.837	8	$^3J_{9A-8}=3.9$	185.6	10 or	
		$^3J_{9B-8}=6.0$	182.6	7	
4.461	11	$^3J_{12A-11}=4.1$	130.1	15	
		$^3J_{12B-11}=3.0$	129.3	16	
4.022	9A	$^3J_{9A-8}=3.9$	127.8	17	
		$^2J_{9A-9B}=10.7$	69.8	8	
3.938	6A	$^2J_{6A-6B}=17.0$	65.9	9	
3.899	9B	$^3J_{9B-8}=6.0$	63.4	11	
		$^2J_{9B-9A}=10.6$	38.5	13	
3.869	13A	$^2J_{13A-13B}=12.8$	37.0	6	
3.772	13B	$^2J_{13B-13A}=12.8$	35.9	12	
3.762	6B	$^2J_{6B-6A}=17.0$			
3.338	12A	$^3J_{12A-11}=4.1$			
		$^2J_{12A-12B}=14.1$			
3.095	12B	$^3J_{12B-11}=2.9$			
		$^2J_{12B-12A}=14.1$			

fraction and the one being assigned because this seems to be the case in most of these complexes as will be discussed in detail in Chapter 3.

The most interesting feature of the ^{13}C NMR spectrum was in large shifts of the amide carbons. These significant downfield shifts arose from the fact that upon coordination, the NH of the amide loses its proton and some of its ability to back donate electron density to the carbonyl together with the positive inductive effect of the metal ion. The other ^{13}C shifts showed only small changes as a result of complexation.

2.6 Complex Formation

The complexation of rhenium and technetium to the chelant would mostly involve the initial chelation of the thiol, the softer and most nucleophilic donor group, followed by the loss of either a phosphine or chloride, depending on the starting material. A combination of the chelate effect and the drive of the metal to minimize its metal-oxo core charge would then see the amides complex followed by the thioether with a concomitant loss of chlorides or phosphines. It seems likely that the amides complex through the oxygen and then the nitrogens upon deprotonation. The driving force becomes the formation of five membered chelant rings containing the more stable amide nitrogen donor. This then forms a neutral complex.

The presence of a thioether in this particular N_2S_2 ligand confers different complexing properties on this chelant. The thioether acts as a softer donor to the TcO^{3+} core which most likely results in a weaker bond to the technetium. This may then impart a less restrictive type of chelant ring as seen for the cysteine residue. The sulfur of the

mercaptoacetamide is a harder donor and contributes a full negative charge to the TcO^{3+} core. It is expected that this bond would be shorter and cause more rigidity in the chelant ring. Modelling studies and crystal structures would be necessary to fully elucidate the structure and complex formation of this ligand.

2.7 Experimental Section

S-Tritylthioglycolic Acid, **1**

The method of Brenner *et al.*[34] was followed. A mixture of 24 g (0.092 mol) of triphenylmethanol, 6.5 mL (0.092 mol) mercaptoacetic acid and 80 ml glacial acetic acid was heated to 70°C. Boron trifluoride etherate (16 ml, 0.125 mol) was then added and the resulting reddish-brown mixture was stirred for 1 hour at room temperature. The reaction mixture was then poured into a beaker of ice cold distilled water (250 ml) and refrigerated overnight. The resulting colorless solid was collected by vacuum filtration, washed with water, then ether and recrystallized in benzene to give 9.54g (31 %) of **1**. The compound showed: mp: 154-158°C (Lit. 158.5-160°C [34]) ; TLC: $R_f = 0.53$ (10%MeOH/DCM); ^1H NMR (CDCl_3) [500 MHz]: δ 7.29 (m, 5H-aryl), 3.03 (s, 2H, CH_2); ^{13}C NMR (CDCl_3) [50 MHz]: δ 175.8 (s, COOH), 143.82 (s, trityl-**ipso**), 129.44 (s, trityl-**ortho**), 128.07 (s, trityl-**meta**), 127.89 (s, trityl-**para**), 67.20 (s, CPh_3), 34.44 (s, S- CH_2).

S-Tritylthioglycolic-*N*-Succinimido Ester, **2**

The method of Brenner *et al.* [34] was followed. To a mixture of 5 g (0.015 mol) of *S*-tritylthioglycolic acid and 1.7 g (0.015 mol) *N*-hydroxysuccinimide in distilled

acetonitrile (25 mL), 3.16 g (0.0165 mol) of EDAC was added. The reaction was protected from the light and allowed to stir for 2.5 h whereupon a colourless precipitate formed. This was collected by vacuum filtration giving 4.12 g (69%) of **2**. The compound showed : mp:177-179°C (Lit.178.5-179.5°C [34]); TLC: $R_f=0.71$ (5% MeOH/DCM); $^1\text{H NMR}$ (CDCl_3) [200MHz]: δ 7.200 (m, 15H, aryl), 3.118 (s, 2H, SCH_2), 2.696 (s, 4H, CH_2CH_2); $^{13}\text{C NMR}$ (CDCl_3) [50MHz]: δ 167.75 (2C, CO), 164.19 (CO), 142.68 (trityl-**ipso**), 128.62 (trityl-**ortho**), 127.37 (trityl-**meta**), 126.28 (trityl-**para**), 67.17 (CPh_3), 30.55 (CH_2).

p-Toluenesulfonic acid salt of S-benzyl-L-cysteine methyl ester, 3

The method of Valliant [27] was followed. A mixture of 5 g (0.0024 mol) of S-benzyl-L-cysteine and 16.34 g (0.095 mol) of *p*-toluenesulfonic acid was refluxed in the presence of excess methanol (200 mL) and protected from light for a period of 48 hours. The solvent was then removed *in vacuo* and 20 mL of diethyl ether was added and the whole triturated. The resultant colourless precipitate was collected by vacuum filtration and washed with 20 mL of ether to give 8.426 g (88 %) of **3**. The compound showed: mp: 72-73 °C; TLC: R_f : 0.51 (5%MeOH/DCM); $^1\text{H NMR}$ (CDCl_3) [200 MHz]: δ 7.70, 7.17 (m, 9H, aryl), 4.29 (m, 1H, CHCH_2), 3.65 (s, 3H, OCH_3), 3.60 (s, 2H, SCH_2Ph), 2.96 (d, 2H, $^3\text{J}=6.1$ Hz, CHCH_2S), 2.32 (s, 3H, $\text{CH}_3\text{-Ph}$); $^{13}\text{C NMR}$ (CDCl_3) [50 MHz]: δ 168.00 (COOCH_3), 142.05, 138.92, 129.18, 129.00, 128.63, 127.37, 126.39 (aryl), 53.55 (CHCH_2), 52.62 (OCH_3), 36.16 (CH_2Ph), 31.09 (CHCH_2), 21.42 (CH_3Ph).

N-t-Boc-L-serine-benzyl-L-cysteine methyl ester, 4

The method of Valliant [27] was followed. Compound **3** (5g, 12.5 mmol) was dissolved in 25 mL DCM and extracted with 25 mL of 10% Na₂CO₃. The aqueous layer was then back extracted with 2 x 25 mL DCM. The organic layers were combined and dried over Na₂SO₄. The solvent was removed by rotary evaporation and 50 mL of fresh DCM were added. To this was added 2.2 g (11 mmol) of N-t-Boc-L-serine and 3.6 g (18.75 mmol) of EDAC. The mixture was allowed to stir overnight in the presence of 1.5 mL (12.5 mmol) Hunig's base (DIPEA) under protection from light. The reaction mixture was then extracted with 0.1M HCl (2 x 20 mL), 0.1M NaHCO₃ (2 x 20 mL) and distilled water (2 x 20 mL). The organic layer was dried over Na₂SO₄ and the solvent removed by evaporation at reduced pressure (Buchi Rotovapour) to produce a golden, thick liquid which was dissolved in 25 mL diethyl ether. The solution was extracted with 0.1M HCl (1 x 20 mL), 0.1M NaHCO₃ (1 x 20 mL) and distilled water (1 x 20 mL). The organic layer was collected and dried over Na₂SO₄ and then placed in the freezer overnight. Colourless crystals were deposited and collected by vacuum filtration to give 3.26 g (72%) of **4**. The compound showed: mp: 59-60°C (Lit. 78-79°C [27]); TLC R_f = 0.45 (5%MeOH/DCM); ¹H NMR (CDCl₃) [200 MHz]: δ 7.26 (m, 5H, aryl), 4.75 (m, 1H, CHCH₂S), 4.15 (m, 1H, CHCH₂OH), 3.72 (s, 3H, OCH₃), 3.69 (s, 2H, SCH₂Ph), 3.66 (m, 1H, CHCH₂OH), 2.85 (m, 2H, CHCH₂S), 1.44 (s, 9H, (CH₃)₃C); ¹³C NMR (CDCl₃) [50 MHz]: δ 172.24 (COOCH₃), 172.01 (amide CO), 158.10 (carbamate CO), 131.20, 128.90, 128.60, 127.31 (aryl), 80.01 (C(CH₃)₃), 63.01 (CHCH₂OH), 54.56 (OCH₃), 52.74 (CHCH₂S), 51.57 (CHCH₂OH), 36.39 (SCH₂Ph), 33.12 (CHCH₂S), 30.86 (C(CH₃)₃).

L-Serine-S-benzyl-L-cysteine methyl ester ditrifluoroacetate salt, 5

Compound **4** (1.16 g , 2.9 mmol) was dissolved in 5 mL of trifluoroacetic acid (TFA). With rapid stirring, triethylsilane was added dropwise until the colour dissipated and the whole was allowed to stir. A colourless precipitate developed after 2 hours and this was removed by vacuum filtration and the filtrate quickly transferred to a round-bottomed flask. The mixture was diluted by the addition of 20 mL DCM and the new solvent removed in vacuo several times. DCM (20 mL) was added and then removed under a N₂ stream with stirring to completely remove the last traces of TFA. A light grey solid of **5** remained. The compound showed : TLC R_f=0.00 (5% MeOH/DCM).

S-Tritylthioglycolic-L-serine-S-benzyl-L-cysteine methyl ester, 6

Compound **5** (1g, 2.5 mmol) as the crude solid, was dissolved in 25 mL of 50/50 MeOH/DCM. To this was added 0.94 g (2.2 mmol) of S-tritylthioglycolic N-hydroxysuccinimido ester **2**. Diisopropylethylamine (DIPEA) (2 mL) was then added and the mixture stirred for 48 h. The solvent was removed by rotary evaporation and the residue dissolved in 2 mL DCM. The product was then isolated using radial chromatography with 50/50 CHCl₃/MeOH as eluent to give 600 mg (44 %) of **6** as a colourless solid. The compound showed: mp:45-47°C; TLC R_f= 0.53(5%MeOH/DCM); ¹H NMR (CDCl₃) [500 MHz]: See Table 2-1; ¹³C (CDCl₃) [125 MHz]: See Table 2-1.

KTcOCl₄, 15

To a beaker equipped with a stir bar, 140 mg (0.8 mmol) of NH₄TcO₄ and 19 mL

of 12M HCl were added. The mixture was stirred for 10 minutes and 70 mg (0.8 mmol) of KCl were added. This was heated to 40°C and evaporated slowly under a stream of N₂. A dark green crystalline solid was deposited to give 198 mg (87%) of **15**. The compound showed: IR(cm⁻¹, KBr disk) 984 cm⁻¹ (ν_{Tc=O}).

ReOCl₃(PPh₃)₂, 26

The method of Chatt and Rowe [43] was followed. Rhenium metal (1.498 g , 8 mmol) was oxidized by the addition of 10 mL of 30% H₂O₂. To the mixture was added 20 mL of distilled water and this was gently heated overnight and the solution evaporated to a volume of 5 mL. Concentrated HCl (7 mL) was then added and this mixture was allowed to stir for 0.5 h. To this was added 4.2g (16 mmol)of triphenylphosphine in hot ethanol solution (20 mL). A yellow-green solid was collected by vacuum filtration to give 3.6g (54%) of **26**. The compound showed: IR (KBr disk) 969 cm⁻¹ (ν_{Re=O}).

ReO-mer-ser-cys-OMe, 11

Compound **6** (60 mg, 0.1 mmol) was dissolved in 2 mL of TFA. With rapid stirring, Et₃SiH was then added dropwise until the colour dissipated and the whole was allowed to stir. A colourless precipitate developed after 2 h. This was removed by vacuum filtration and the filtrate quickly transferred to a round-bottomed flask. The mixture was diluted with the addition of 20 mL DCM and the solvent removed in vacuo several times. DCM (20 mL) was added and then removed under a N₂ stream with stirring to completely remove the last traces of TFA. The residue was then dissolved in 50/50

MeOH/THF (10 mL). A 1M sodium acetate buffer (1 mL) was added with 82 mg (0.1 mmol) of $\text{ReOCl}_3(\text{PPh}_3)_2$. The mixture was refluxed for 18 h, cooled and the solvent removed in vacuo. The orange-red residue was brought up in MeOH (5 mL) and refrigerated to precipitate out triphenylphosphine and other impurities. A precipitate formed and was removed by filtration through a glass wool plug. The residue was concentrated to 500 μL . The material was purified by reverse phase HPLC using a Vydac 201HS10110 semi-preparative column (9.4 x 250 mm). The conditions used for purification were developed by use of an analytical column and involved using a partial gradient from 10-25% acetonitrile/water to separate the polar products. The non-polar products were then eluted off in a 70-100% acetonitrile/water gradient. Fraction 3 for all runs gave **11** and this was used for analysis. The compound showed: MS(-ES) m/z 569/571 (60/100%); IR (KBr disk) 922 cm^{-1} ($\nu_{\text{Re=O}}$); $R_f=0.0$ (25%MeOH/DCM); $^1\text{H NMR}$ (CD_3CN) [500 MHz]: See Table 2-2; $^{13}\text{C NMR}$ (CD_3CN) [125 MHz]: See Table 2-2.

TcO-mer-ser-cys-OMe, **13**

Compound **6** (75 mg, 0.125 mmol) was dissolved in 2 mL of TFA. With rapid stirring, Et_3SiH was then added dropwise until the colour dissipated and the whole was allowed to stir. A colourless precipitate developed after 2 h and this was removed by vacuum filtration and the filtrate quickly transferred to a round-bottomed flask. The mixture was diluted with the addition of 20 mL DCM and the solvent removed in vacuo several times. DCM (20 mL) was then added and then removed under a N_2 stream with stirring to completely remove the last traces of TFA. The residue was dissolved in

absolute ethanol (5 mL) and a solution of **7** (35.4 mg, 0.125 mmol) in absolute ethanol (5 mL) was added. The pH was adjusted to neutral with 1M sodium methoxide in absolute ethanol. After stirring for 4 h, the solvent was removed under a stream of N₂ and 200 μL of MeOH added. The material was purified by reverse phase HPLC using a Vydac 201HS10110 semi-preparative column (9.4 x 250 mm). The conditions used for purification were developed with the use of an analytical column and involved using a partial gradient from 10-25% acetonitrile/water to separate the polar product. The non-polar products were then eluted off in a 70-100% acetonitrile/water gradient. Fractions 3 and 4 were used for analysis from runs 3-7 and contained **13**. The compound showed: MS(-ES) m/z 483 (100%); IR (cm⁻¹, KBr disk) 964 cm⁻¹ (ν_{Tc=O}); R_f=0.0 (25%MeOH/DCM); ¹H NMR (CD₃CN) [500 MHz]: See Table 2-3; ¹³C (CD₃CN) [125 MHz]: See Table 2-3.

Chapter 3
Technetium(V) Oxo Complex of an
 $N_2N'_1S_1$ Peptidic Chelator

3.0 Introduction

The search for new technetium imaging agents has branched into other combinations of the N_xS_y type with the purpose of finding new, highly specific radiopharmaceuticals. The next stage of the journey was the synthesis of a N_3S (triamide monothiol) ligand based on the amino acid glycine. One such drug developed by Nosco *et al.* [49] and called MAG_3 , consisted of three glycine residues and a mercaptoacetyl group (Fig. 3-1). This compound is currently in use as a highly successful renal imaging agent. The very stable MAG_3 complex with its carboxyl group is also potentially useful as a

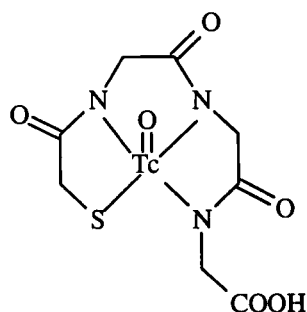


Figure 3-1 MAG_3 Structure

bifunctional chelant. For example, the carbonyl group could be used as a coupling site and provide a way of introducing ^{99m}Tc or rhenium isotopes onto lysines in antibodies [45, 50]. The in vivo stability of the $Tc N_3S$ chelate is close to the stability of the $Tc N_2S_2$ DADT or

based chelants [48]. This chapter deals with the synthesis and properties of one such N_3S chelant and its ability to coordinate with Tc(V).

3.1 Chelant Design

For several years, Resolution Pharmaceuticals Inc. have actively investigated the ^{99m}Tc labelling of small biologically active peptides (5-30 amino acid residues). The goal was to develop a target specific diagnostic radiopharmaceutical; in particular, one which would image *in vivo* inflammation. Several methods existed for labelling peptides with ^{99m}Tc , as has been discussed in earlier chapters. The route chosen is termed a “final step labelling bifunctional chelant” approach. In this scenario, the chelant is bound to the targeting molecule and isolated as a pure compound first. Chelation with Tc(V) is then carried out and the technetium transported to the target area by the specificity of the target molecule. Resolution developed a chelant (RP294), N,N'-dimethylglycine-L-serine-L-cysteine-glycine-NH₂, **15**, based on amino acids in which, via the carboxyl terminus, a biologically active peptide sequence could be bound. Preliminary molecular modelling had shown **15** would coordinate strongly to TcO^{3+} . In addition to peptides, **15** would also be

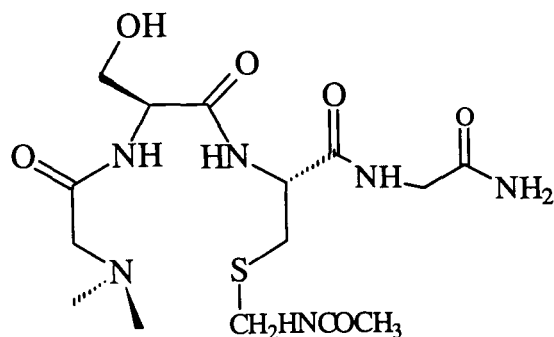


Figure 3-2 RP294 Chelant, **15**

an ideal bifunctional chelator for the labelling of proteins, monoclonal antibodies and small molecules. In order to better understand the coordination of this peptidic chelator to ^{99m}Tc at the tracer level (10^{-7} - 10^{-6} M), studies were undertaken to study its coordination to ^{99}Tc , where relatively large quantities of complex can be prepared. In this chapter, the synthesis and characterization of the ^{99}Tc complex of dimethylglycine-L-serine-L-cysteine-glycine-NH₂, **15**, is presented.

3.2 NMR Spectroscopy of Chelant RP294

Dimethylglycine-L-serine-L-cysteine-glycine-NH₂ was prepared in excellent yields using solid phase methods on an automated peptide synthesizer [51]. The C terminus was capped with an amide moiety to avoid any problems that a free, charged carboxylate might introduce during complexation. The cysteine thiolate was protected by an acetoamidomethyl moiety during synthesis and was retained until just before coordination experiments were attempted as free thiol groups tend to oxidize readily to form disulphides on standing. RP294 was extremely hygroscopic and was soluble in water and aqueous acetonitrile solution but was not soluble in organic solvents. It was purified by High Performance Liquid Chromatography (HPLC) at Resolution Pharmaceuticals and was characterized at McMaster using NMR spectroscopy and electrospray mass spectrometry (ESMS). ^1H and ^{13}C assignments are given in Table 3-1 and an expansion of the aliphatic spectrum of the proton region can be seen in Fig. 3-3.

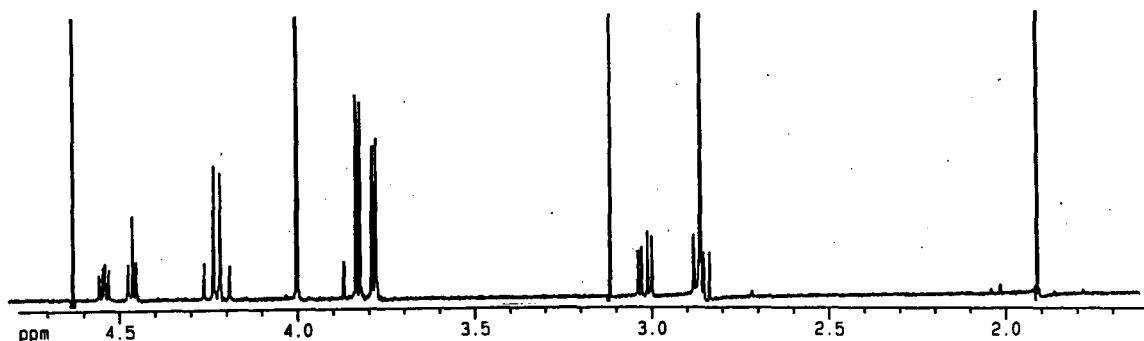


Figure 3-3 500 MHz ^1H NMR spectrum of aliphatic region of 15 in D_2O

The use of NMR spectroscopy for the analysis of amino acid chelating systems has become vital in the determination of the structure and conformation of the uncoordinated and coordinated forms of the chelants. The method used in assigning the spectra is a standard one. It generally begins with the assignment of the proton spectrum based on Wuthrich's tables [41]. Initial assignments are conveniently made for the α protons of each amino acid residue and some coupling constants can be calculated. A 2D COSY spectrum is then recorded to assign the majority of the remaining proton spectrum. Any proton couplings unassigned at that point because of severe signal overlap can be resolved through use of the Selective TOCSY experiment, a technique which is illustrated later in this chapter. The ^{13}C spectrum is then recorded and, while some assignments can be made directly, full assignment is readily made with the aid of a ^1H - ^{13}C HSQC correlation experiment. This connects the carbons to their directly bonded protons. The Heteronuclear Multiple Bond Correlation or HMBC experiment then allows for the connectivity of the amino acid residues to be found. In this experiment, three and four bond couplings between the ^{13}C and ^1H nuclei are correlated and thus the ^{13}C correlation

of an amide to the α proton of the next amino acid residue on the carboxyl side is identified. An example of this is shown in Fig. 3-4.

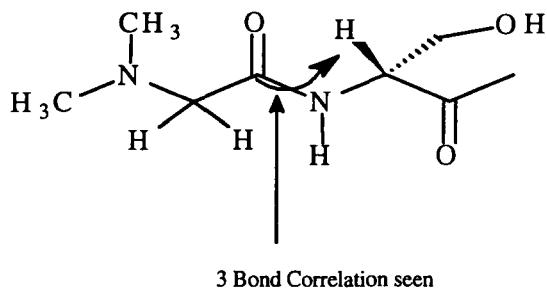
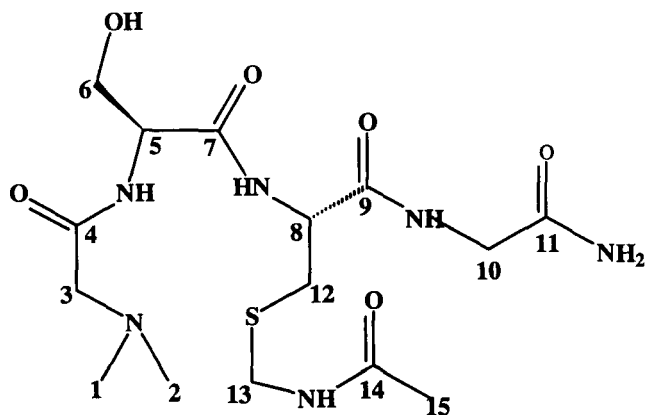


Figure 3-4 HMBC Connectivity

Conformational information can come from the use of a Nuclear Overhauser Effect (NOE) experiment. This is an experiment in which the change in intensity of the resonance of one nucleus is affected by the spin populations of a proximate nucleus. The process occurs through a dipole-dipole relaxation mechanism which is dependent on the separation of nuclei in a $1/r^6$ manner. Thus “through-space” correlations can be found and conformational information about which portions of the peptide are close together can be gained [52].

The main purpose of examining RP294 using ^1H NMR was to be able to determine whether a complex had been formed with the TcO^{3+} core by observing the changes in both chemical shifts and coupling constants. It is interesting to note some of the normal features of the ^1H spectrum of RP294 in order to see and understand what happens to the molecule upon chelation to the metal. The singlets found in the simple RP294 spectrum for example provided the first clues that complex formation had

Table 3-1 ^1H and ^{13}C NMR assignments of RP294

^1H Assignment			^{13}C Assignment	
δ (ppm)	Assignment	J (Hz)	δ (ppm)	Assignment
4.53	8	$^3J_{8-12A}=5.6$	174.34	11
		$^3J_{8-12B}=8.5$	173.83	14
4.45	5	$^3J_{5-6}=5.5$	172.37	9
4.21	10	$^2J_{10A-10B}=14.1$	171.56	7
3.99	3		165.62	4
3.82	13A	$^2J_{13A-13B}=17.1$	61.06	6
3.81	13B	$^2J_{13B-13A}=17.1$	58.12	3
3.77	6	$^3J_{6-5}=5.5$	55.56	5
3.01	12A	$^2J_{12A-12B}=14.2$	53.44	8
		$^3J_{12A-8}=5.6$	43.84	1 & 2
2.86	12B	$^3J_{12B-8}=8.5$	42.18	13
		$^2J_{12B-12A}=14.2$	40.90	10
2.85	1&2		31.55	12
1.90	15		22.05	15

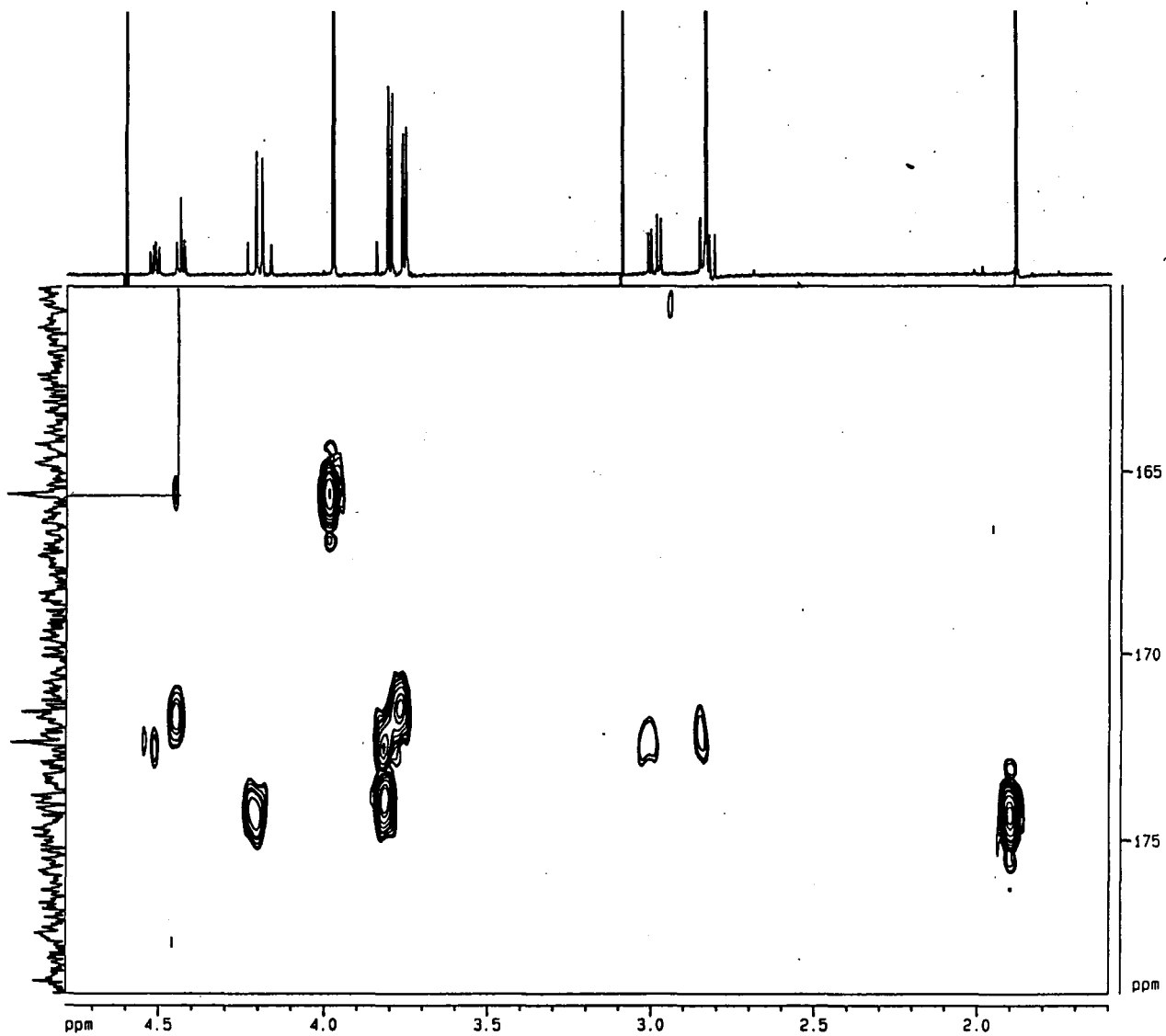


Figure 3-5 HMBC of 15

occurred when Tc(V) was added. Thus, for the uncomplexed RP294, the singlet for the N,N-dimethyls at 2.85 ppm was most noteworthy. The glycine CH₂ also produced a singlet at 3.99 ppm. The α proton for the serine showed an averaged coupling constant to the β protons (X of an A₂X system) and showed a triplet at 4.45 ppm. The β protons for the serine were found as the A₂ part of the A₂X spin system and were a doublet at 3.77 ppm. The cysteine protons formed an ABX spin system with the α proton a doublet of doublets at 4.53 ppm and the β protons at 3.01 and 2.86 ppm respectively.

HSQC and HMBC spectra were recorded to correlate the ¹H-¹³C signals and then confirm the connectivity of the dimethyl glycine to the serine and the serine to the cysteine. All of the carbons were accounted for and the chemical shifts are presented in Table 3-1. It was expected that upon complexation the most drastic changes would occur in the α carbon shifts as well as in the β carbon of the cysteine residue as that atom would become part of a chelant ring. The HMBC shown in Fig. 3-5, illustrates the connection between the amide carbon of the dimethyl glycine (165.62 ppm) and the α proton of the serine (4.45 ppm). As expected, a 3 bond correlation between the carbonyl carbon of the serine and the α proton of the cysteine can also be found to complete the connection between the amino acids.

3.3 Technetium Complex of RP294 , **16**

The neutral Tc(V) oxo complex of RP294 ([TcO(RP294)] (**16**) was prepared by the use of a reduction/substitution reaction of deprotected RP294 with NH₄TcO₄, tin (II) chloride and sodium gluconate (Fig. 3-6). The sodium gluconate provided an

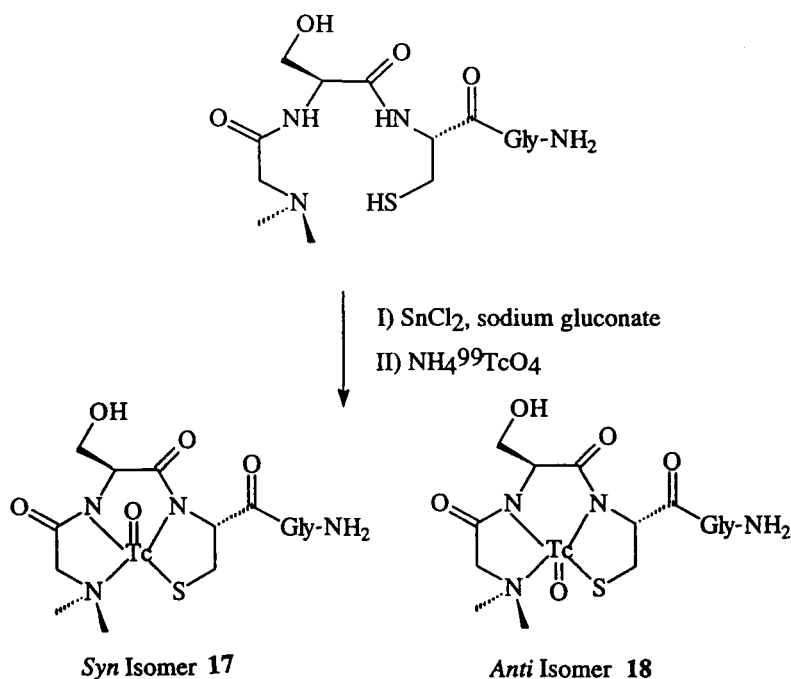


Figure 3-6 *Synthesis of 16*

opportunistic intermediate as a Tc-gluconate complex can form, while also fulfilling other duties as a buffer. The crude [TcO(RP294)] was found to be soluble in aqueous solution and slightly soluble in methanol. Analysis by TLC gave a coloured spot with an R_f value of 0.4 in a 50/50 CH₃OH/CH₂Cl₂ developing solution. The crude reaction mixture consisting of unreacted RP294, NH₄TcO₄, SnCl₂, SnCl₄, sodium gluconate and [TcO(RP294)] was purified by size exclusion gel chromatography using distilled, deionized water as the eluant. Several attempts had been made to purify this compound using such traditional chromatographic methods such as ion exchange, silica gel and preparative-plate thin-layer chromatography but in no cases were acceptable yields of purified chelates obtained. Success was only achieved when separation was attempted based on the size of the components in the reaction mixture.

The infrared spectrum of [TcO(RP294)] showed a stretching frequency of 977cm⁻¹ for the metal-oxo bond. This is the characteristic band found in other technetium-oxo

complexes [53, 54]. In general, the $\nu_{\text{Tc}=\text{O}}$ band can be seen from 880-1020 cm^{-1} depending on the donor atoms in the chelate. Mass spectral data for $[\text{TcO}(\text{RP294})]$ were obtained by ESMS in the positive ion detection mode. The molecular ion was not found but the sodium adduct $\text{M}+\text{Na}^+$ at 484 was present and this was the 100% ion which confirmed that the $[\text{TcO}(\text{RP294})]$ complex was of a mononuclear, monoligand nature.

The infrared and ESMS data did not however show the presence of two diastereomers. The occurrence of two isomers is not new in technetium-oxo complexes of amino/amido-thiolato ligands[55, 56, 57] and it was strongly suspected in the present case, as work on the rhenium complex was being carried out simultaneously at Resolution and HPLC analysis had shown two fractions of equal magnitude [48]. When examined with

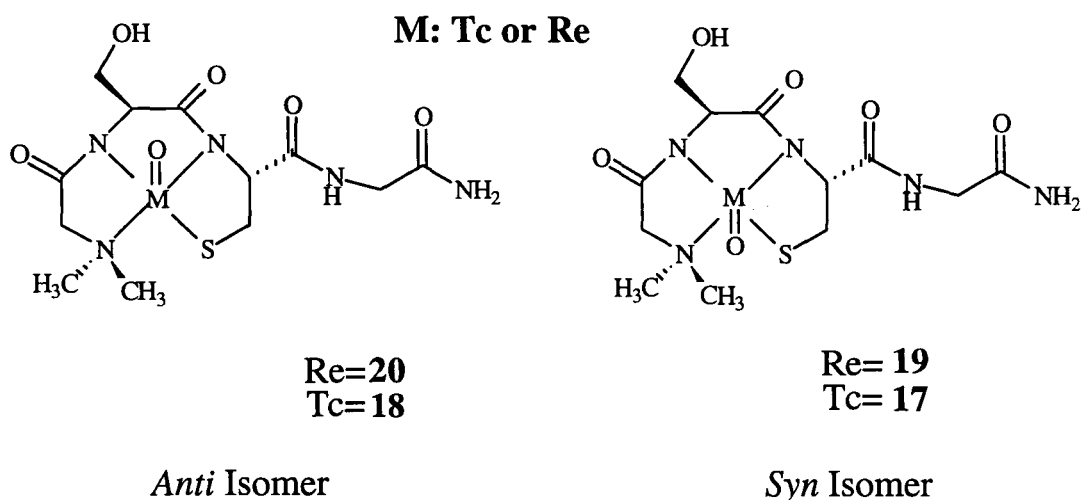


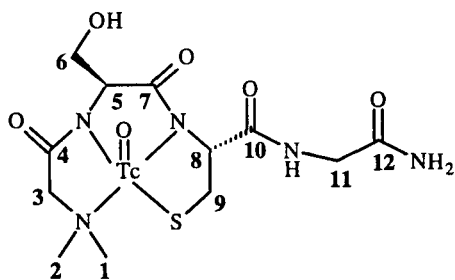
Figure 3-7 *Syn and anti isomers of MO(RP294)*

ESMS, these fractions showed only ions associated with the Re complex. These two HPLC fractions represented the two isomers of $[\text{ReO}(\text{RP294})]$: **20** and **19**, the serine CH_2OH group being in the *syn* or *anti* conformation with respect to the Re oxo bond (Fig. 3-7). The assignment of one isomer being *syn* and the other being *anti* was based

initially on the relative intensities of their respective NMR peaks (from HPLC peaks their areas were 1.1:1). Later, a single crystal x-ray structure of the *syn* isomer was obtained and it was possible to correlate this structure with one of the NMR isomers through dihedral angle data and coupling constants [48].

For the [TcO(RP294)] complex, ^1H and ^{13}C NMR spectra were recorded in D_2O at room temperature. The ^1H spectrum showed a complex array of overlapping ^1H NMR resonances from 2.3 to 5.7 ppm indicative of the presence of more than one isomer and the ^{13}C NMR spectrum showed resonances from 40 to 190 ppm. Assignments of the ^1H resonances are given in Table 3-2.

In the ^1H NMR spectrum of uncoordinated RP294, the two methyls from the glycine were chemically equivalent and a singlet was observed. Upon coordination of the chelant to TcO^{3+} , the two methyl groups became nonequivalent and two singlets were observed for the hydrogen atoms of each methyl group for each isomer. The greatest change was found in the chemical shift between the pairs of methyls on each isomer. The methyl closer to the metal in each isomer, in a pseudoaxial orientation, was downfield from the original by 0.6 ppm. The methyl further away, in a pseudoequatorial orientation, shifted upfield by 0.3 ppm. In addition, the two methylene hydrogen atoms in the dimethylglycine residue became nonequivalent with one adopting a pseudoequatorial position and the other a pseudoaxial one. The same type of chemical shift change can be seen as the pseudoaxial protons closest to the metal shifted downfield from 3.99 to 4.1 and 4.6 ppm respectively, and those pseudoequatorial and farthest away shifted upfield to 3.7 and 3.99 ppm. These changes in the ^1H NMR resonances for the

Table 3-2 ^1H NMR Assignment for (TcO[RP294])

<i>Anti Diastereomer</i>			<i>Syn Diastereomer</i>		
Proton	δ (ppm)	J(Hz)	Proton	δ (ppm)	J(Hz)
1	2.360		1	2.462	
2	3.429		2	3.450	
3A	$\sim 4.6^\Phi$	$^2J_{AB}=15.5$	3A	4.130	$^2J_{AB}=12.0$
3B	3.741	$^2J_{AB}=15.5$	3B	3.986	$^2J_{AB}=12.0$
5	4.788	$^3J_{6A-5}=3.1$	5	4.525	$^3J_{6A-5}=2.7$
		$^3J_{6B-5}=1.9$			$^3J_{6B-5}=2.7$
6A	4.233	$^3J_{6A-5}=3.5$	6A	4.121	$^3J_{6A-5}=2.7$
		$^2J_{6A-6B}=11.9$			$^2J_{6A-6B}=12.0$
6B	3.825	$^3J_{6B-5}=1.9$	6B	3.991	$^3J_{6B-5}=2.7$
		$^2J_{6A-6B}=12.0$			$^2J_{6A-6B}=12.0$
8	5.676	$^3J_{8-9A}=5.3$	8	5.293	$^3J_{8-9A}=1.2$
		$^3J_{8-9B}=6.5$			$^3J_{8-9B}=7.8$
*9A	3.742	$^3J_{9A-8}=6.75$	9A	3.874	$^3J_{9A-8}=1.2$
		$^2J_{9A-9B}=?$			$^2J_{9A-9B}=13.0$
*9B	3.742	$^3J_{9B-8}=6.75$	9B	3.767	$^3J_{9B-8}=7.8$
		$^2J_{9B-9A}=?$			$^2J_{9B-9A}=13.0$
*11A	3.834	$^2J_{11A-11B}=17.2$	*11A		$^2J_{11A-11B}=17.2$
*11B	3.741	$^2J_{11B-11A}=17.2$	*11B		$^2J_{11B-11A}=17.2$

$^\Phi$ under water peak

† selective tocsy unable to give resolution to determine J_{AB}

* *syn* and *anti* terminal glycine protons indistinguishable

dimethylglycine residue from the free RP294 to [TcO(RP294)] demonstrated the coordination of the dimethylglycine N_{amine} to the Tc centre.

Changes to the serine and cysteine ¹H NMR resonances from the uncoordinated RP294 to the Tc complex were also observed. Because the x-ray structure of the *syn* Re isomer **19** was available, it was used as a guide in the assignment of the isomer for the technetium complex. In **19**, if the cysteine residue is examined, a dihedral angle of 86° is found for the H_A-H_X protons and this leads to a small coupling constant for J_{AX} (~1.2 Hz) through use of the PCMODEL program [58]. The H_B-H_X protons have a dihedral angle of 32° and shows a larger coupling constant for J_{BX} (~7.5 Hz). Identical coupling patterns were found for the cysteine residue in one of the diastereomers of the technetium complex of RP294 and the rhenium information was then used as a tool to help identify which isomers were which.

Dramatic changes were seen in the cysteine α protons' chemical shift from coordination. The α proton for the cysteine was found at 5.7 ppm for one diastereomer and 5.3 ppm for the other. This represented a shift of 1.2 and 0.8 ppm from the original uncomplexed α proton. The *syn* isomer gave J_{AX}=1.2 Hz and J_{BX}=7.8 Hz and the *anti* isomer gave a J_{AX}=5.3 and J_{BX}= 6.5 Hz. If the crystal structure for the rhenium complex is viewed as noted above, it becomes apparent how the isomers can be assigned as the 5.3 ppm signal led to the expected coupling pattern for the *syn* isomer. The 5.7 ppm signal must therefore belong to the *anti* isomer.

The cysteine β protons were much more difficult to assign. The 2D COSY did not provide enough information to pick out all of the peaks related to the spin systems

because of severe overlap. To aid in this, selective TOCSY experiments were recorded to assign the β protons because each isomer's α proton were in uncluttered regions of the spectrum and could be selected for discrete irradiation. The *anti* isomer protons were found at 3.7 ppm. The selective TOCSY experiment in this case was unable to separate

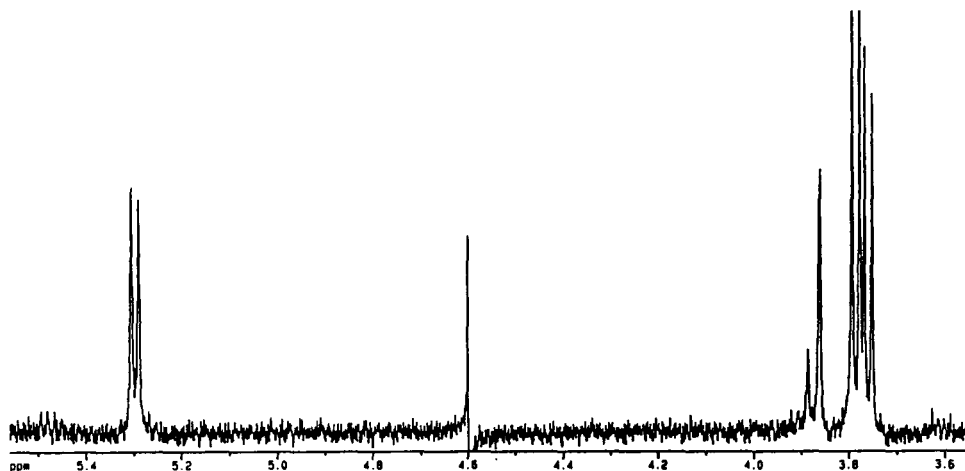


Figure 3-8 Selective TOCSY irradiation of Cys α proton at 5.3 ppm

the peaks and provide a J_{AB} coupling constant because only two lines were recorded showing H_A and H_B had chemical shifts very close together. For the *syn* isomer, the protons were assigned H_A at 3.87 ppm and H_B at 3.76 ppm. In this case, the doublets of doublets were clearly visible with the selective TOCSY and the coupling constants were readily calculated. Figure 3-8 shows one such experiment on the *syn* α proton where irradiation of the α proton at 5.3 ppm resulted in a doublet of doublets.

The coupling constants for the *syn* cysteine β protons indicated that the dihedral angles were close to 90° for the small coupling constant ($J_{AX}=1.2$ Hz) and $20-30^\circ$ for the

larger ($J_{\text{BX}}=7.8$ Hz). This is in accordance with the crystal structure of the rhenium complex. The *anti* isomer produced a coupling constant that suggested a dihedral angle of between 45° and 130° for both of the β protons which would indicate that there is appreciable distortion when this 5-membered, chelate ring has formed.

The serine α protons shifted downfield approximately 0.3 and 0.1 ppm for the two isomers. When comparing the crystal structure of the *syn* [ReO(RP294)], **19**, the α proton can be seen to be directed away from the metal. A slight downfield shift was found for the $\text{H}\alpha$ of **19** as the serine became part of the chelant ring and thus, by analogy, the $\text{H}\alpha$ of the *syn* isomer **17** at 4.52 ppm could be assigned as it too displayed only a slight downfield shift. The *anti* isomer, in which the α proton is on the same side as the metal-oxo group, was assigned the signal at 4.79 ppm and it is again of interest to note that this proton was the most affected by the metal and displayed the largest chemical shift change.

The β proton assignments for the serine were made through use of the 2D COSY. As Fig. 3-9 shows, the spectrum was quite complex because the simple A_2X system that

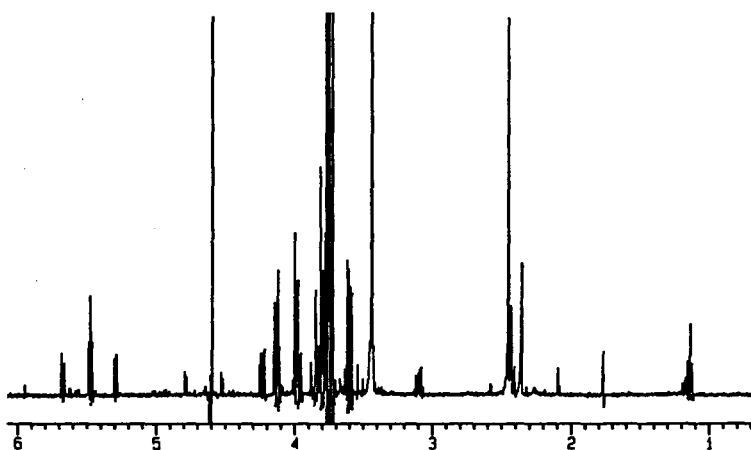


Figure 3-9 500 MHz ^1H NMR spectrum of the aliphatic region of 16 in D_2O

phase, has a very strong preference for the conformation in which it sits just above the metal-oxo bond in the *syn* isomer and opposite it in the *anti* isomer (Fig. 3-10). Again, examination of the solid state crystal structure of [ReO(RP294)] shows that the OH group is gauche to the chelant ring; that is, the conformation is the same in the solid state as preferred in solution.

The coupling constants for both the *syn* and *anti* isomer differ only slightly. The *syn* 3J s were both 2.7 Hz indicating that the dihedral angles were approximately 60° . The *anti* β protons were $^3J_{6A}$ at 3.5 Hz and $^3J_{6B}$ at 1.9 Hz. This is indicative of dihedral angles around 60° also. If the analogous [ReO(RP294)] crystal structure is referred to, the protons exhibit that type of arrangement. The crystal has, for the *syn* isomer, calculated coupling constants of $^3J_{6A}=1.7$ Hz (68°) and $^3J_{6B}=2.8$ Hz (49°). Thus it is possible to assign the *syn* isomer while further confirming the preferred gauche conformation of both isomers (*vide supra*).

It was necessary to use the same crystal structure analogy when assigning the protons for the dimethylglycine because the HMBC experiment that was recorded was too weak to see any correlations. By analogy, the *syn* and the *anti* isomers were assigned by 2J values. The two hydrogen atoms of the methylene groups α to the coordinated dimethylglycine N_{amine} atom became nonequivalent as the CH_2 groups could no longer freely rotate about the $C2-N_{\text{amide}}$ bond and each diastereomer had distinctly different 2J values. One was 15.5 Hz and the other 12.0 Hz. The *syn* [ReO(RP294)], **18**, had $^2J=12.0$ Hz for the dimethylglycine CH_2 protons and thus the corresponding CH_2 with $^2J=12.0$ Hz and chemical shifts 4.130 ppm and 3.986 ppm were assigned to the *syn* Tc complex **17**.

The two CH₃ groups were assigned to the *syn* isomer because of the long range coupling observed in the 2D COSY spectrum. The *anti* assignments were then made by default. The *anti* isomer produced the greatest change with the chemical shifts between the A and B proton being 0.9 ppm (see Table 3-2). It is also interesting to note that the *anti* isomer produced a large coupling constant of 15.5 Hz. This may be the result of hyperconjugation between the neighbouring carbonyl π system and the methylene group. This would indicate that one of the methylene protons would be at approximately 90° to the plane of the carbonyl system [59]. Modelling studies of this isomer would be necessary to further investigate this.

3.4 *Syn and Anti Interconversion*

The presence of *syn* and *anti* isomers in the sample of [TcO(RP294)] purified by gel chromatography was demonstrated by the ¹H NMR spectra discussed above. HPLC had been done on the corresponding [ReO(RP294)] complex at Resolution Pharmaceuticals and the chromatogram showed the presence of two peaks corresponding to each isomer with retention times that were 0.2 minutes apart. In this case, the isomers seemed to interconvert back to a 1:1 mixture after 18 hours as monitored by the reinjection of each isomer in a further HPLC experiment [48]. The conversion of an *anti* N₂S₂ complex to a *syn* diastereomer in the presence of excess ligand and with 3 hours of heating has been reported by Kung [46, 50] but the conversion was only 5-10%. No conversion of the *syn* to *anti* isomers was reported. This was not the case with [ReO(RP294)] as both isomers seemed to interconvert equally. It was therefore important

to determine if the interconversion was the result of an oxygen exchange catalysed by the presence of water or some other mechanism. The [TcO(RP294)] interconversion was investigated using H_2^{18}O as use of an HPLC was prohibited because of radioactive contamination. The experiment examined the incorporation of ^{18}O by monitoring the appearance of a 486(M+Na+2 amu) peak in the ESMS in negative ion mode. The 486 peak is indicative of the complex, **16**, with one sodium and one ^{18}O incorporated.

In a strictly qualitative manner, the results indicated that an exchange of isomers was occurring as the ^{18}O was being incorporated into the complex. The conversion took approximately one week to achieve a 1:1 ratio at room temperature in ^{18}O enriched water. This suggested that the interconversion was being made possible by the coordination of a water molecule in the sixth position, trans to the Tc-oxo bond. Figure 3-11 illustrates one possible mechanism. In this dissociative mechanism, the tertiary terminal amine is protonated resulting in a bond breakage. This then allows for the space necessary for a water molecule to bind in the 5th position, trans to the metal-oxo bond. The water molecule coordinates and then loses a proton to become a coordinated hydroxide. This is then followed by the formation of a TcO^{2+} group. Protonation of the alternate oxygen atom and the regeneration of the $\text{M-N}_{\text{amine}}$ bond produces an intermediate that now has the Tc-oxo group on the opposite side of the $\text{N}_2\text{N}'_1\text{S}_1$ plane. The protonation of the hydroxide, followed by the release of the water molecule results in the formation of the other isomer. Since H_2^{18}O was the only source of the ^{18}O atoms in this experiment, the incorporation of the ^{18}O atom into the Tc complex confirms the role of water in the interconversion and supports the proposed mechanism.

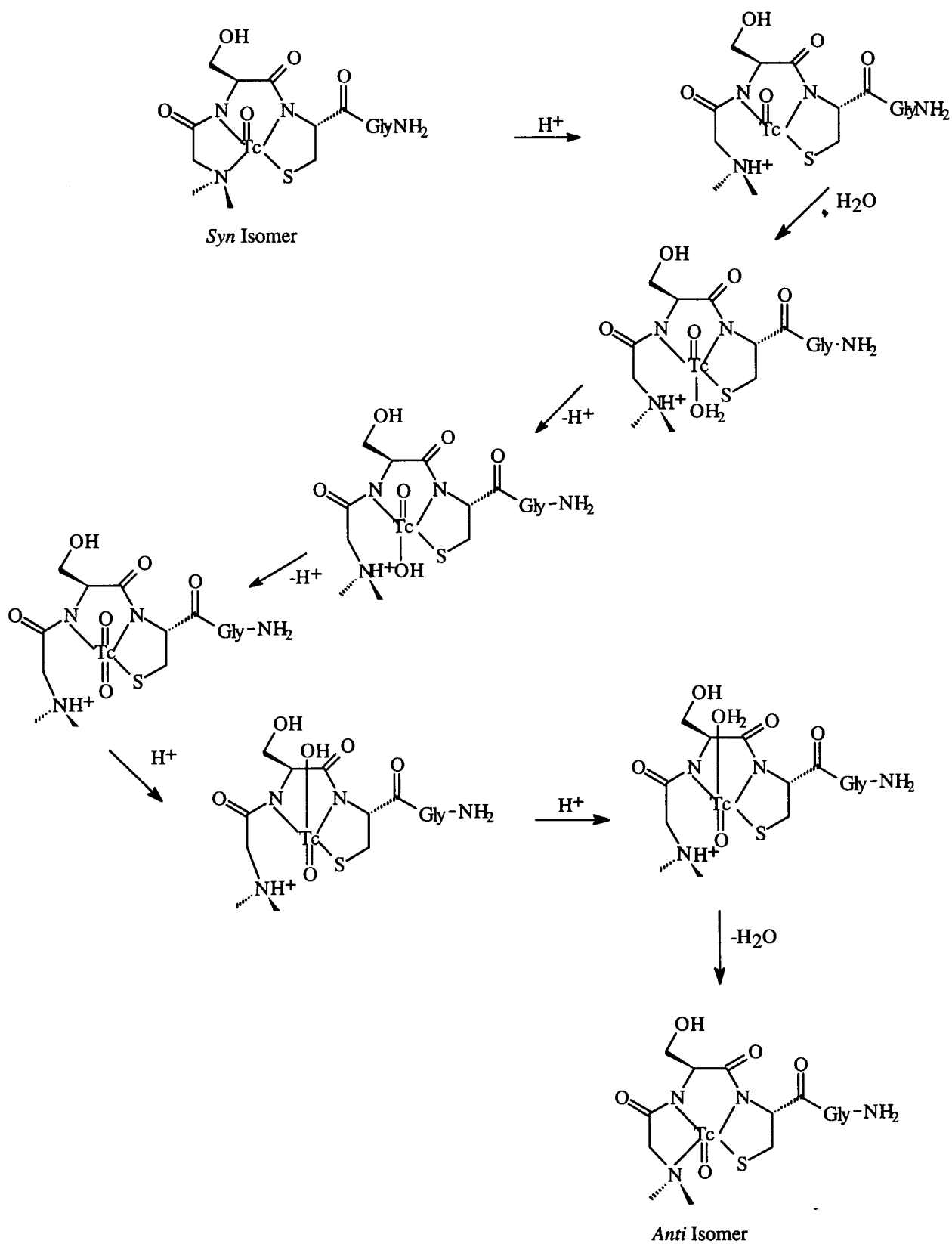


Figure 3-11 ^{18}O syn and anti interconversion mechanism

Another experiment was performed to confirm that the oxygen being exchanged was the metal-oxo one and not one of the amides or a carboxylate in the complex. The $[\text{Tc}^{18}\text{O}(\text{RP294})]$ sample was dried and used to make a KBr pellet. If the incorporation of the ^{18}O atom had occurred into the TcO^{3+} core, there would be a change in the $\text{Tc}=\text{O}$ stretching frequency. The infrared spectrum did show two stretching frequencies at 977 cm^{-1} and 932 cm^{-1} . Only the band at 977 cm^{-1} is present in $[\text{Tc}^{16}\text{O}(\text{RP128})]$ and a calculation based on Hooke's law for vibration and isotopic substitution gave the expected frequency of a Tc^{18}O stretch as 928 cm^{-1} . This experiment provided further confirmation of the proposed mechanism.

3.5 $^{99\text{m}}\text{Tc}$ Tracer Studies

This work was done to provide Resolution Pharmaceuticals Inc. with information on the formation of a ^{99}Tc complex with RP294 and was to mimic the use of $^{99\text{m}}\text{Tc}$ as the chelant portion of a radiopharmaceutical that is discussed in Chapter 4. An experiment was performed where the $^{99\text{m}}\text{Tc}$ complex of RP294 was prepared at the tracer level in the same manner as with the ^{99}Tc complex, with the exception that the tin(II) chloride, sodium gluconate and RP294 were present in large excess as is common in radiopharmaceutical preparations. A radiochemical yield of greater than 94% was obtained in consecutive labelling experiments.

The $^{99\text{m}}\text{Tc}$ and Re complexes of RP294 were co-injected into the HPLC (Fig. 3-12) to determine if their structural characteristics were similar. The Re complex was observed using a UV detector, while the $^{99\text{m}}\text{Tc}$ complex was monitored with a radiometric gamma

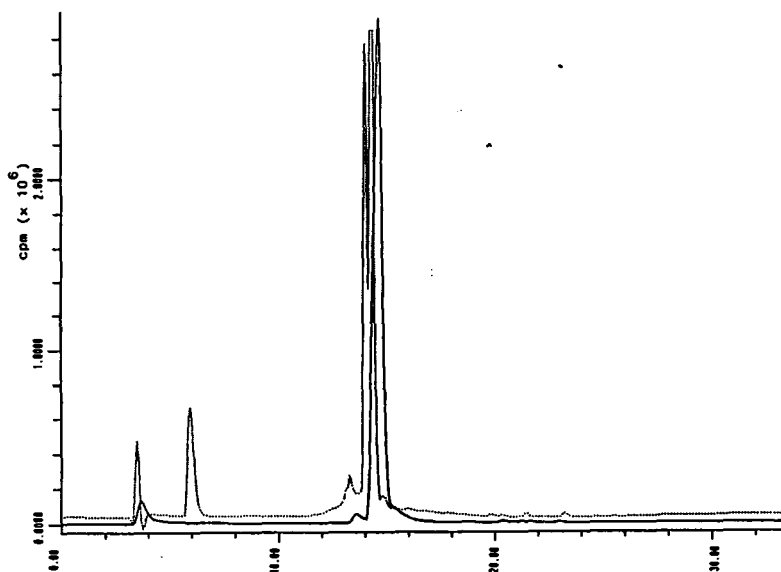


Figure 3-12 HPLC Coinjection of Re and Tc complexes of RP294
 $\lambda_{obs} = 254 \text{ nm}$; gamma detector at 140.4 keV

detector. Two peaks at 13.99 and 14.27 minutes were seen that corresponded to the isomers of the [ReO(RP294)]. The radiometric peak was seen at 14.62 minutes. This delay was due to the fact that the detectors were set up in series. The similar retention times of the Re and ^{99m}Tc complexes support the hypothesis that the ^{99m}Tc complex has a similar structure to the Re complex.

3.6 Experimental Section

Dimethylglycine-L-serine-L-cysteine-glycine-NH₂ (RP294), 15

Dimethylglycine-L-serine-L-cysteine-glycine-NH₂ was prepared via a solid phase peptide synthesis method [51] on an Applied Biosystems Inc. Model 433A peptide synthesizer. Sasarin resin and Fmoc protected amino acids were used. Prior to the addition of each amino acid residue to the peptide chain, the Fmoc protection group was removed with 15% piperidine in N-methylpyrrolidone (NMP). Each amino acid residue was

activated with 0.45 M N-hydroxybenzotriazole (HOBT) and 0.45 M O-benzotriazol-1-yl-N,N,N',N'-tetramethyl uronium hexafluorophosphate (HBTU) in dimethylformamide (DMF), in the presence of diisopropylethylamine (DIPEA). The peptide was cleaved off the sasarsin resin using 95% aqueous trifluoroacetic acid and the sasarsin resin removed by filtration. The addition of the filtrate to *tert*-butylmethyl ether at 0°C caused the precipitation of the crude product. The crude RP294 was purified by HPLC. In RP294, the cysteine thiolate was protected with an acetoamidomethyl (ACM) group and the C terminus was capped with an amide moiety. Mass spectrum (ESMS): $m/z = 421$ ($[M+1]^+$, $[C_{15}H_{29}N_6O_6S_1]^+$). Reverse Phase C-18 HPLC retention time: $R_t = 4.7$ min. 1H and ^{13}C NMR spectral data are given in Table 3-1.

Synthesis of the ^{99}Tc complex of RP294, 16

RP294 (379mg, 0.917 mmoles) was dissolved in 3 mL of distilled water. Tin(II) chloride (205 mg, 1.08 mmoles) and sodium gluconate (200 mg, 0.917 mmoles) were added to the peptide solution, followed by NH_4TcO_4 [61] (151 mg, 0.812 mmoles). The solution was stirred at room temperature for 6 hours. The colour of the solution changed to orange-red. The solution was frozen and lyophilized overnight, yielding a red solid. The product was purified using a 1 cm x 15 cm column packed with Sephadex G10 resin and washed with 20 mL of distilled deionized water which was also used as the eluant. Twenty fractions of 2 mL each were collected and the orange-pink fractions collected, evaporated to dryness and examined with 200 MHz NMR spectroscopy. Fractions 13-19 were chosen to be examined in more detail on a 500 MHz NMR spectrometer. Yield: 225

mg (60% for the combined fractions). Compound **16** showed: TLC: $R_f = 0.0$ in 50/50 DCM/MeOH; Mass spectrum (ESMS): $m/z = 484$ ($[M+Na]^+$ (100%), $[C_{12}H_{20}N_5Na_1O_6^{99}Tc_1S_1]$); IR(cm^{-1} , KBr disk); $977\text{ cm}^{-1}(\nu_{Tc=O})$; 1H NMR spectral data are given in Table 3-2; ^{13}C NMR (D_2O) [125 MHz] 187.8, 174.0, 71.4, 70.5, 68.9, 68.1, 62.2, 60.2, 56.5, 56.4, 56.2, 54.8, 54.5, 54.2, 42.3, 42.2, 42.1, 40.8, 40.6.

*Exchange of ^{18}O into **16***

A sample of the [TcO(RP294)] (15 mg, 0.031 mmoles) was dissolved in 50 μL (2.8 μmol) of ^{18}O enriched water. The solution was left at room temperature and mass spectra taken at timed intervals using the ESMS in positive ion mode. ESMS: $m/z = 484$ ($[C_{12}H_{20}N_5Na_1O_6^{99}Tc_1S_1]$) and 486 ($[C_{12}H_{20}N_5Na_1O_5^{18}O_1^{99}Tc_1S_1]$). The relative ratios for each spectrum recorded were based on peak % intensity. Spectra were taken initially at 15 minute intervals, then 1 hour intervals and finally 24 hour intervals.

Chapter 4

Chelation of a Nine Amino Acid Peptide to ^{99m}Tc

4.0 Introduction

Over the past thirty years, biospecific imaging agents have evolved from large proteins, like antibodies, to antibody fragments (eg. Fab fragments) to smaller “molecular recognition units” such as Fv fragments, antigen binding domain fragments and small biologically active peptides. The smaller size of these molecules confers some desirable properties, such as higher target-to-background ratios and faster blood clearance, that are favourable for imaging. Molecular engineering techniques now permit the peptide to carry the radionuclide binding group in its structure while maintaining high affinity binding to the receptor site. An important component to this kind of system is the ability to radiolabel these agents with high specific activity using short-lived radionuclides, particularly ^{99m}Tc . Recently, the application of small, radiolabeled, biologically active peptides for external imaging of a variety of biological processes has received considerable interest. These applications have ranged from the current widespread use of somatostatin analogs for imaging numerous types of tumours to the development of radiolabeled chemotactic peptides for infection imaging [62].

Resolution Pharmaceuticals Inc. has been active in the research area of small biologically active radioimaging agents. Recently they have developed a nine amino acid peptide (RP128) which has been shown to image areas of infectious and non-infectious inflammation. A market exists for a radioimaging agent that could be used for

inflammation and in particular for abdominal/gastrointestinal inflammation. Resolution based its agent on the Tuftsin tetrapeptide, threonine-lysine-proline-arginine (TKPR). [63].

The tuftsin receptor was selected as an attractive target for imaging inflammation because TKPR is a natural immunostimulant derived from Immunoglobulin G (IgG) through proteolytic cleavage in the spleen and by a neutrophil-derived enzyme (leukokinase). It stimulates a number of functional responses by phagocytes including phagocytosis, respiratory burst and antigen presentation. Tuftsin has been investigated as a potential therapeutic for cancer and viral infection and some efficacy has been observed. The antagonist, TKPPR, with an added proline, has a four-fold greater receptor affinity than tuftsin and was chosen as the targeting domain to avoid the elicitation of any biological activity that might occur if the tuftsin sequence was used [64,65,66].

RP128, **21**, uses the method of bifunctional chelation discussed previously. It is based on two separate substructures, the biologically active portion, TKPPR, and the chelant/spacer portion consisting of dimethylglycine-serine-cysteine-glycine in which the glycine acts as the spacer (Fig. 4-1). This chelant has been discussed above in Chapter 3 in detail. The goal of the present work was to mimic the binding of $^{99m}\text{TcO}(\text{RP128})$ and $\text{ReO}(\text{RP128})$ by binding RP128 to the longer lived ^{99}Tc . Once complexation was achieved, detailed analysis of the structure and properties of the complex could then be carried out. The results are discussed in detail in this chapter.

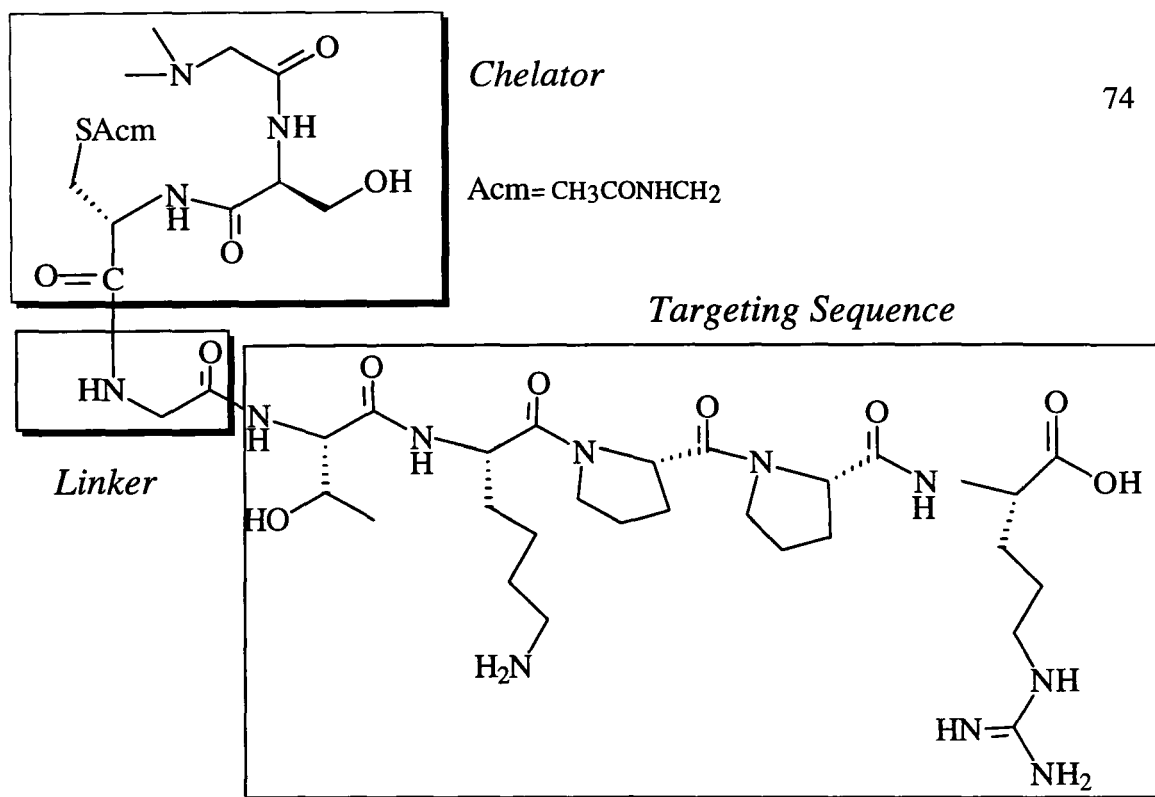


Figure 4-1 The bifunctional chelant RP128, 21

4.1 NMR Spectroscopy of RP128, 21

As in Chapter 3, extensive NMR spectroscopic analysis was necessary in order to show that the chelating portion of the molecule was the only portion to be affected by the coordination of technetium. Proton and carbon-13 NMR spectra were initially assigned by J. Valliant [66], were refined by the writer and the results are shown in Table 4-1. The proton and carbon-13 resonances were assigned by looking for unique peaks which could be ascribed to a particular group within a side chain. By use of the COSY, HSQC and HMBC spectra, the rest of the amino acid residue could then be assigned. For example, the doublet at 1.060 ppm was thought to be the methyl of the threonine (H-17). This was confirmed by COSY correlation to H-16, the β proton for threonine, which in turn showed a COSY correlation

Proton	δ (ppm)	Carbon	δ (ppm)
H-1	2.834	C-2	58.14
H-31 OR H-26	2.228	C-4	55.50
H-31 OR H-26	2.179	C-7	53.49
H-30, H-25	1.907	C-34	52.39
H-11	1.889	C-19	51.41
H-35, H-20	1.818	C-24 OR C-29	47.99
H-35	1.678	C-24 OR C-29	47.81
H-36, H-22	1.557	C-1	43.86
H-21	1.348	C-13	42.60
H-17	1.060	C-9	40.90
		C-37	40.51
		C-23	39.28
		C-8	31.59
		C-20	29.89
		C-26 OR C-31	29.28
		C-26 OR C-31	28.24
		C-35	27.80
		C-22	26.34
		C-25 OR C-30	24.67
		C-25 OR C-30	24.58
		C-36	24.37
		C-11	22.08
		C-21	21.89
		C-17	18.92

to H-15, the α proton of the threonine. From the HSQC spectra, the protons could be correlated easily to their respective carbons, once the protons were reasonably assigned. The carbonyl peaks could then be assigned by the use of the HMBC spectra. Typically, a correlation could be seen between the alpha proton of one residue and the carbon of its neighbouring amide.

There were several residues whose resonances were not as obvious as that of the threonine or where the spin system overlapped with other spin systems. Such was the case for the proline residues. Selective TOCSY experiments were useful in overcoming these problems. For example, by irradiating the resonance at 4.327 ppm, which was assigned to one of the proline α protons, the complete spin system, if the spin-lock time was long enough, would reveal the whereabouts of the other multiplets associated with that proline. A confirmation from the COSY experiment would assure the correct assignment for all of the peaks. It was in this manner that the complete NMR spectrum of RP128 was assigned.

4.2 Synthesis of $^{99}\text{TcO}(\text{RP128})$, 23

The synthesis of the technetium complex of RP128 required that the sulfur of the cysteine residue be deprotected (Fig. 4-2) by reaction with mercuric acetate. This process was attempted using 2-mercaptoethanol as the mercury scavenger however this scavenger was difficult to remove completely and thus caused interference in the complexation process and in later NMR analyses. Hydrogen sulfide was used in its stead and it provided excellent scavenger capabilities and all traces of it could be removed by exposure of the

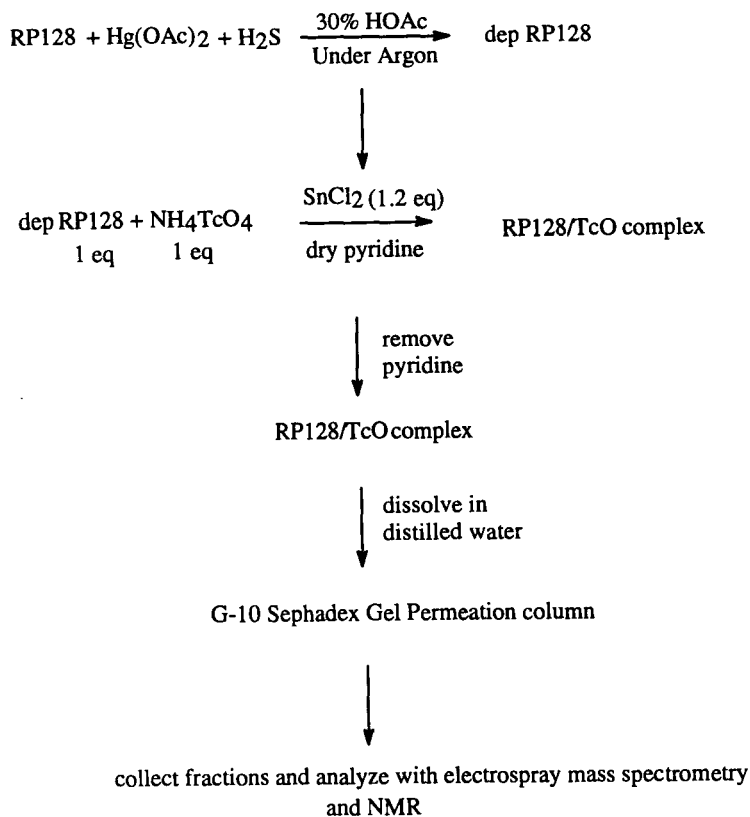


Figure 4-2 Reaction scheme for RP128 coordination of technetium

sample to high vacuum. Lyophilization of the deprotected sample was found necessary to prevent side reactions from occurring. The occurrence of complex formation was determined using ESMS in the positive ion mode. Various attempts were made to complex the deprotected ligand to ^{99}Tc . Substitution reactions had been tried with tetrabutylammonium tetrachlorooxo technetium ($\text{Bu}_4\text{NTcOCl}_4$) and an ethylene glycol ligated to Tc, $[\text{TcO}_2(\text{eg})_2]^-$. These either failed to produce a complex or resulted in an ESMS spectrum that showed many ions but none of the expected $m+2H$ ratio for a 1:1

Tc:RP128 complex. With $\text{Bu}_4\text{NTcOCl}_4$, this was especially true. The large cation Bu_4N^+ produced a huge interfering ion that obliterated all other signals in the mass spectrometer. A reduction/substitution strategy was eventually tried as a means of avoiding this interference. The experiment, outlined in Fig. 4-2, involved taking the lyophilized ligand, dissolving it in dry pyridine and then adding the pertechnetate and tin (II) chloride. The ESMS gave a 522 peak in the positive ion mode that corresponded to the $(\text{M}+2\text{H})^{2+}$ ion, where protonation had occurred probably at the lysine and arginine residues respectively. This would be expected as the pKa values for their side chain amines are quite high, 10.80 and 13.20 for lysine and arginine, respectively. The crude $\text{TcO}(\text{RP128})$ was an orange-red material, soluble in water and slightly soluble in methanol. Analysis by TLC gave an R_f value of 0.0 in 50% MeOH/DCM developing solution. An infrared spectrum was run on a combined sample of 3 fractions from one run. As Fig. 4-3 shows, a strong peak can be

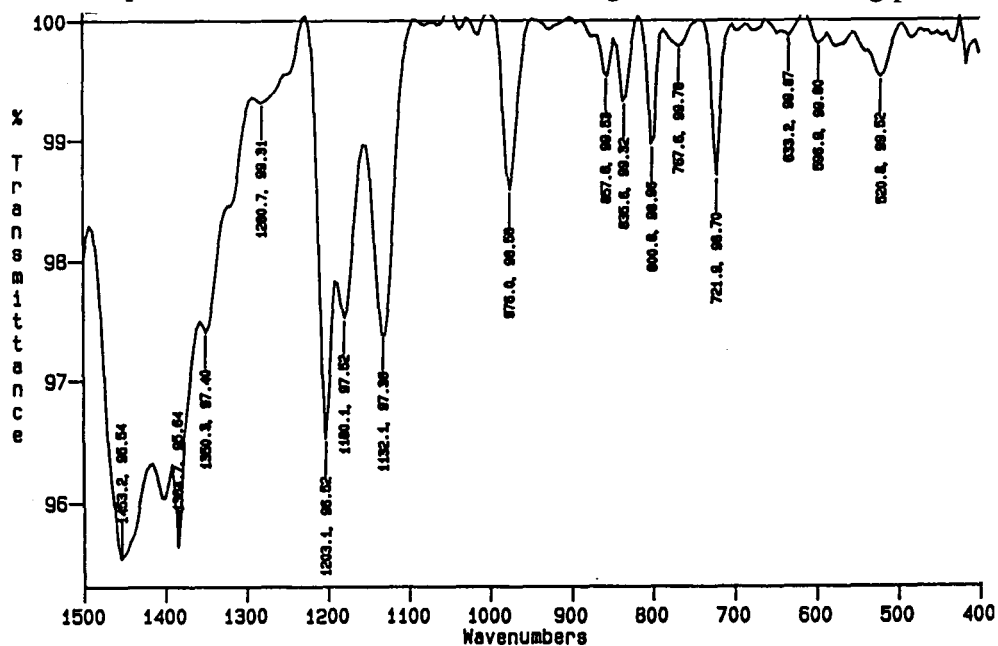


Figure 4-3 Infrared spectrum of 23

seen at 976 cm^{-1} which is characteristic of other technetium-oxo complexes.

It was imperative to obtain a clean, pure sample in order to run the extensive NMR analysis that was necessary. This became quite a problem once the synthesis of **23** was achieved. Early attempts to purify the compound had been made using various chromatographic techniques and supports such as silica gel, cellulose-paper and preparative plate thin-layer chromatography. None of these methods produced definitive results. As Fig. 4-2 shows, separation was finally achieved by size exclusion gel chromatography using distilled, deionized water as the eluant. Fractions were collected as the water ran through the column under gravity. Those fractions that were orange-pink coloured were all examined using 200 MHz NMR spectroscopy for the presence of TcO(RP128) impurities. This procedure provided several excellent samples and these were used for the 500 MHz NMR analysis.

4.3 NMR Spectroscopy of ⁹⁹TcO(RP128), 23

It was expected that two isomers would be present in the fractions of **23** analyzed by NMR spectroscopy as this had been true with the chelant complex TcO(RP294). What was vital to the project was to determine if the targeting area of the molecule had been affected by the chelation of technetium. Thus those peaks associated with the TKPPR portion of the molecule were closely examined to see if any had shifted.

As expected, two isomers were very apparent upon examination of the ¹H NMR spectrum (Fig. 4-4). Table 4-2 gives a complete assignment of the proton peaks for

Table 4-2: ^1H Assignment of TcO(RP128)

<i>Anti Isomer</i>			<i>Syn Isomer</i>		
Assignment	δ (ppm)	J (Hz)	Assignment	δ (ppm)	J (Hz)
7	5.694	$^3J_{AX}=5.0$	7	5.307	$^3J_{AX} = 1.2$
		$^3J_{BX} = 6.6$			$^3J_{BX} = 7.7$
4	4.794	$^3J_{AX} = 3.0$	4	4.600*	$^3J_{AX} = 2.9$
		$^3J_{BX} = 1.8$			$^3J_{BX} = 2.4$
5A	4.243	$^3J_{AX} = 3.1$	5A	4.130	$^3J_{AX} = 2.9$
		$^2J_{AB} = 11.9$			$^2J_{AB} = 11.9$
5B	3.880	$^3J_{BX} = 1.9$	5B	3.962	$^3J_{BX} = 2.4$
					$^2J_{AB} = 11.9$
8A [‡]	3.757	$^3J_{AX} = 5.0$	8A	3.874	$^3J_{AX} = 1.2$
		$^2J_{AB} = ?$			$^2J_{AB} = 12.9$
8B [‡]	3.757	$^3J_{BX} = 6.6$	8B	3.783	$^3J_{AX} = 7.8$
		$^2J_{AB} = ?$			$^2J_{AB} = 13.0$
2A	4.600*	$^2J_{AB} = 16.1$	2A	4.145	$^2J_{AB} = 12.0$
2B	4.129	$^2J_{AB} = 16.1$	2B	3.994	$^2J_{AB} = 12.0$
1A	2.376		1A	2.448	
1B	3.444		1B	3.455	
13A	3.834	$^2J_{AB} = 17.0$	13A	3.834	$^2J_{AB} = 17.0$
13B	3.765	$^2J_{AB} = 17.0$	13B	3.765	$^2J_{AB} = 17.0$

* Peaks hidden under water.

[‡] Selective TOCSY unable to give $^2J_{AB}$

Note: The remaining RP128 peaks remained unchanged for their uncoordinated shifts.

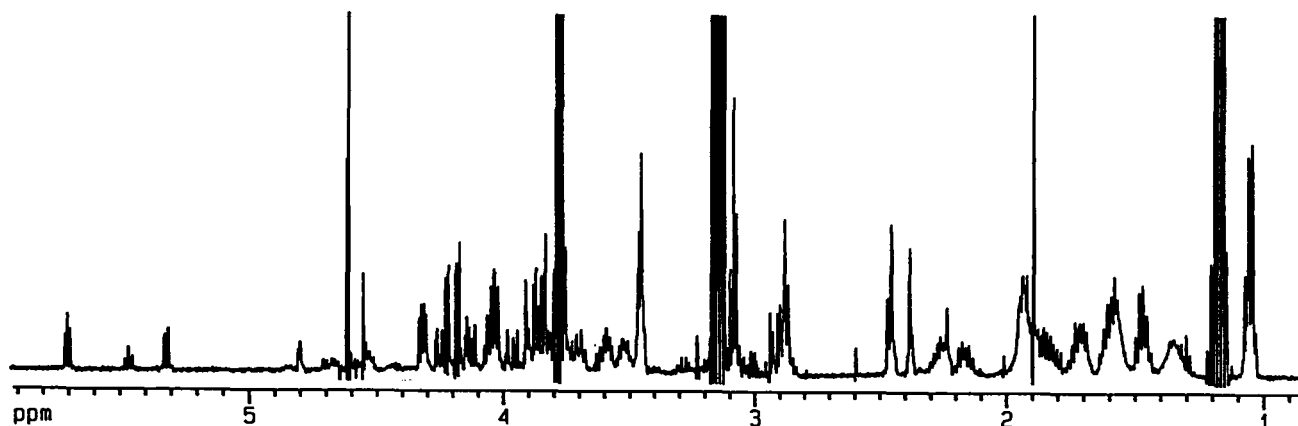


Figure 4-4 500 MHz ^1H NMR of the aliphatic region of **23** in D_2O both the *syn* and *anti* isomer. A brief comparison of these peaks with that of $\text{TcO}(\text{RP294})$, **16**, showed that changes had occurred. The benchmarks for these complexes were the dimethylglycine as well as the α protons for both the serine and cysteine residues. The methyls of the terminal glycine exhibited chemical shifts that were identical to that of its chelate counterpart $\text{TcO}(\text{RP294})$. The α proton for serine was found at 4.794 ppm for the *anti* isomer and was determined to be under the water peak (4.600 ppm) for the *syn* isomer. This was in concurrence with the chelate **16**. The α proton for the cysteine was found at 5.694 ppm for the *anti* isomer and 5.307 ppm for the *syn* isomer. Again very little chemical shift change was found for this proton when compared to $\text{TcO}(\text{RP294})$.

The coupling constants also remained unchanged between chelate **16** and the fully coordinated molecule **23**. The serine β protons showed the same type of coupling as in

the chelant with the serine preferring a specific conformation, holding the OH moiety over the plane of the molecule and the β protons *gauche* to the α proton. The slight difference between the two isomers in coupling constants was caused by the slight variation in the overall structure and how the β protons situated themselves between the two amide carbonyls. The cysteine β protons proved to be as difficult as the TcO(RP294) in terms of the assignment. They exhibited the same coupling constants as their counterparts in **16**. They even exhibited a difficulty in assignment that required a Selective TOCSY experiment to divine. This mimicking of coupling constants indicated that the chelated RP128 forms a similar type of square-based pyramid complex as TcO(RP294). Again, it can be seen that the linker glycine is unaffected by the chelation of the technetium. The AB protons were unchanged from their chelant positions and had the same coupling constants ${}^2J_{AB} = 17.0$ Hz.

Examination of the NMR results of the targeting portion of the [TcO(RP128)], **23**, (Fig. 4-4) showed that few changes occurred with chelation. As mentioned above, the linker portion was unaffected by the chelation process. As Table 4-3 shows, when comparing the peaks between the uncoordinated RP128 and the Tc bound RP128 in the targeting portion, few major changes are seen. The α proton of the arginine could not be located clearly but was most likely unaffected by the chelation. HPLC analysis was done on the ${}^{99m}\text{TcO}(\text{RP128})$ by coinjecting it with its rhenium analogue $\text{ReO}(\text{RP128})$ (prepared at Resolution Pharmaceuticals Inc.) as shown in Figure 4-4. As seen previously with the RP294 complex **16**, the two complexes eluted off the column at the same time, a good indication that the two structures are identical, and further confirming the idea that these

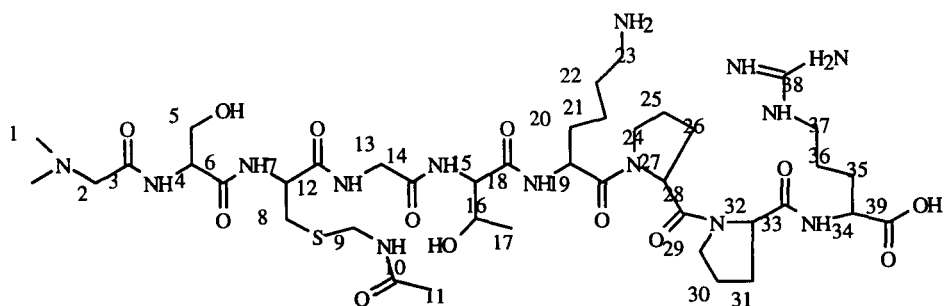


Table 4-3 Proton Comparison in Targeting Portion of RP128 and TcO(RP128)

Proton	Rp128 (ppm)	23 (ppm)
27	4.600	4.600
19	4.517	4.519
32	4.327	4.302
34	4.235-4.206	4.209 (?)
15	4.235-4.206	4.148
16	4.055	4.034
24 or 29	3.732	3.582
24 or 29	3.524	3.515
37	3.097	3.078
23	2.859	2.866
31 or 26	2.228	2.253
31 or 26	2.179	1.161
30 or 25	1.907	1.931
30 or 25	1.907	1.855
35 or 20	1.818	1.702
36 or 22	1.557	1.585
21	1.348	1.466
17	1.060	1.047

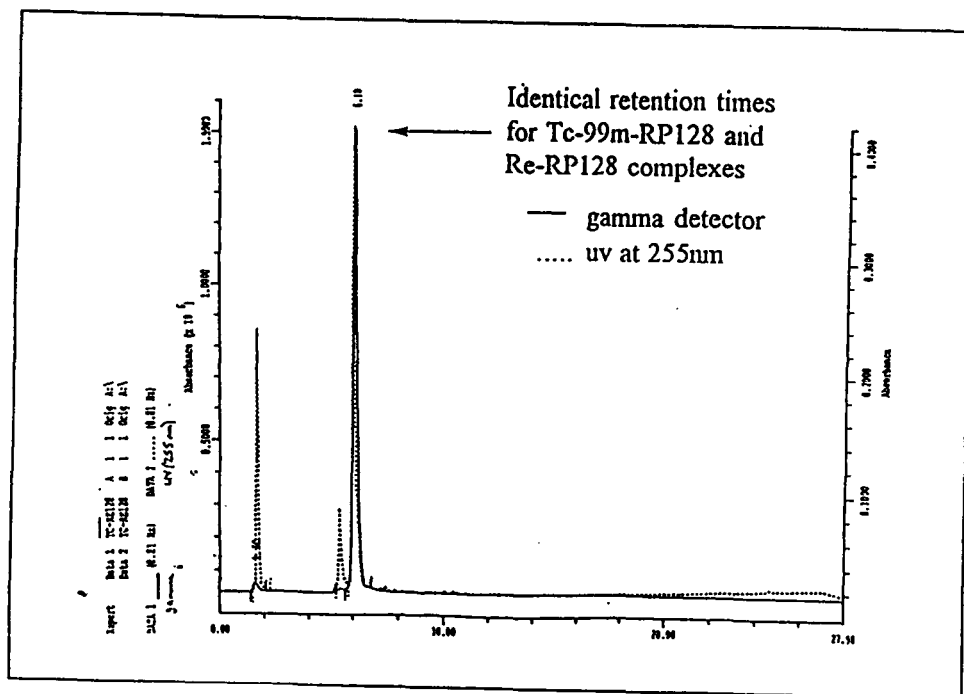


Figure 4-5 HPLC of $^{99m}\text{TcO}(\text{RP128})$ and $\text{ReO}(\text{RP128})$

compounds are analogs of one another.

4.4 $^{99m}\text{TcO}(\text{RP128})$ As an Imaging Agent

In an attempt to mimic the radiopharmaceutical kit that RP128 was being developed for, the exact same reaction that was carried out by the reagents supplied in the kit was repeated using ^{99}Tc as a substitute for ^{99m}Tc . The kit reaction involves the use of pertechnetate, tin (II) chloride and sodium gluconate. The reaction produced an ESMS in the positive ion mode that reflected the kit reaction. A 522 m/z (MH+2) ion was seen indicating that the reaction had occurred and produced the exact same result as those carried out in the laboratory by the present author.

Figure 4-6 is an actual radioimage of a patient that had $^{99m}\text{TcO}(\text{RP128})$ administered to him/her. This subject was a rheumatoid arthritis sufferer. As the

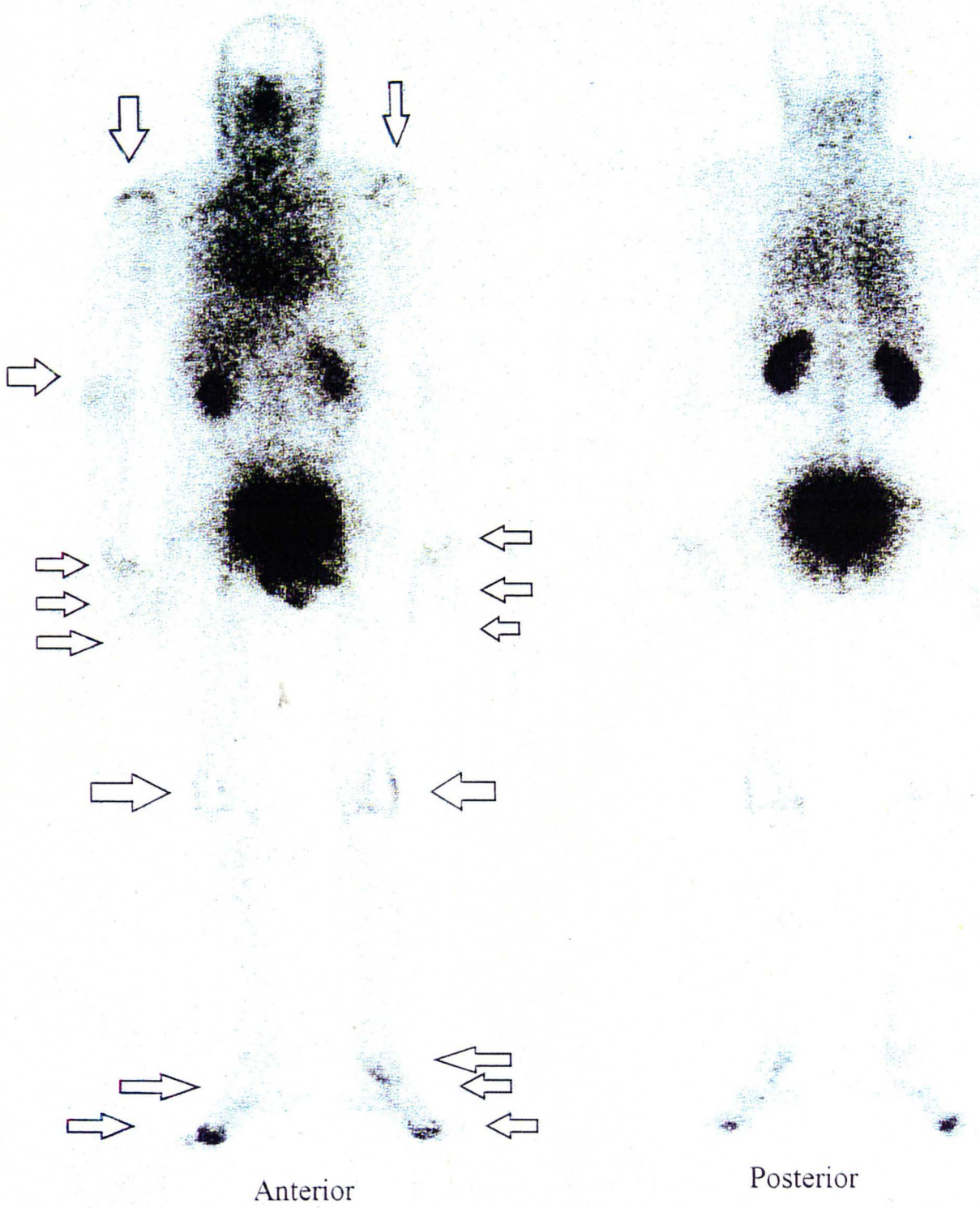


Figure 4-6 ^{99m}Tc scintigraph of rheumatic arthritis sufferer
(Supplied by Resolution Pharmaceuticals Inc.)

scintigraph shows, inflammation can be seen in all of the expected areas for these types of patients. The most pronounced areas are those of the joints, mainly in the hands and the feet.

At present, RP128 is in Phase II trials. It is being developed mostly as an imaging agent for both infectious and non-infectious inflammation and tests done to date have indicated that it is a strong candidate for the imaging of bowel disease. Inflammatory bowel disease (IBD) has been used as a model for RP128 imaging and the results have been quite encouraging. RP128 shows promise as a targeting agent for abdominal/gastrointestinal inflammation imaging [63].

4.5 Experimental Section

DmGSCGTKPPR (RP128), 21

RP128 was prepared via a solid phase peptide synthesis method [49] on an Applied Biosystems Inc. Model 433A peptide synthesizer. Sasarin resin and Fmoc protected amino acids were used. Prior to the addition of each amino acid residue to the peptide chain, the Fmoc protection group was removed with 15% piperidine in N-methylpyrrolidine (NMP). Each amino acid residue was activated with 0.45 M N-hydroxybenzotriazole (HOBt) and 0.45 M O-benzotriazol-1-yl-N,N,N',N'-tetramethyluronium hexafluorophosphate (HBTU) in dimethylformamide (DMF), in the presence of diisopropylethylamine (DIPEA). The peptide was cleaved off the sarsin resin using 95% aqueous trifluoroacetic acid and the sarsin resin removed by filtration. The addition of the filtrate to *tert*-butylmethyl ether at 0°C caused the precipitation of the crude product. The

crude RP128 was purified by HPLC in acetonitrile and water. In RP128, the cysteine thiolate was protected with an acetoamidomethyl (ACM) group. Compound **19** showed: mass spectrum (ESMS): $m/z = 1002$ ($[M+1]^+$); Reverse Phase C-18 Column HPLC in acetonitrile/water with retention time: $R_t = 5.6$ min; ^1H and ^{13}C NMR spectroscopy: see Table 4-1.

Deprotection of RP128, 22

RP128 (20 mg, 0.020 mmoles) was dissolved in 2 mL of 30% acetic acid. Mercury(II) acetate (12.7 mg, 0.040 mmoles) was added to the solution and the solution was stirred under argon at room temperature for 1 hour. H_2S gas was then bubbled through the solution for 5 minutes, causing black HgS to precipitate. The precipitate was removed by vacuum filtration, and the filtrate was frozen and lyophilized overnight. The resulting residue was used immediately in the reaction with the Tc starting material.

Synthesis of the ^{99}Tc complex of RP294, 23

Deprotected RP128, **22**, (20mg, 0.020 mmoles) was dissolved in 2 mL of dry pyridine. Tin(II) chloride (4.6 mg, 0.024 mmoles) and NH_4TcO_4 [61] (3.3 mg, 0.018 mmoles) in 1 mL of dry pyridine were added to the peptide solution. The solution was stirred at room temperature for 1 h. The colour of the solution changed to orange-red. The solution was frozen and lyophilized overnight, yielding a red solid. The product was purified using a 1 cm x 15 cm column packed with Sephadex G10 resin and washed with 20 mL of distilled deionized water which was also used as the eluant. Twenty fractions of

2 mL each were collected and the orange-pink fractions collected, evaporated to dryness and examined by 200 MHz NMR spectroscopy. Fractions 13-19 were found to be the most pure of the compound **23** and were chosen to be examined in more detail on a 500 MHz NMR spectrometer. Compound **23** showed: TLC: $R_f = 0.0$ in 50/50 DCM/MeOH; mass spectrum (ESMS): $m/z = 522$ ($[M+2H]^{2+}$ (100%); IR (KBr disk); 976 cm^{-1} ($\nu_{\text{C=O}}$); ^1H NMR spectral data are given in Tables 4-2 and 4-3.

Chapter 5

Conclusions and Future Work

5.0 Conclusions

In the beginning of this thesis several objectives were given as the purpose to this study. All of them have been met. The main objective was to synthesize a novel tripeptide-based chelant for technetium and rhenium. This was achieved with the synthesis of a mercaptoacetamide-serine-cysteine chelant that was successfully coordinated to both rhenium and technetium. In each case only one diastereomer of the Re/Tc chelate was produced in detectable amounts. This is an unusual feature of this particular ligand. It was also expected that the benzyl group would be displaced upon complexation. As this did not happen it makes for an interesting future study as to why this should be so, because rhenium and technetium complexes prepared under similar conditions have been reported to de-benzylate. Other future work on these rhenium and technetium complexes would involve crystallization of both species to fully assign the major diastereomer obtained and further refine the geometry. Modelling studies would also be necessary to fully understand the various aspects of the NMR studies and the mechanism of complexation, and the basis for the preferential formation of one diastereomer over the other.

The chelation of technetium to RP294 was achieved with great success. Adequate separation was provided by size-exclusion chromatography such that a detailed NMR analysis of the complex in solution could be carried out. It led to the discovery of the

presence of two isomers. Each isomer's proton NMR was assigned and demonstrated interesting properties for both the *syn* and *anti* species. This led to the discovery of the preference of the serine hydroxyl positioning itself over the basal plane of the coordination complex in both isomers. Oxygen-18 studies showed that the isomers interconverted and a mechanism was proposed. Future work would involve the growth of a crystal and an x-ray structure for both the *syn* and *anti* isomers to allow for a full examination of the NMR data produced in this study. Modelling studies would also provide some further insight into some of the coupling patterns and chemical shifts seen in the NMR analysis.

The nonapeptide, DmGSCGTKPPR, RP128 was complexed to technetium and the resulting complex was purified to give detailed NMR spectra. The results were as expected; the chelant area was the most affected by coordination while the targeting sequence remained untouched. Again, two isomers were found but the changes remained in the chelant area of the molecule. Further NMR studies need to be done to determine if there are any effects of closely situated protons in the chelant area to the target area such as would be achieved by a Nuclear Overhauser Effect experiment. A crystal structure of either the radiopharmaceutical itself or with the technetium present would provide very useful information on the solid state conformation of the molecule(s).

References

1. Spies, H; Johannsen, B. Topics in Current Chemistry: Technetium and Rhenium, Yoshiria, K.; Omori, T. (Eds.) Springer, New York, **1996**, pp. 79-121.
2. Breitz, H.B.; Weiden, P.L.; Vanderheyden, J.-L.; Appelbaum, J.W.; Bjorn, M.J.; Fer, M.F.; Wolf, S.B.; Ratliff, B.A.; Seiler, C.A.; Foisie, D.C.; Fisher, D.R.; Schroff, R.W.; Fritzberg, A.R.; Abrams, P.G. *J. Nucl. Med.* **1992**, 33, 1099.
3. Deutsch, E.; Libson, K.; Jurrison, S.; Lindoy, L.F. *Progr. Inorg. Chem.* **1993**, 30, 75.
4. Davison, A. Technetium in Chemistry and Nuclear Medicine, Deutsch, E.; Nicolini, M.; Wagner H.N Jr. (Eds.), Cortina International, Verona, Italy, **1983**, p3.
5. Bandoli, G.; Mazzi U.; Roncari, E.; Deutsch, E.; *Coord. Chem. Rev.* **1982**, 44, 191.
6. Melnik, M.; Van Lier, J.E. *Coord. Chem. Rev.* **1987**, 77, 275.
7. Mazzi, U. *Polyhedron* **1989**, 8, 1683.
8. Franklin, K.J.; Howard-Lock, H.E.; Lock, C.J.L. *Inorg. Chem.* **1982** 17, 1377.
9. Morgan, G.; Deblaton, M.; Hussein, W.; Thornback, J.; Evard, G.; Durant, F.; Stach, J.; Abram, U.; Abram, S. *Inorg. Chim. Acta* **1991**, 190, 257.
10. Deutsch, E.; Libson, K. Technetium in Chemistry and Nuclear Medicine, Deutsch, E.; Nicolini, M.; Wagner H.N Jr. (Eds.), Cortina International, Verona, Italy, **1983** p29.
11. Mazzi, U.; Nicolini, M. Bandoli, G.; Refosco, F.; Tisato, F.; Moresco, A.; Duatti, A. Technetium and Rhenium Chemistry and Nuclear Medicine 3, Nicolini, M.; Bandoli, G. (Eds.) Cortina International, Verona, Italy, Raven Press, New York, New York **1990**, p39.

12. Volkert, W.; Jurrison, S. Topics in Current Chemistry: Technetium and Rhenium, Yoshiria, K.; Omori, T. (Eds.) Springer, New York, **1996**, p123-148.
13. Volkert, W.A.; Hoffman, T.J.; Seger, R.M. *Eur. J. of Nuc. Med.* **1984**, 9, 511.
14. Troutner, D.E.; Volkert, W.A.; Hoffman, T.J.; *J. Appl. Radiat. Isotopes* **1984**, 35, 467.
15. Morgan, G.F.; Deblaton, M. Thornback, J. *J. Nucl. Med.* **1991**, 32, 500.
16. Abrams, M.J.; Davison, A.; Jones, A.G.; Costello, C.E.; Pang, H. *Inorg. Chem.* **1983**, 22, 2798.
17. Jones, A.G.; Abrams, M.J. *Nucl. Med. Biol.* **1984**, 22, 225.
18. Holman, B.L.; Jones, A.G.; Lister-James, J.; Davison, A.; Abrams, M.J.; Kirshenbaum, J.M.; Tumeh, S.S.; English, R.J. *J. Nucl. Med.* **1984**, 25, 1350.
19. Kelly, J.D.; Forster, A.M.; Higley, B.; Archer, C.M.; Booker, F.S.; Canning, L.R.; Chiu, F.W.; Edwards, B.; Gill, H.K.; McPartlin, M.; Nagle, K.R.; Latham, I.A.; Pickett, R.D.; Storey, A.E.; Webbon, P.M. *J. Nucl. Med.* **1983**, 34, 222.
20. Higley, B.; Smith, F.W.; Smith, T.; Gemmell, H.G.; Gupta, P.D.; Gvozdanic, D.V.; Graham, D.; Hinge, D.; Davidson, J.; Lahiri, A. *J. Nucl. Med.* **1993**, 34, 30.
21. Steigman, J.; Eckleman, W.C.; The Chemistry of Technetium in Medicine, National Academy Press, Washington, D.C., **1992**.
22. Chilton, H.M.; Thrall, J.H. Pharmaceuticals in Medical Imaging, Swanson, D.; Chilton, H.; Thrall, J. (Eds.) Macmillan Publishing, New York, New York, **1990**, p305.

23. Nowotnik, D. Technetium Bifunctional Chelating Agents 1996 from the Internet
<http://www.bcpl.lib.md.us/~dnowotni/bfca/>
24. Babich, J.W.; Graham, W.; Barrow, S.W.; *J. Nucl. Med.* **1993**, 34, 2176.
25. Jurrison, S.; Schlemper, E.O.; Troutner, D.E.; *Inorg. Chem.* **1986**, 25, 543.
26. Neirinckx, R.D.; Canning, L.; Piper, I.M.; *J. Nucl. Med.* **1987**, 28, 191.
27. Valliant, J.F. *Ph.D. Thesis*, McMaster University, **1997**.
28. Thakur, M.L. *Nucl. Med. Comm.* **1995**, 16, 724.
29. Bruch, M.; Dybowski, C. NMR Spectroscopy Techniques, Bruch, M. (Ed.) Marcel Dekker, Inc. New York, New York, **1996**, p61-104.
30. McLafferty, F.W.; Turecek, F. Interpretation of Mass Spectra, University Science Books, Mill Valley, California **1993**, p106.
31. Kung, H.F.; Molnar, M.; Billing, J.; Wicks, R.; Blau, M.J. *J. Nucl. Med.* **1984**, 25, 326.
32. Edwards, D.S.; Cheesman, E.H.; Watson, M.W.; Maheu, L.J.; Nguyen, S.A.; Dimitre, L.; Nason, T.; Watson, A.D.; Walovitch, R. Technetium and Rhenium Chemistry and Nuclear Medicine 3, Nicolini, M.; Bandoli, G. (Eds.) Cortina International, Verona, Italy, Raven Press, New York, New York **1990**, p433.
33. Knight, L.C.; Radcliffe, R.; Maurer, A.H.; Rodwell, J.D.; Alvarez, V.L. *J. Nucl. Med.* **1994**, 35, 282.
34. Brenner, D.; Davison, A.; Lister-James, J.; Jones, A.G. *Inorg. Chem.* **1984**, 23, 3793.
35. Carey, F.A.; Sundberg, R.J. Advanced Organic Chemistry, Plenum Press, New York, New York, **1990**, p229-231.

36. Bell, R. *Personal communication*.
37. Carey, F.A.; Sundberg, R.J. Advanced Organic Chemistry, Plenum Press, New York, New York, 1990, p478.
38. Maharaj, R. *Ph.D. Thesis*, 1993.
39. Bodanszky, M. Peptide Chemistry, Springer-Verlag, Berlin Heidelberg, 1988, p63-68.
40. Pearson, D.; Blanchette, M.; Baker, M.; Guidon, C. *Tet. Lett.* 1989, Vol. 30, No. 21, 2739.
41. Wuthrich, K. NMR of Proteins and Nucleic Acids, John Wiley and Sons, Inc. New York, New York, 1986, p17.
42. Bruch, M. NMR Spectroscopy Techniques, Bruch, M. (Ed.) Marcel Dekker, Inc. New York, New York, 1996, p145-238.
43. Chatt, J.; Rowe, G.A. *J. Am. Chem. Soc.* 1962, 4019.
44. Kung, H.F.; Guo, Y.; Yu, C.; Billings, J.; Subramanyam, V.; Calabrese, J.C. *J. Med. Chem.* 1989, 32, 433.
45. Hansen, L.; Ciri, R.; Taylor, A.J.; Marzilli, L. *Inorg. Chem.* 1992, 31, 2801.
46. Francesconi, L.C.; Graczyk, G.; Wehrli, S.; Shaikh, S.N.; McClinton, D.; Liu, S.; Zubieta, J.; Kung, H.F. *Inorg. Chem.* 1993, 32, 3114.
47. Oneil, J.P.; Wilson, S.R.; Katzenellenbogen, J.A.; *Inorg. Chem.* 1994, 33, 319.
48. Wong, E.; Fauconnier, T.; Bennett, S.; Valliant, J.F.; Nguyen, T.; Lau, F.; Lu, L.; Pollak, A.; Bell, R.A.; Thornback, J.; *submitted for publication, April 1997 to Inorg. Chem.*
49. Nosco, D.L.; Manning, R.G.; Fritzberg, A. *J. Nucl. Med.* 1986, 27, 939 (abs.)

50. Hansen, L.; Marzilli, L.G.; Eshima, D.; Malveaux, E.J.; Folks, R.; Taylor A. Jr. *J. Nucl. Med.* **1994**, 35, 1198.
51. Merrifield, R.B., *J. Am. Chem. Soc.* **1963**, 85, 2149.
52. Rizo, J.; Bruch, M. NMR Spectroscopy Techniques, Bruch, M. (Ed.) Marcel Dekker, Inc. New York, New York, **1996**, p 285-415.
53. Pietzsch, H.J.; Spies, H.; Hoffman, S.; Scheller, D. *Appl. Radiat. Isot.* **1990**, Vol. 41, No. 2, p 185.
54. Pirmettis, I.C.; Papadoupoulos, M.S.; Mastrostamatis, S.G.; Raptopoulou, C.P.; Terzis, A.; Chiotellis, E. *Inorg. Chem.* **1996**, 35, 1685.
55. Jones, A.G.; Davison, A.; Technetium in Chemistry and Nuclear Medicine, Deutsch, E. ; Nicolini, M.; Wagner H.N Jr. (Eds.), Cortina International, Verona, Italy, **1983**, p25.
56. Bryson, N.; Dewan, J.; Lister-James, J.; Jones, A.; Davison, A. *Inorg. Chem.* **1988**, 27, 2154.
57. Rao, T.; Adhikesavalu, D.; Camerman, A.; Fritzberg, A.R. *J. Am. Chem. Soc.* **1990**, 112, 5498.
58. PCMODEL Version 4.0, Serena Software, Bloomington, Ind.
59. Cordier, C.; Gruselle, M.; Jaouen, G.; Hughes, D.; McGlinchey, M.J. *Mag. Res. Chem.* **1990**, 28, 835.
60. Kung, H.F.; Liu, B.L.; Pan, S. *Appl. Radiat. Isot.* **1989**, 40, 677.
61. Peacock, R.D.; The Chemistry of Technetium and Rhenium, Elsevier Publishing Company, London, **1966**, p33.

62. Fischman, A.J.; Babich, J.W.; Strauss, H.W.; *J. Nucl. Med.* **1993**, 34, 2253.
63. Peers, S.H.; Tran, L.L.; Eriksson, S.J.; Ballinger, J.; Goodbody, A.E. *J. Nucl. Med.* **1993**, 36, 114p.
64. Gershonov, E.; Granoth, R.; Tzeheval, E.; Gaoni, Y.; Fridkin, M. *J. Med. Chem.* **1996**, 39, 4833.
65. Nishioka, K.; Satoh, P.S.; Constantopoulos, A.; Nayjar, V.A. *Biochim. Biophys. Acta* **1973**, 310, 230.
66. Fridkin, M.; Gottlieb, P. *Molecular and Cellular Biochemistry* **1981**, 41, 73.
67. Valliant, J.F. *personal communication*.

Appendix I

Experimental Methods

Analytical TLC was performed on silica gel 60-F₂₅₄ (Merck) plates with detection by long wavelength ultra violet light unless specified otherwise. Chromatography was performed with use of a chromatotron (Harrison Research Model 7924T) that used a 4 mm plate (EM Science silica gel 60 PF₂₅₄ containing gypsum). The mobile phase consisted of a gradient which starts off with 100% of the less polar solvent moving to 100% of the other solvent. All commercial reagents were used as supplied. Solvents were distilled, under nitrogen, from calcium hydride. Nitrogen was dried by passing it through calcium sulphate. All reactions were protected from light and carried out under a slow flow of nitrogen unless stated otherwise. Solvents were evaporated with a rotary evaporator (20 mmHg) at elevated temperatures (30-50°C). Melting points were recorded on a Gallenkamp capillary tube melting point apparatus.

Selected NMR spectra were recorded on a Bruker Avance DRX-500 spectrometer. Proton spectra were acquired at 500.130 MHz with a 5 mm broadband inverse probe with triple axis gradient capability. Spectra were obtained in 8 scans in 32K data points over a 4.006 kHz spectral width (4.096 s acquisition time). Sample temperature was maintained at 30 °C by a Bruker Eurotherm variable temperature unit. Gaussian multiplication (line broadening: -1.5 Hz, Gaussian broadening: 0.2) was used to process the free induction decay (FID) which was zero-filled to 64K before Fourier

transformation. Coupling constants (J) were reported in Hz.

Proton COSY two dimensional NMR spectra were recorded in the absolute value mode with the pulse sequence $90^\circ - t_1 - 45^\circ - \text{ACQ}$ and included pulsed field gradients for coherence selection. Spectra were acquired in 1 scan for each of the 256 FIDs that contained 2K data points in F2 over the previously mentioned spectral width. The ^1H 90° pulse width was $6.6 \mu\text{s}$. A 1.0 s relaxation delay was employed between acquisitions. Zero-filling in F1 produced a 1K x 1K data matrix with a digital resolution of 3.91 Hz/point in both dimensions. During two dimensional Fourier transformation a sine-bell squared window function was applied to both dimensions. The transformed data were then symmetrized.

Carbon-13 NMR spectra were recorded at 125.758 MHz with a 5 mm broadband inverse probe with triple axis gradient capability. The spectra were acquired over a 28.986 kHz spectral width in 32K data points (0.557 s acquisition time). The ^{13}C pulse width was $4.0 \mu\text{s}$ (30° flip angle). A relaxation delay of 0.5 s was used. Exponential multiplication (line broadening: 4.0 Hz) was used to process the FID which was zero-filled to 64K before Fourier transformation.

Inverse detected $^1\text{H} - ^{13}\text{C}$ two dimensional chemical shift correlation spectra were acquired in the phase sensitive mode and used the pulsed field gradient version of the HSQC pulse sequence. The FID's in the F2 (^1H) dimension were recorded over a 3.655 kHz spectral width in 1K data points. The 128 FID's in the F1 (^{13}C) dimension were obtained over a 21.368 kHz spectral width. Each FID was acquired in 2 scans. The fixed

delays during the pulse sequence were a 1.0 s relaxation delay and a polarization transfer delay of 1.786 ms. The 90° ^1H pulse was 6.6 μs while the ^{13}C 90° pulse was 11.6 μs . The data were processed with a sine-bell squared window function shifted by $\pi/2$ in both dimensions and linear prediction to 256 data points in F1 followed by zero-filling to 1K.

The pulsed field gradient version of the HMBC pulse sequence was used to acquire the inverse detected ^1H - ^{13}C two dimensional chemical shift correlation spectra through two- and three-bond coupling interactions in the absolute value mode. The FID's in the F2 (^1H) dimension were recorded over a 3.655 kHz spectral width in 1K data points. The 128 FID's in the F1 (^{13}C) dimension were obtained over a 21.368 kHz spectral width. Each FID was acquired in 2 scans. The fixed delays during the pulse sequence were a 1.0 s relaxation delay, a 3.3 ms delay for the low pass J-filter and 0.08 s delay to allow evolution of the long-range coupling. The 90° ^1H pulse was 6.6 μs while the ^{13}C 90° pulse was 11.6 μs . The data were processed with a sine-bell window function in both dimensions and linear prediction to 256 data points in F1 followed by zero-filling to 1K.

Compounds studied by NMR were dissolved in the appropriate deuterated solvents (Isotec, Inc.) to a concentration of approximately 15.0 mg mL⁻¹ whenever possible. Chemical shifts are reported in ppm relative to TMS. The residual solvent signals were used as internal references for the ^1H and ^{13}C spectra, respectively.

All other NMR spectra were recorded on a Bruker AC-200 spectrometer. Proton spectra were acquired at 200.133 MHz with a 5 mm dual frequency probe. Spectra were

obtained in 8 scans in 16K data points over a 2.403 KHz spectral width (3.408 s acquisition time). Spectra were acquired at ambient probe temperature. The free induction decay (FID) was processed with exponential multiplication (line broadening: 0.1 Hz) and was zero-filled to 32K before Fourier transformation.

Carbon-13 NMR spectra were recorded at 50.323 MHz with the 5 mm QNP probe. The spectra were acquired over a 12.195 kHz spectral width in 16K data points (0.672 s acquisition time). The ^{13}C pulse width was 1.5 μs (42° flip angle). A 0.5 s relaxation delay was used. The FIDs were processed with exponential multiplication (line broadening: 3.0 Hz) and zero-filled to 32K before Fourier transformation.

Infrared spectra were recorded on a Bio Rad FTS-40 Fourier transform spectrometer. Solid samples were prepared in Nujol or as KBr pellets in the region of 4000-400 cm^{-1} .

Electrospray ionization mass spectrometry was performed with 50/50 $\text{CH}_3\text{CN}/\text{H}_2\text{O}$ as the mobile phase at a flow rate of 15 μL per minute, with the use of a Brownlee Microgradient syringe pump. Samples were dissolved in 50/50 $\text{CH}_3\text{CN}/\text{H}_2\text{O}$ with the addition of 1 drop of 0.1% ammonium hydroxide for samples to be analysed in the negative mode, or 1 drop of 0.1% TFA for samples that were to be analyzed in the positive mode. Full scan ESMS experiments were performed with a Fisons Platform quadrupole instrument.